t No. FHWA-RD-76-91

ICATION OF FRACTURE MECHANICS FOR OVED DESIGN OF BITUMINOUS CONCRETE

Vol.1. Plan of Research, State-of-the-Art, and Mathematical Investigations

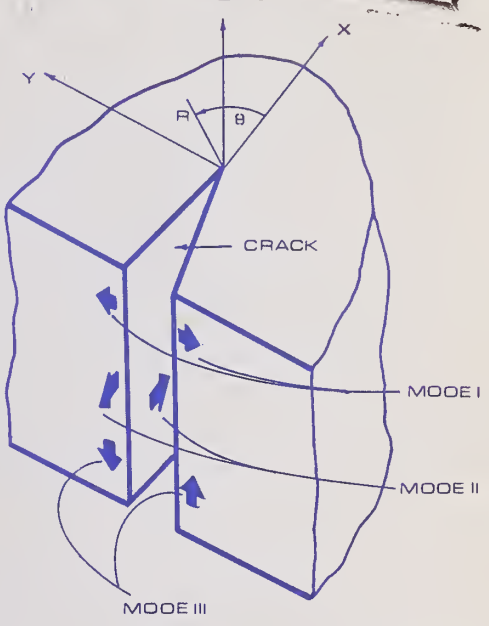

June 1976
Final Report

Document is available to the public through the National Technical Information Service, Springfield, Virginia 22161

Prepared for
FEDERAL HIGHWAY ADMINISTRATION
Offices of Research & Development
Washington, D. C. 20590

NOTICE

This document is disseminated under the sponsorship of the Department of Transportation in the interest of information exchange. The United States Government assumes no liability for its contents or use thereof.

The contents of this report reflect the views of the contracting organization, which is responsible for the facts and accuracy of the data presented herein. The contents do not necessarily reflect the official views or policy of the Department of Transportation. This report does not constitute a standard, specification, or regulation.

FHWA DISTRIBUTION NOTICE

This report is being distributed by FHWA memorandum to interested researchers. A limited number of additional copies are available upon request from the Paving and Structural Materials Group of the Materials Division, Office of Research.

Technical Report Documentation Page

1. Report No.	2. Government Accession No.	3. Recipient's Catalog No.
FHWA-RD-76-91		

4. Title and Subtitle: APPLICATION OF FRACTURE MECHANICS FOR IMPROVED DESIGN OF BITUMINOUS CONCRETE Vol. 1. Plan of Research, State-of-the-Art, and Mathematical Investigations.

5. Report Date: June 1976

6. Performing Orgonization Code: RF-3736

7. Author(s): K. Majidzadeh, C. Buranarom & M. Karakouzian

8. Performing Orgonizotion Report No.

9. Performing Orgonization Name and Address:
Ohio State Research Foundation
Dept. of Civil Engineering
Columbus, Ohio 43210

10. Work Unit No. (TRAIS): FCP 34A2-202

11. Contract or Grant No.: DOT-FH-11-8157

12. Sponsoring Agency Name and Address:
Offices of Research and Development
Federal Highway Administration
U.S. Department of Transportation
Washington, D.C. 20590

13. Type of Report and Period Covered: Final Report

14. Sponsoring Agency Code: M-0326

15. Supplementary Notes: This contract is one study in the Federally Coordinated Program of Highway Research and Development, Project 4A, Minimize Early Deterioriation of Bituminous Concrete, and Task 2, Improved Mixture Design and Performance Through Use of Stiffness, Fatigue and Fracture Criteria. FHWA Contract Manager: S.R.Spelman(HRS-22)

16. Abstract: In this study, the State-of-the-Art of fatigue and fracture concepts and mathematical developments of stress-intensity factor were reviewed. The interrelation between normalized stress-intensity factor crack length and beam on elastic foundation are discussed.

The effect of material constituents influencing the fatigue and fracture response of asphaltic mixtures are discussed. The sensitivity analysis included the effect of mixture constituents such as asphalt, filler and polymeric and fibrous additives. In this study, a number of fatigue models for asphaltic concrete were also investigated.

In this volume, the State-of-the-Art of fatigue and fracture concepts and mathematical development of stress-intensity factor are reviewed. The mathematical relation between the normalized stress-intensity factor, crack length and beam on elastic foundation geometry are presented. Nomographs are developed to aid in solution of stress-intensity variation with crack length. The limits of analysis and restriction of the theory are discussed. Typical examples demonstrating the applicability of concepts developed are presented.

This is the first of a two volume series. The other volume in the series is:

Vol. No.	FHWA No.	Short Title
2	76-92	Evaluation of Improved Mixture Formulations, and the Effect of Temperature Conditions on Fatigue Models.

17. Key Words	18. Distribution Statement
Stress intensity factor, fracture mechanics, beam on elastic foundations, normalized stress-intensity, crack length, viscoelastic fracture and fatigue, crack propagation.	No restrictions. This document is availiable to the public through the National Technical Information Service, Springfield, Virginia 22161.

19. Security Classif. (of this report)	20. Security Classif. (of this page)	21. No. of Pages	22. Price
Unclassified	Unclassified	211	

Form DOT F 1700.7 (8-72) Reproduction of completed page authorized

ACKNOWLEDGMENT

This report is prepared as a part of the research investigation entitled "Application of Fracture Mechanics for Improved Design of Bituminous Concrete," and conducted by the Department of Civil Engineering, Materials Division, The Ohio State University Research Foundation. The financial support for this study was provided by the U.S. Department of Transportation under contract no. FH-11-8157.

A number of graduate and undergraduate students plus the staff of the Materials Division of Ohio State University have assisted in this investigation. The authors gratefully acknowledge the following persons for their help: G. Bokowski, M. Dat, G. Ilves and F. Makdisi-Ilyas. Special thanks are also due to Ms. Cheryl Helm and Ms. Carole Painter for typing, correcting and revising the manuscript.

TABLE OF CONTENTS

LIST OF FIGURES

NOTATIONS

a	fundamental length of the beam
B	widths of the beam and the foundation
b	$B/2$
c	vertical crack length
d	depth of the beam
d_f	depth of the elastic foundation
d_i	the Williams' stress function coefficients
E_b	modulus of elasticity of the beam
E_f	modulus of elasticity of the foundation
I_b	moment of inertia of the beam
K_1	opening mode stress-intensity factor
K_1'	normalized stress-intensity factor
l	effective length of the beam in the boundary collocation procedure
m	number of boundary stations
n	one-half the number of the Williams' stress function coefficients
P	total applied load
p	applied uniform load per unit length or applied sinusoidal load on the beam
p_0	amplitude of the applied sinusoidal load
Q	reaction of the foundation
q	reactive sinusoidal load per unit width on the foundation

q_0	amplitude of q
r	radial distance from the tip of the vertical crack
u	horizontal displacement
v	vertical displacement
w	surface deflection of the beam
x,y	rectangular coordinates
α	a dimensionless parameter
$1/\beta$	a fundamental length of the beam in the conventional theory of beams on elastic foundations
ϵ	one-half of the applied uniform loaded length
ϵ_x, ϵ_y	strain components
$1/\lambda$	a wave length of the sinusoidal loads
σ_x, σ_y τ_{xy}	stress components
σ_{max}	maximum tensile stress in the beam
$\sigma_{p_{max}}$	maximum tensile stress in the beam due to a concentrated load
$\sigma_{s_{max}}$	maximum tensile stress in the beam due to a uniform load
ν_f	Poisson's ratio of the foundation
ϕ	Airy's stress function
χ	Williams' stress function
ψ	a dimensionless parameter
θ	an angle in radians measured counter-clockwise from the vertical axis

PART I. PLAN OF RESEARCH

I. INTRODUCTION

The rational design of pavements must lead to the prediction of their performance during their service life. The overall pavement performance as measured by its serviceability and maintainability under induced environmental and loading conditions, in turn, depends upon the structural integrity of the component layers. The engineering properties of paving materials and geometrical variables such as thickness and relative position of various component layers greatly contribute to the structural integrity of pavement systems. The pavement material and its structural arrangement need to be selected to provide optimum serviceability under induced load and environmental factors. Recognizing that pavement failures can be placed into three broad categories of durability, stability, and fatigue and fracture, bituminous concrete needs to be selected and designed so as to resist detrimental forces of load and environment and provide satisfactory performance.

This study is concerned with the evaluation of fatigue and fracture resistance of bituminous concrete. It is aimed at an investigation of the characteristics and behavior, and improvements of these mixtures as related to resistance to cracking. As it has been shown in the literature review, two approaches to such a problem study are possible; namely, one leading to a phenomenological characterization and evaluation of asphaltic concrete material; and the other based on the mechanistic approach developed at Ohio State University. The mechanistic approach utilizes the fracture mechanics concept

to study the damage processes and to evaluate the fatigue and fracture resistance of asphaltic mixtures.

The phenomenological characterization of fatigue in bituminous mixtures has been extensively studied within the past few decades. In a recent report, Saraf (49) has presented a detailed review of various testing and analytical procedures used for the phenomenological characterization of fatigue life of bituminous mixtures. This review of literature indicates that various methods and analytical procedures have been employed in the past to study the fatigue response of asphaltic mixes in the laboratory. The phenomenological approach to fatigue is credited to Monismith (29-36), Pell (41-43) and others (5,7,18) in which the fatigue life of a flexible pavement, N_f, is related to the maximum tensile stress, σ, or tensile strain, ϵ, developed in the under-side of the bituminous layer by semi-empirical relations of the form:

$$N_f = c_1 \left(\frac{1}{\sigma} \right)^{m_1} \quad \text{for controlled stress tests} \qquad (1.1)$$

and

$$N_f = c_2 \left(\frac{1}{\epsilon} \right)^{m_2} \quad \text{for controlled strain tests} \qquad (1.2)$$

where c_1, c_2, m_1, m_2, are constants to be determined experimentally on simply-supported or cantilever beams using prescribed testing procedures.

According to these equations, for a repetitive loading of a controlled-stress nature, specimens with high initial moduli or stiffness tend to perform

*Underlined numbers in parentheses refer to the list of references.

most satisfactory. The reverse is true for controlled-strain fatigue experimentation. Therefore, the interpretation of the test results and the selection of mix characteristics required for pavement design are dependent upon the mode of loading. It has been argued (47) that since the constants c and m vary with the type of test and boundary conditions, they cannot be considered as true material constants.

Despite such inherent limitations, the phenomenological approach provides a reasonably simple procedure which has been universally adopted by various research organizations. In addition to the variations in the testing procedures such as recommended by Monismith et.al., phenomenological evaluation of bituminous concrete has also been carried out using different geometrical setups.

Bazin (2), Savin (50) and Coffman (5) have used trapezoidal-shaped cantilever beam samples in their laboratory investigations. Jiminez and Gallaway (18) used an apparatus designated as a "deflectometer" and a rotating bending fatigue machine has been used by Pell (41-43) in this study of asphaltic concrete fatigue.

Similarly, researchers have argued that for a better simulation of fatigue response of pavements in service, the mode of loading needs to be selected either as controlled stress or controlled strain depending upon the pavement thickness and other geometrical considerations (1). In controlled

stress or controlled load testing as represented by equation 1.1, the nominal stress or load is maintained constant throughout the duration of the test. If the nominal stress level is maintained constant, the testing is under the controlled strain or controlled deflection mode (see equation 1.2).

The available experimental results have indicated that the fatigue life of a given sample in controlled strain tests is usually higher than in controlled stress tests (28, 29, 30) when compared with the same initial nominal stress.

Most of the previous phenomenological investigations of fatigue response of asphaltic mixes have been carried out using simple loading histories, in which the maximum and minimum amplitudes of load or strain were constant for each cycle. Although this criterion has provided basic information regarding the mechanism of fatigue failure in a given sample, it is far from the true loads sustained by pavements in service. Compound loadings have also been attempted by Deacon and Monismith (7) to study their effects on fatigue response.

Frequency of load application in fatigue tests has also been considered as an important testing variable. Monismith, et.al. (27) reported that the frequency of load application in the range of 3.0 to 30.0 cycles per minute had no effect on the specimen's fatigue behavior. The subsequent work of Deacon and Monismith (7) has shown that the increase in the rate of loading significantly decreased the fracture life for the type of test employed at rates between 30 and 100 applications per minute.

Raithby and Sterling (42,43) have similarly shown that the rest periods between successive loading cycles have a beneficial effect on fatigue performance, both by increasing the resistance to cracking and by reducing the rate of loss of dynamic stiffness due to repeated loading. Rest periods on the order of one second increased the number of cycles to failure by a factor of upto 5, when compared with the life under continuous sinusoidal cyclic loading. The improvement in life was less at high temperatures; it also appeared to be influenced by the magnitude of the applied cyclic stress, although this effect was not clearly established. A comparison of fatigue performance under square, sinusoidal, and triangular wave forms indicated some significant differences, but these were small compared to the effects of rest periods. It should be noted that the effect of rest periods on the crack growth process has been recently investigated by Majidzadeh and Kauffmann (26) by testing beams on elastic founcations with rest periods of 0.0, 0.4 and 0.8 seconds. They reported that for such test conditions, there were no significant effects of rest periods on the crack growth process.

In summary, it should be pointed out that although the phenomenological approach has gained universal acceptance, it bears the limitation that it cannot take into account the crack initiation and propagation. Nor can it fulfill the mechanistic model representation of fatigue and fracture of bituminous or other paving materials.

To take into account the role played by crack propagation and the consequent redistribution of stresses within a layered pavement system, a mechanistic model was developed at Ohio State University (23), (27), (47) in the late 1960's. It was considered essential that the design strategy should incorporate the formation and development of failure mechanisms and describe such processes involved in terms of invariant material properties, loading, geometry and boundary conditions.

The mechanistic scheme is a rational strategy which utilizes the principles of fracture mechanics to explain the mechanism of damage, the progression of crack growth, and the prediction of the fatigue life of pavements. Such a design scheme, as shown in Figure 1, is based on the postulate that the fatigue life, N_f, can be described by the process of crack initiation, growth and ultimate fracture. The material parameters required for a detailed fatigue and fracture characterization are parameters associated with and identified by these three damage processes:

$$N_f = F\left[c_o, A, n, K, K_{IC}\right] \tag{1.3}$$

The parameter K_{IC} is the fracture toughness describing the final stages of crack propagation. The crack growth process, however, has been shown to be expressed in terms of A, n and K by either a simplified power law equation:

$$dc/dN = A\,K^n \tag{1.4}$$

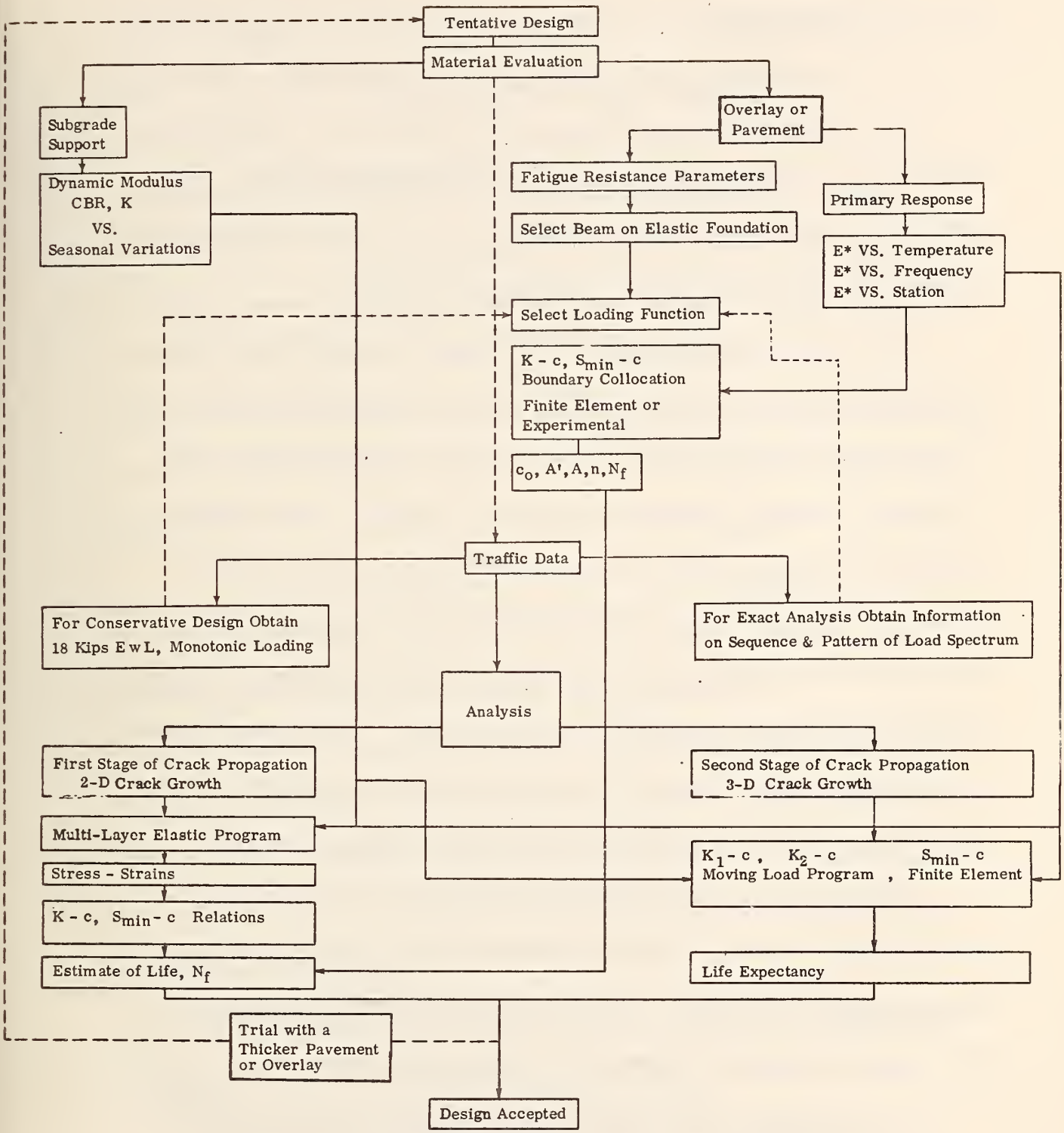

The Mechanistic-Fatigue Subsystem

Figure 1.1

or in a generalized form of

$$dc/dN = A_1 K^{n_1} + A_2 K^{n_2} + A_3 K^{n_3} \qquad (1.5)$$

where A_i , n_i = material constants and K = stress-intensity factor. The critical value of the stress-intensity factor, K_{IC}, is a material constant which describes the failure criterion for both fatigue and fracture.

The analysis of fatigue and fracture of pavement systems, using the mechanistic method, as shown in Figure 1, is a two-step process; that is, (i) the material characterization to obtain parameters describing the crack resistance of paving mixtures and (ii) solution of boundary-value problems to obtain an estimation of the stress-strain distribution within the layered system. The previous research at the Ohio State University (26) and the theoretical development of fracture mechanics at other institutions have provided various methods of solution for crack problems. The computer program and analysis procedures presented in research reports (26) (27) are typical of such analysis procedures available for the design of pavement systems.

With respect to material characterization task, the proposed mechanistic analysis procedure requires the determination of material constants affecting fatigue and fracture. It also requires the sensitivity analysis of these material constants as affected by pertinent testing variables.

As an example, the previous studies have indicated that the prediction of the fatigue life of pavements from laboratory tests is independent of the

mode of loading or specimen geometry. Failure by cracking is defined in terms of the stress-intensity factor and catastrophic failure by the critical stress-intensity factor. The results of these studies carried out at the Ohio State University have also indicated that the crack propagation law, in a more formalized form, is applicable to asphaltic mixtures tested in various geometries, boundary conditions, temperatures and modes of loading. The effect of random block loading and the levels of variable amplitude on the crack propagation has also been formulated (26). The mathematical models incorporating the effect of plastic yielding at crack tip locations have also been investigated. The results of these researches have led to the following general conclusions:

(i) The crack propagation model $dc/dN = A K^n$ satisfactorily explains the fatigue performance of bituminous material, the stress-intensity factor being the dominant parameter controlling the crack growth.

(ii) Theoretical solutions have been developed that accurately predict the stress distribution in cracked bodies and the stress-intensity factor for beams on elastic foundations, slabs on elastic foundation, etc. The agreement of theoretical stress-intensity factors and the experimental values have been found to be excellent.

(iii) The fatigue crack propagation process in bituminous materials is considered as a stress interaction type phenomenon.

(iv) For the range of variables investigated, it was found that the rest period has little or no effect on the fatigue life of pavements.

(v) The sequence of load application has a significant effect on the fatigue life of asphaltic materials, causing a delay in the rate of crack propagation.

(vi) The fatigue life of pavement slabs subjected to loads of variable amplitude can be predicted from tests on beams resting on an elastic solid.

(vii) The constant n in the power law $dc/dN = A\ K^n$ varies depending upon the material characteristics such as asphalt content, gradation, etc.

(viii) The mechanistic approach to predict cracking of flexible pavements is applicable in the range of temperatures from 41° to 90°F.

(ix) The critical stress-intensity factor, K_{IC}, is the failure criterion for low temperatures.

(x) The concepts of linear fracture mechanics can be used to predict the fatigue life of pavements by means of the analysis encompassed by the mechanistic approach. The application of this method to a typical flexible pavement has been demonstrated in previous studies (27,28).

To utilize this mechanistic model for pavement design purposes, it is required that the material characteristics responsible for the fracture and fatigue resistance of asphaltic mixtures to be determined in the laboratory under field simulated conditions. In this respect, therefore, this study has been aimed at the application of mechanistic concepts to optimization of mix

variables and improve the fatigue and fracture life of expectancy of the bituminous mixtures. To achieve such objectives, it should be demonstrated that fracture and fatigue principles are applicable to a variety of bituminous mixtures and can provide an estimate of the crack resistance characteristics of these materials. In addition, the analytical and experimental fracture mechanics to be used for mixture optimization must be simple enough to lend itself to routine material characterization and mix design purposes. It must also recognize the effects of variability in the material characteristics, such as aggregate size distribution, asphalt content, and other mixture variables. The scope of this study includes the following.

II. SCOPE

A. Selection of Testing and Analytical Procedures for Fracture Resistance

This phase of the study involves a detailed review of literature and preparation of a state of the art report of the applicability of fracture mechanics concepts to the evaluation of fatigue and fracture resistance characteristics of bituminous concrete materials.

It is also aimed at selecting the most promising existing laboratory testing procedures, modified as necessary, and to verify these procedures through laboratory testing of bituminous concrete mixtures. Consideration shall be given to the following items during verification: specimen type, size, geometry, and method of support; mixture type and maximum size of aggregate; and test temperature.

With respect to the testing temperature, the study will investigate the agreement between elastic and viscoelastic analysis at 77°F, to measure the effect of time dependent material response on fatigue crack propagation.

To evaluate the results and test procedures best suited for crack resistance studies, analytical techniques such as finite element, boundary collocation or other new and innovative techniques will be used to determine which test procedure best defines crack resistance.

B. Sensitivity of Various Mix Parameters and Evaluation of Formulations for Improvement of Fracture Resistance

This phase of the study involves the evaluation of the effect of asphalt source, consistency and amount, aggregate grading, type and maximum size; air-void content and type, and the amount of conventional fillers on the fracture-resistant qualities of the mixtures.

This phase will also include an evaluation of the effects of polymeric additives to the asphalt and the effects of admixtures such as asbestos, rubber, sulfur and synthetic constituents on fracture resistance.

C. Recommendations for Routine Mixture Design and Testing and Suggested Formulations for Fracture-Resistant Mixtures

It is the aim of the study to recommend a mixture design procedure that will enable optimization of fracture-resistant qualities of typical mixtures which can be used on a routine basis. Mixtures formulations required for

optimizing the fracture-resistant characteristics of typical mixtures will also be recommended using the results of the sensitivity analysis of mixtures variables as developed in Phase II.

PART I

LIST OF REFERENCES

1. Barksdale, Richard R., "Compressive Stress Pulse Times in Flexible Pavements for Use in Dynamic Testing," HRB Record 345, Highway Research Board, 1971.

2. Bazin, P. and Saunier, J. B., "Deformability, Fatigue and Healing Properties of Asphalt Mixes," Proceedings, Second International Conference on the Structural Design of Asphalt Pavements, University of Michigan, 1967.

3. Bosson, Geoffrey, "The Flexure of an Infinite Elastic Strip on an Elastic Foundation," Philosophical Magazine, Seventh Series, Vol. 27, 1939.

4. Cherpanov, Genady P. and Halmanov, H., "On the Theory of Fatigue Crack Growth," Engineering Fracture Mechanics, Pergamon Press, Great Britain, Vol. 4, pp. 219-230, 1972.

5. Coffman, Bonner S., and Ilves, George J., and Edwards, William F., "The Fatigue of Flexible Pavements," Engineering Experiment Station, The Ohio State University, Report EES 296B-1, February 1971.

6. Culley, R. W., "Relationship Between Hardening of Asphalt Cements and Transverse Cracking of Pavements in Saskatchewan," Proceedings, Association of Asphalt Paving Technologists, Vol. 38, 1969.

7. Deacon, J. A. and Monismith, C. L., "Laboratory Flexural-Fatigue Testing of Asphalt Concrete with Emphasis on Compound Loading Test," HRB Record 158, Highway Research Board, 1967.

8. Drennon, Clarence B. and Kenis, William J., "Response of a Flexible Pavement to Repetitive and Static Loads," HRB Record 337, Highway Research Board, 1970.

9. Epps, J. A. and Monismith, C. L., "Influence of Mixture Variables on the Flexural Fatigue Properties of Asphalt Concrete," Proceedings, Assoc. of Asphalt Paving Technologists, Vol. 38, 1969.

10. Gotolski, William H., et.al., "Study of Physical Factors Affecting Durability of Asphaltic Pavements," HRB Record 231, Highway Research Board, 1968.

11. Grumm, Fred J., "Designing Foundation Courses for Highway Pavements and Surfaces," California Highway and Public Works, Vol. 20, No. 3, March 1942.

12. Hetenyi, M., "Beams on Elastic Foundation," Ann Arbor, Michigan, University of Michigan Press, 1946.

13. Heukelom, W. and Klomp, A. J. G., "Road Design and Dynamic Loading," Proceedings, Association of Asphalt Paving Technologists, Vol. 33, 1964.

14. Heukelom, W. and Klomp, A. J. G., "Dynamic Testing as a Means of Controlling Pavements During and After Construction," Proceedings, First International Conference on Structural Design of Asphalt Pavements, University of Michigan, 1962.

15. Howeedy, M. Fayek, and Herrin, Moreland, "Behavior of Cold Mixes Under Repeated Compressive Loads," HRB Record 404, Highway Research Board, 1972.

16. Hveem, F. N., "Pavement Deflections and Fatigue Failures in Design and Testing of Flexible Pavements," HRB Bulletin 114, Highway Research Board, 1955.

17. Irwin, G. R., "Fracture Mechanics," Structural Mechanics, Proceedings First Naval Symposium, Pergamon Press, New York, 1960.

18. Jimenez, R. A. and Gallaway, B. M., "Behavior of Asphaltic Concrete Diaphragms to Repeated Loadings," Proceedings, First International Conference on the Structural Design of Asphalt Pavements, University of Michigan, 1962.

19. Kirk, J. M., "Relations Between Mix Design and Fatigue Properties of Asphaltic Concrete," Proceedings, Third International Conference on the Structural Design of Asphalt Pavements, University of Michigan, 1972.

20. Layman, A. H. and Phillips, S. W., "A Study of the Flexural Properties of Certain Black Base Mixtures," Proceedings, Association of Asphalt Paving Technologists, Vol. 38, 1969.

21. Lee, Dah-Yinn, "Development of a Laboratory Durability Test for Asphalts," HRB Record 231, Highway Research Board, 1968.

22. Majidzadeh, K., Kauffman, E. M., and Saraf, C. L., "Analysis of Fatigue of Paving Mixtures from the Fracture Mechanics Viewpoint," Fatigue of Compacted Bituminous Aggregate Mixtures, ASTM STP 508, American Society for Testing and Materials, 1972.

23. Majidzadeh, K., Ransamooj, D. V., and Fletcher, T. A., "Analysis of Fatigue of a Sand Asphalt Mixture," Proceedings, Association of Asphalt Paving Technologists, Vol. 30, 1969.

24. Majidzadeh, K., Chan, A. T., and Ramsamooj, D. V., "Fatigue and Fracture of Bituminous Paving Mixtures," Annual Meeting of the Highway Research Board, January, 1970.

25. Majidzadeh, K. and Kauffmann, E. M., "Analysis of Fatigue and Fracture of Bituminous Paving Mixtures-Phase II," The Ohio State University Research Foundation Final Report, Project RF 2845, September 1971.

26. Majidzadeh, K., Kauffman, E. M., and Chang, C. W., "Verification of Fracture Mechanics Concepts to Predict Cracking of Flexible Pavements," The Ohio State University Research Foundation Final Report, Project RF 3200, June 1973.

27. Majidzadeh, K. and Ramsamooj, D. V., "Development of Testing Procedures and a Method to Predict Fatigue Failures of Asphalt Concrete Pavement Systems," The Ohio State University Research Foundation Final Report, Project RF 2873, March 1971.

28. Mendelson, Alexander, "Plasticity: Theory and Application," The MacMillan Company, New York, 1968.

29. Monismith, C. L., "Flexibility Characteristics of Asphaltic Paving Mixtures," Proceedings, Association of Asphalt Paving Technologists, Vol. 27, 1958.

30. Monismith, C. L., Secor, K. E., and Blackmer, E. W., "Asphalt Mixture Behavior in Repeated Flexure," Proceedings, Association of Asphalt Paving Technologists, Vol. 30, 1961.

31. Monismith, C. L., "Asphalt Mixture Behavior in Repeated Flexure," Report No. TE 64-2, University of California, Berkeley, 1964.

32. Monismith, C. L., "Asphalt Mixture Behavior in Repeated Flexure," Report No. TE 65-9, University of California, Berkeley, 1965.

33. Monismith, C. L., "Asphalt Mixture Behavior in Repeated Flexure," Report No. TE 66-6, University of California, Berkeley, 1966.

34. Monismith, C. L., "Asphalt Mixture Behavior in Repeated Flexure," Report No. TE 67-4, University of California, Berkeley, 1967.

35. Monismith, C. L., Epps, J. A., and Kasianchuk, D. A., "Asphalt Mixture Behavior in Repeated Flexure," Report No. TE 68-8, University of California, Berkeley, 1968.

36. Monismith, C. L., and Epps, J. A., "Asphalt Mixture Behavior in Repeated Flexure," Report No. TE 69-6, University of California, Berkeley, 1969.

37. Moore, Raymond K., and Kennedy, Thomas W., "Tensile Behavior of Asphalt Treated Materials Under Repeated Loadings," Proceedings, Third International Conference on the Structural Design of Asphalt Pavements," University of Michigan, 1967.

38. Paris, Paul C., and Sih, George C., "Stress Analysis of Cracks," Fracture Toughness Testing and Its Applications, ASTM STP 381, American Society for Testing and Materials, 1965.

39. Paris, P., and Erdogan, F. J., "A Critical Analysis of Crack Propagation Laws," Journal of Basic Engineering, Transaction of ASME, Series D, Vol. 85, 1963.

40. Paris, Paul C., "The Fracture Mechanics Approach to Fatigue," Fatigue-An Interdisciplinary Approach, Proceedings, 10th Sagamore Army Materials Research Conference, Syracuse University Press, 1964.

41. Pell, P. S. and Taylor, I. F., "Asphalt Road Materials in Fatigue," Proceedings, Association of Asphalt Paving Technologists, Vol. 38, 1969.

42. Pell, P. S., "Fatigue Characteristics of Bitumen and Bituminous Mixes," Proceedings, First International Conference on the Structural Design of Asphalt Pavements, University of Michigan, 1962.

43. Pell, P. S., "Fatigue of Asphalt Pavement Mixes," Proceedings, Second International Conference on the Structural Design of Asphalt Pavements, University of Michigan, 1967.

44. Porter, O. J., "Foundations for Flexible Pavements," Proceedings, Highway Research Board, Vol. 22, 1942.

45. Raithby, K. D. and Sterling, A. B., "The Effect of Rest Periods of Fatigue Performance of a Hot Rolled Asphalt Under Reversed Axial Loading," Proceedings, Association of Asphalt Paving Technologists, Vol. 39, 1970.

46. Raithby, K. D., and Sterling, A. B., "Some Effects of Loading History on the Fatigue Performance of Rolled Asphalt," Great Britain, Transport and Road Research Laboratory, TRRL Report LR 496, 1972.

47. Ramsamooj, D. V., "Analysis and Design of the Flexibility of Pavements," Ph.D. Thesis, The Ohio State University, 1970.

48. Santucci, L. E., and Schmidt, R. J., "The Effect of Asphalt Properties on the Fatigue Resistance of Asphalt Paving Mixtures," Proceedings, Association of Asphalt Paving Technologists, Vol. 38, 1969.

49. Saraf, Chhote Lal, "Effect of Mix Variables on the Fatigue Response of Asphaltic Mixes," Ph.D. Dissertation, The Ohio State University, 1973.

50. Savin, G. N., "Stress Concentration Around Holes," Pergamon Press, New York, 1961.

51. Sisko, A. W., "Tensile Strength of Asphalt Films and Road Life," HRB Record 231, Highway Research Board, 1968.

52. Srawley, John E., "Plane-Strain Fracture Toughness," Fracture, An Advanced Treatise, edited by Liebowitz, H., Vol. IV, Chapter 2, 1969.

53. Taylor, I. F., "Asphaltic Road Materials in Fatigue," Thesis, University of Nottingham, October 1968.

54. Tetelman, A. S., and McEvily, A. J., "Fracture of Structural Materials," John Wiley and Sons, Inc., New York, 1967.

55. Vallerga, B. A., Finn, F. N. and Hicks, R. G., "Effects of Asphalt Aging on the Fatigue Properties of Asphalt Concrete," Proceedings, Second International Conference on the Structural Design of Asphalt Pavements," University of Michigan, 1967.

56. Vallerga, B. A., and Halstead, W. T., "Effects of Field Aging on Fundamental Properties of Paving Asphalts," HRB Record 361, Highway Research Board, 1971.

57. VanDijk, W., Quedeville, A., and Uge, P., "The Fatigue of Bitumen and Bituminous Mixes," Proceedings, Third International Conference on the Structural Design of Asphalt Pavements, University of Michigan, 1972.

58. Walker, Richard D., et.al., "Significance of Layer Deflection Measurements," HRB Bulletin 321, Highway Research Board, 1962.

59. Westergaard, H. M., "Bearing Pressures and Cracks," Journal of Applied Mechanics, Transactions ASME, Vol. 61, 1939, pp. A-49-A-53.

60. Zube, E., and Skog, J., "Final Report on the Zaca-Wigmore Asphalt Test Road," Proceedings, Association of Asphalt Paving Technologists.

PART II. A STATE-OF-THE-ART REVIEW

I. FRACTURE MECHANICS

A. A General Review

One of the important aspects of modern structural analysis is the selection of a criterion of failure which could provide an accurate estimate of factors affecting failure. The traditional design criterion often does not account for the existence of flaws and inherent defects causing premature structural distress. The classical approach, which is based on the selection of a limiting applied stress as compared with the material yield stress, σ_y, might not always guarantee a fail-safe design strategy.

It has been shown that the theoretical strength of materials which depends on the forces of molecular cohesion are many-fold larger than actual observed values of strength. It is obvious that material defects, imperfections within the crystalline structures, and other forms of flaws resulting from manufacturing and handling are responsible for such a discrepancy. The existence of such flaws as joints, cracks, etc., cause a redistribution of stresses and stress concentration in the vicinity of structural discontinuities. The high elevation of stresses at such localized regions of the body can often result in catastrophic failure of the structure, even at normal stress levels much less than the yield strength of the material.

To account for such discrepancies between the observed and theoretical failure limits, a classical theory of fracture mechanics has been set forth to provide a rational and refined analysis of the degradation of the strength due to inherent flaws. In brief, in the fracture mechanics approach, the existence of flaws are assumed to be responsible for the elevation of stresses at crack tip locations. When the applied load is increased, the stresses around the flaws reach a limiting value and fracture becomes possible.

The basis of linear fracture mechanics is the paper by Griffith (13) which was unrecognized for thirty years. In 1920, Griffith proposed that brittle bodies fail because of the presence of numerous internal cracks or flaws which produce local stress concentrations. He also stated that the elastic body under stress must transfer from an unbroken to a broken state by a process during which a decrease in potential (elastic) energy takes place. He postulated that fracture instability is reached when the increase in free surface energy (surface tension), caused by the extension of the crack, is balanced by the release of elastic-strain energy in the volume surrounding the crack. The Griffith equation for propagation of an internal crack of length $2c$ in an infinite thin plate under a uniform stress, σ, normal to the plane of the crack, is:

$$\sigma^2 \geq \frac{(2\gamma)\, E}{\pi c} \tag{2.1}$$

where γ = the specific surface energy

E = the modulus of elasticity

c = crack length.

In many engineering materials such as ceramics and glass, fracture occurs with hardly any deformation. However, in metals and other engineering materials, plastic deformation always takes place, and Griffith's classical surface tension concept is not suitable. Both Orowan (52, 53) and Irwin (17, 18, 19) independently came to the conclusion that the slight plastic flow which occurs in the brittle-fracture case, absorbs a large amount of additional energy required to create new surfaces.

Mathematically, Griffith's criteria for crack propagation is:

$$\delta U \geq \delta U_{ST} \tag{2.2}$$

where δU is the decrease in potential energy due to increased crack surface,

δU_{ST} is the increase in surface energy due to increased crack surface.

Irwin's criteria for crack propagation can be represented as:

$$\delta U \geq \delta U_{ST} + \delta U_{PL} \tag{2.3}$$

where δU_{PL} is the plastic energy dissipated due to increased crack surface.

Irwin recognized that the plastic energy dissipated is much larger than the surface energy dissipated and therefore, proposed to ignore the latter.

The terms above involving increase in energy quantities are evaluated with respect to the increased crack surface δA and hence, the change in energies could be referred to as rates of energy input or dissipation.

The theory by Griffith on energy balance and its subsequent modification by Irwin and Orowan are necessary conditions for the onset of fracture. As such, this theory cannot conveniently characterize all types of fracture observed in fracture tests. Irwin thus proposed that the local stress field surrounding the crack tip be used in place of the total input-output energy rate for such characterizations.

The relationship between δU_σ, the input energy rate, and the local stress field can be obtained by considering the situation where a short segment, δx, of a two-dimensional crack is closed by imposing a force, $\sigma^*_{yy}(-\delta x, 0)$, on the crack surface as shown in Figure 2.1 (21)(32). The total strain-energy absorption rate in this reverse-loading problem is equal to δU_σ, which in turn is equal to the strain-energy release rate, G, for a crack extension of δx, or

$$\delta U_\sigma = G \cdot \delta x = \int_0^{\delta x} u_y(0,0) \cdot \sigma^*_{yy}(-\delta x, 0)\, dx \qquad (2.4)$$

where $u_y(0, 0)$ is the crack closing displacement when the crack closes from the origin of the x-y coordinate for a length of δx.

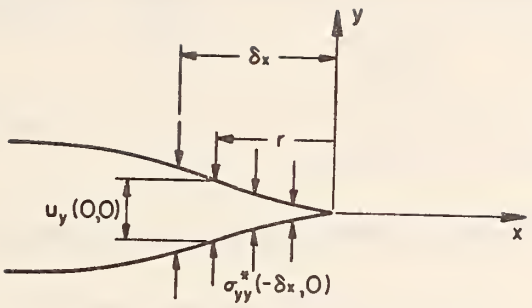

Figure 2.1. Closing of a Crack Tip

It can be assumed further that the plastically yielded region ahead of the crack tip does not change the state of stress significantly. As a result, $u_y(0,0)$ and $\sigma^*_{yy}(-\delta x,0)$ can be obtained by the elastic stresses and elastic displacements obtained through the known elastic state in the vicinity of the crack tip. In particular, $u_y(0,0)$ is the crack-closing displacement with the crack tip located at the origin of the coordinates $(0,0)$ and $\sigma^*_{yy}(-\delta x,0)$ is the associated closing stress which is equal to the normal stress ahead of the crack tip located at $(-\delta x,0)$. Therefore, all problems in linear fracture mechanics can now be converted to problems in linear elasticity for which solutions are possible.

It is also shown that all linear elastic solutions to problems involving cracks in homogeneous, isotropic material show an inverse square root dependency of the crack tip singularity.

Considering the "Mode I" crack tip deformation problem, as shown in Figure (2.1), Westergaard's stress function, frequently used to solve two-dimensional problems in cracked structures in the vicinity of the crack tip, is:

$$Z_1 = \frac{f(\rho)}{\sqrt{\rho}} \tag{2.5}$$

where $\rho = re^{i\theta}$ (in polar coordinates.

As $\rho \longrightarrow 0$, however, the complex analytical function, $f(\rho)$, approaches a real constant, $\frac{K_I}{\sqrt{2\pi}}$, where K_I is the opening mode of stress-intensity factor and is defined as:

$$K_I = \lim_{r \to 0} \sigma_{yy}(r, \theta = 0) \cdot \sqrt{2\pi r} \tag{2.6}$$

The local stresses in terms of local coordinates for Mode I fracture are:

$$\begin{Bmatrix} \sigma_{xx} \\ \sigma_{yy} \\ \sigma_{xy} \end{Bmatrix} = \frac{K_I}{\sqrt{2\pi r}} \cos\frac{\theta}{2} \begin{Bmatrix} 1 - \sin\frac{\theta}{2} \sin\frac{3\theta}{2} \\ 1 + \sin\frac{\theta}{2} \sin\frac{3\theta}{2} \\ \sin\frac{\theta}{2} \cos\frac{3\theta}{2} \end{Bmatrix} \tag{2.7}$$

Similarly, the local displacement components in the x and y directions, u_x and u_y, can be expressed in terms of K_I as;

$$\begin{Bmatrix} u_x \\ u_y \end{Bmatrix} = \frac{(1+\nu)}{\sqrt{2\pi}\ E} K_I\, r^{\frac{1}{2}} \begin{Bmatrix} \cos\frac{\theta}{2}\left(\chi - 1 - 2\sin^2\frac{\theta}{2}\right) \\ \sin\frac{\theta}{2}\left(\chi + 1 - 2\cos^2\frac{\theta}{2}\right) \end{Bmatrix} \tag{2.8}$$

where $\chi = 3 - 4\nu$ for plane strain

$= (3 - \nu)/(1 + \nu)$ for plane stress

ν = Poisson's ratio

E = the modulus of elasticity.

The substitution of $\theta = \pi$ in Eq. (2.8) gives $u_x = 0$ and

$$u_y(0,0) = \frac{(1+\nu)\, r^{\frac{1}{2}}}{\sqrt{2\pi}\ E} \cdot K_I (\chi + 1) \tag{2.9}$$

or

$$u_y(0,0) = \frac{4(1-\nu^2)}{\sqrt{2\pi}\ E}\ r^{\frac{1}{2}}\ K_I \text{ for plane strain} \tag{2.10a}$$

and

$$u_y(0,0) = \frac{4}{\sqrt{2\pi}\ E}\ r^{\frac{1}{2}}\ K_I \text{ for plane stress} \tag{2.10b}$$

The imposing stress $\overset{*}{\sigma}_{yy}(-\delta x, 0)$ is obtained by shifting the origin in Figure (2.1) from (0,0) to $(-\delta x, 0)$ and evaluating σ_{yy} in Eq. (2.7b) for $r = \delta x - r$, $\theta = 0$. This gives,

$$\overset{*}{\sigma}_{yy}(-\delta x, 0) = \frac{K_I}{\sqrt{2\pi}\ (\delta x - r)} \tag{2.11}$$

The strain-energy release rate due to a crack extension of δx in a state of plane strain is then given by

$$\delta U_\sigma = G_I\ \delta x = \frac{2(1-\nu^2)}{\pi E} \cdot K_I^2 \int_0^{\delta x} \left(\frac{r}{\delta x - r}\right)^{\frac{1}{2}} dr \tag{2.12}$$

which upon substitution $r = \delta x \sin^2$ and evaluation of the integral gives

$$G_I\ \delta x = \frac{(1-\nu^2)}{E}\ K_I^2 \cdot \delta x$$

or

$$G_I = \frac{(1-\nu^2)}{E}\ K_I^2 \quad \text{(plane strain)} \tag{2.13}$$

For a plane stress condition, a similar relation can be obtained by simply substitute Eq. (2.10b) instead of Eq. (2.10a) in Eq. (2.4). This gives $G_I = K_I^2/E$ for plane stress. The subscript I denotes the opening mode fracture.

At the onset of fracture, the elastic energy release rate, following the Griffith-Irwin theory, can be replaced by an equivalent material constant designated by the critical strain-energy-release rate or G_{IC}. Since the stress intensity factor is directly related to G_I, the Griffith-Irwin theory can also

be restated in terms of the stress-intensity factor, K_I, which becomes a material constant K_{IC} at the onset of rapid fracture. This critical stress-intensity factor, K_{IC}, is referred to as the fracture toughness of the material and has the dimensions of (stress $\cdot$ $\sqrt{\text{length}}$) .

With regard to a general state of fracture in which in-plane sliding (Mode II) and tearing (Mode III) are present (Figure 2.2), the stress distribution at the end of cracks can be written as:

$$\sigma_{ij} = r^{-\frac{1}{2}} \left[K_I f_{ij}^{I}(\theta) + K_{II} f_{ij}^{II}(\theta) + K_{III} f_{ij}^{III}(\theta) \right] \qquad (2.14)$$
$$+ \text{ other nonsingular terms.}$$

where r, θ are polar coordinates introduced at the crack tip (Figure 2.3)

K_I, K_{II}, K_{III} and corresponding symbols I, II, and III reflect three modes of fracture.

As was pointed out, the terminal state of fracture can be represented by the critical value of stress-intensity as designated by K_{IC}. The interrelation of Irwin's stress intensity factor K_I and Griffith's energy release rate G_I are represented in Equation (2.13). Although similar relations between G_{II} and K_{II} , and K_{III} and G_{III} can also be written, the physical meanings of K_{IIC} and K_{IIIC} have not been well-defined. Therefore, the Mode I fractures have remained a significant method of analysis. The Mode I critical stress-intensity factor, K_{IC}, as designated by fracture toughness, has also been considered as an important engineering tool which provides the designer with an additional material parameter for crack resistance evaluation.

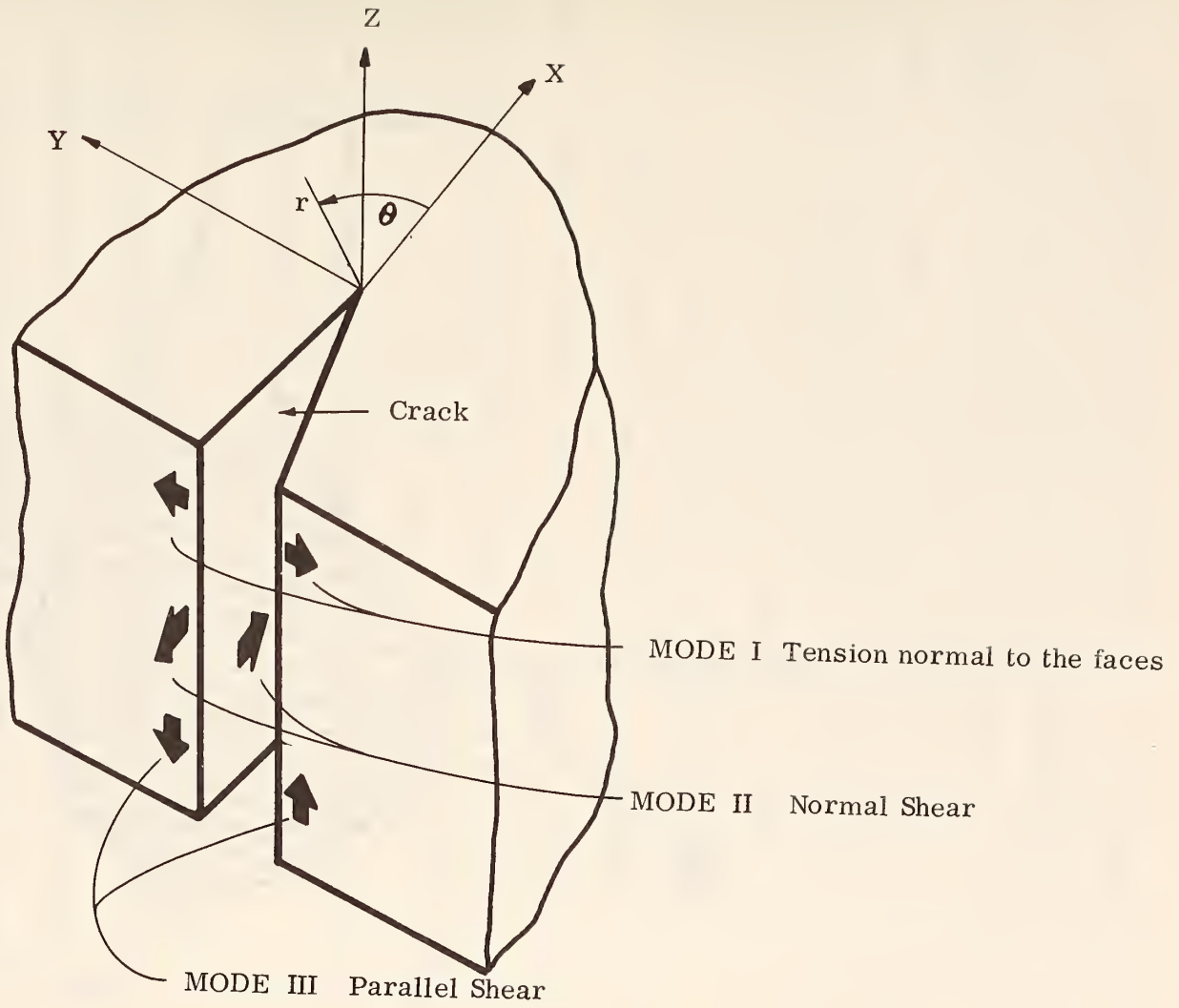

Figure 2.2. Modes of Deformation of a Crack

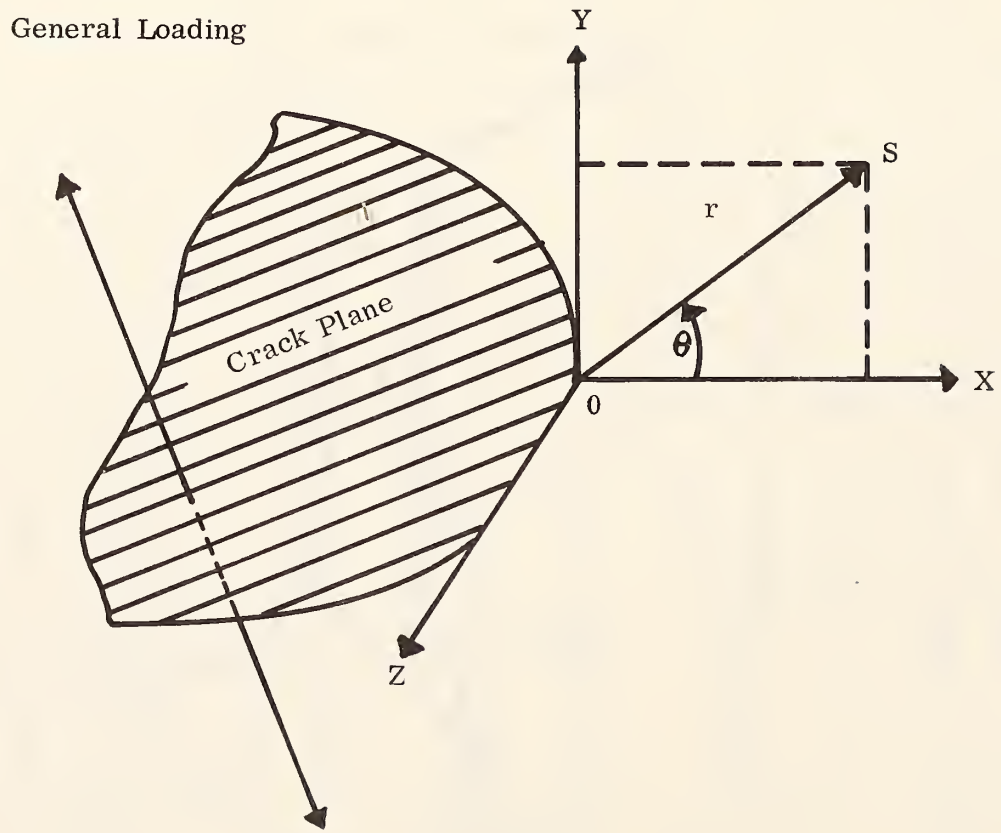

Figure 2.3. Director Theory (70)

The difference between K_I and K_{IC} terms is quite significant and should be clearly understood. The term K_I, or a stress-intensity factor, is determined analytically and is a function of load, geometry and crack size. Hence, the analytical form and the magnitude of K_I varies from one system to another, depending on load and geometrical variables. On the other hand, the fracture toughness, K_{IC}, is a material constant, independent of crack geometry, loading conditions and other physical variables and is analogous to strength.

It should be noted that the K_C concept is primarily restricted to laboratory and material characterizations where the Mode I fracture is applicable. That is, the Griffith-Irwin theory is, in fact, a scalar theory, in that only the critical values of a scalar G_{IC} and/or K_{IC} are known (73). The direction of crack propagation is assumed to be normal to the load and the crack front must be straight (Figure 2.4).

In reality, however, in most structural components the flaws and cracks are seldom aligned perpendicular to the direction of load. Such a deviation invalidates the classical K_C theory of fracture, in which cracks must always be normal to applied tensile stress. As a departure from this classical theory, Sih (73) has presented a theory of fracture based on the field strength of the local strain-energy-density. This theory has the inherent advantage of being capable of treating all mixed mode fracture. The mixed mode fracture analysis is of particular interest in the study of bituminous materials. It has been shown that for mixtures with large size aggregate, when tested as a beam on elastic foundation or in real pavement systems, the crack surface follows a

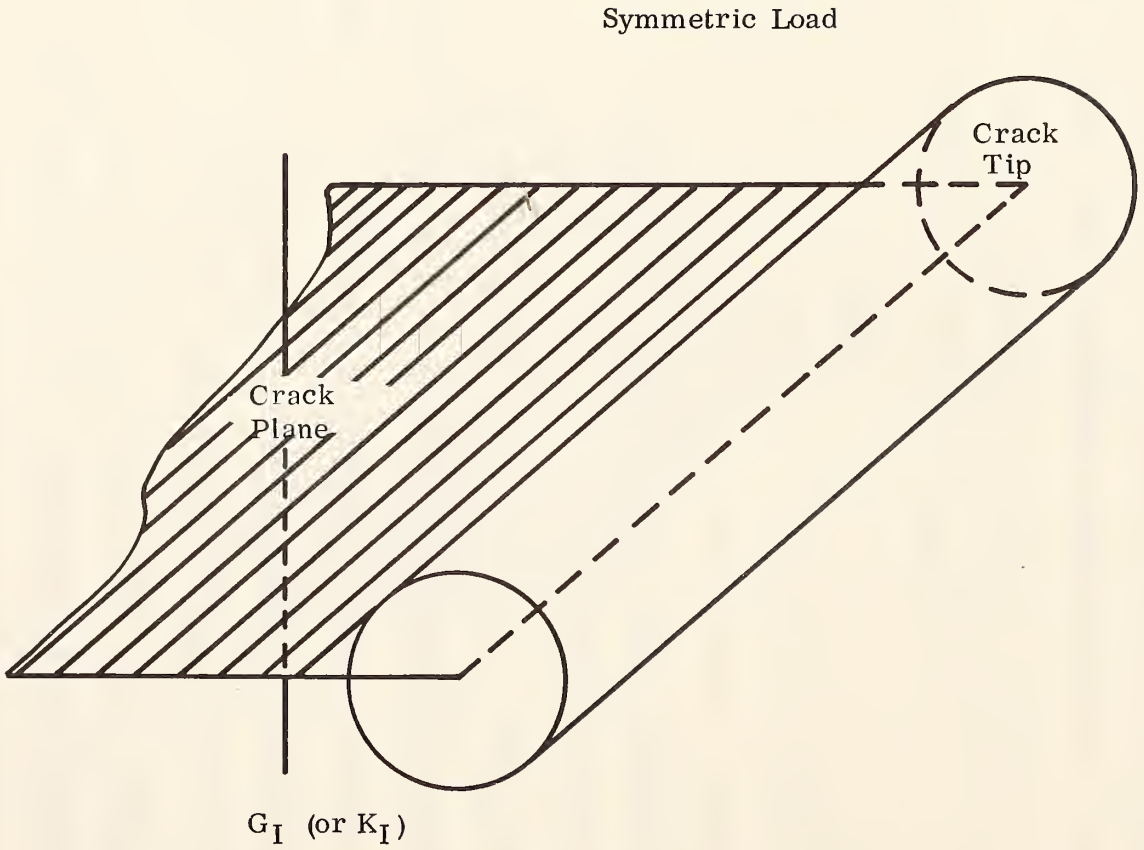

Figure 2.4 Griffith Theory

zig-zag pattern and as a result, the stress component σ_{yy} responsible for the crack growth would no longer remain perpendicular to the crack surface.

Under such conditions, the stress state ahead of the crack will be governed by at least two stress-intensity factors (K_I and K_{II}) instead of a simple parameter, K_I. The elastic stress distribution at the crack tip can be written as:

$$\sigma_{xx} = \frac{K_1}{\sqrt{2r}} \cos\frac{\theta}{2}\left(1 - \sin\frac{\theta}{2}\sin\frac{3\theta}{2}\right) - \frac{K_2}{\sqrt{2r}}\sin\frac{\theta}{2}\left(2 + \cos\frac{\theta}{2}\cos\frac{3\theta}{2}\right)$$

$$\sigma_{xy} = \frac{K_1}{\sqrt{2r}}\cos\frac{\theta}{2}\left(1 + \sin\frac{\theta}{2}\sin\frac{3\theta}{2}\right) + \frac{K_2}{\sqrt{2r}}\sin\frac{\theta}{2}\cos\frac{\theta}{2}\cos\frac{3\theta}{2}$$

$$\tau_{xy} = \frac{K_1}{\sqrt{2r}}\cos\frac{\theta}{2}\sin\frac{\theta}{2}\cos\frac{3\theta}{2} + \frac{K_2}{\sqrt{2r}}\cos\frac{\theta}{2}\left(1 - \sin\frac{\theta}{2}\sin\frac{3\theta}{2}\right)$$

(2.15)

where $K_1 = K_I\sqrt{\pi}$

$K_2 = K_{II}\sqrt{\pi}$

Under such a state of stress, the failure condition can be evaluated using the energy concept. Considering that strain energy of the system in the crack vicinity, ϕ, can be expressed in terms of stresses, for an element $r\,\Delta\,\theta$, Δr ahead of the crack tip, the strain energy function is (Figure 2.3).

$$\frac{d\phi}{dA} = \frac{1+\nu}{2E}\left[\sigma_{xx}^2 + \sigma_{yy}^2 - \frac{\nu}{1+\nu}(\sigma_{xx} + \sigma_{yy})^2 + 2\tau_{xy}^2\right]$$

(2.16)

Then, by inserting the stress components from the previous equation (2.15),

$$\frac{d\phi}{dA} = \frac{1}{r} \left[A_{11} K_1^2 + A_{22} K_2^2 + 2A_{12} K_1 K_2 \right] \tag{2.17}$$

where the term in the bracket is defined as strain-energy-density factor S,

$$S = A_{11}K_1^2 + A_{22}K_2^2 + 2A_{12}K_1K_2 \tag{2.18}$$

A_{11}, A_{12} and A_{22} are constants related to the elastic parameters and element direction as given by:

$$A_{11} = \frac{1+\nu}{8E} \left[(3 - 4\nu - \cos\theta)(1 + \cos\theta) \right]$$

$$A_{12} = \frac{1+\nu}{4E} \sin\theta \left[\cos\theta - (1 - 2\nu) \right] \tag{2.19}$$

$$A_{22} = \frac{1+\nu}{8E} \left[4(1 - \nu)(1 - \cos\theta) + (1 + \cos\theta)(3\cos\theta - 1) \right]$$

For the condition that all three modes of fracture are present, S is written as:

$$S = A_{11}K_1^2 + A_{22}K_2^2 + A_{33}K_3^2 + 2A_{12}K_1K_2 \tag{2.20}$$

where $A_{33} = \frac{1+\nu}{2E}$

If the loading condition and crack propagation is such that Mode I analysis applies, then:

or $$S = \frac{(1+\nu)(1-2\nu)}{2\pi E} K_I^2 \tag{2.21}$$

When unstable crack extension or failure occurs, the parameter S approaches its critical value, given by S_c:

$$S_c = \frac{(1+\nu)(1-2\nu)}{2\pi E} K_{IC}^2 \tag{2.22}$$

where in this case, S_c is a material constant.

Under an in-plane shear condition, where only the Mode II fracture is possible, the local stress field contains K_2 ($K_2 = K_{II}/\sqrt{\pi}$) alone, and the strain-energy-density is written as:

$$S = \frac{1+\nu}{8\pi E} \left[4(1-\nu)(1-\cos\theta) + (1+\cos\theta)(3\cos\theta - 1) \right] K_{II}^2 \tag{2.23}$$

where $K_{II} = \tau\sqrt{\pi c}$

in which τ is applied shear stress and c is the crack length. At the point of crack instability, Sih has shown that

$$S_c = \frac{(1+\nu)}{6E} \left[2(1-\nu) - \nu^2 \right] \cdot \tau_c^2 \, c \tag{2.24}$$

$$S_c = \frac{(1+\nu)}{6\pi E} \left[2(1-\nu) - \nu^2 \right] \cdot K_{IIC}^2 \tag{2.25}$$

Since S_c is a material constant, it can be argued that Equation (2.24) and Equation (2.25) must be equal; and thus setting these equations equal to each other and solving for K_{IIC}^2 ,

$$K_{IIC}^2 = \frac{3\,(1 - 2\nu)}{\left[2\,(1 - \nu) - \nu^2\right]} \cdot K_{I.C}^2 \qquad (2.26)$$

A similar relation can be developed between K_{IC} and K_{IIIC} , when considering the Mode III fracture process.

The preceding relations are derived from Sih's multi-model fractum concept which is based upon the postulation that crack spread occurs in the direction of maximum potential energy density of the system. Considering the potential energy is equal to the negative of the strain energy S, therefore the necessary and sufficient condition for crack growth is the minimum of the strain density,S. The angle $\theta = \theta_0$, which makes S a minimum, determines the angle at which the crack propagates. That is, the crack initiation occurs in a direction determined by the stationary value of:

$$\frac{\partial S}{\partial \theta} = 0 \quad \text{when} \quad \theta = \theta_0 \qquad (2.27)$$

The strain energy density factor, S, can be resolved into two components, one responsible for the change of shape as S_d and/or the change in volume S_v, that is:

$$S = S_d + S_v \qquad (2.29)$$

The crack initiation occurs under conditions of S_{min} for which Sih (73) has shown that fracture occurs along the plane where $S_v > S_d$. On the other hand, the direction $\theta_0 = \cos^{-1}(1-2\nu)$ along which S_{max} occurs (Mode I only), corresponds to maximum yielding on the large dimension of the plastic zone.

For the analysis of fracture problems involving large plastic deformations, the deformation theory of plasticity has been used by Rice (66),(67) to arrive at a parameter needed for characterization of crack tip area. The path independent J integral is a parameter, the value of which depends on the near tip stress-strain field. The path independency of J integral has been shown to be valid for linear, non-linear elastic, and plastic materials under monotonic loading condition. The basis of this formulation is that the path-independent nature of the integral allows integration to be carried out along the path away from the crack tip instead of along a region close to the tip.

The J integral is defined as:

$$J = \int_{\Gamma} W\,dy - T\left(\frac{\partial u}{\partial x}\right) ds \qquad (2.30)$$

where Γ is any contour surrounding a crack tip, W is strain energy density (Fig. 2.5):

$$W = \int_{0}^{\epsilon_{mn}} \sigma_{ij}\, d\,\epsilon_{ij} \qquad (2.31)$$

u, displacement vector, T, traction vector, defined by the outward normal to the contour. Rice (66) has pointed out that the crack tip deformation and

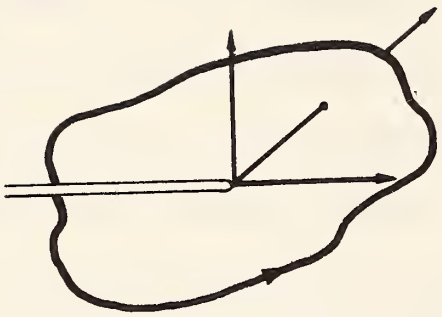

Figure 2.5. Crack Tip Coordinate System and Arbitrary Line Integral Contour

energy conditions are reflected by the J integral. The J integral might be interpreted as the potential energy difference between two identically loaded bodies having neighboring crack size c and $c + \Delta c$. That is,

$$J = -\frac{dU}{dc} \tag{2.32}$$

where U is the potential energy, and c is the crack length. In analogy with the linear crack fracture mechanics, the area between two monotonic load-deflection curves (Fig. 2.6) for cracks of c and $c + \Delta c$ is defined as Area = OABO. That is, J can be determined from experimental load-deflection curves of varying initial crack length. It should be noted that since the deformation theory of plasticity does not permit unloading conditions, the J integral is only applicable to crack initiation rather than crack propagation.

For a linear elastic case, J is identical to G, the energy release rate, and may be expressed as

$$J = G = \frac{P^2}{2B} \cdot \frac{\partial L}{\partial c} = \frac{K^2}{E'} \tag{2.33}$$

where P = applied load
B = width of the material
L = material compliance
c = crack length
E' = E for plane stress and $E/(1 - \nu^2)$ for plane strain.

For a rigid-plastic material, the deformation or displacement Δ is unlimited at the limit load, $P = P_L$, whereas for $P < P_L$, $\Delta = 0$. In this case J is given by

$$J = \frac{\Delta}{B} \cdot \frac{\partial P_L}{\partial c} \tag{2.34}$$

where the derivative $\partial P_L / \partial c$ can be evaluated experimentally. The J

ΔU = Potential energy difference between cracks of lengths c and $c + \Delta c$

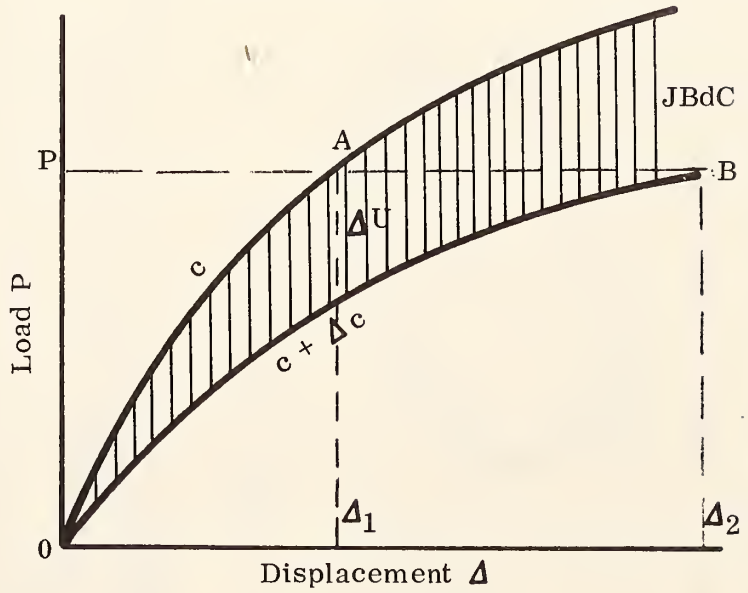

Figure 2.6. Load-Displacement for Two Identically Loaded Cracked Bodies

integral, therefore, can be used as a parameter required for characterization of crack tip problems in both linear and non-linear systems.

B. Crack Tip Stress Analysis For Pavements

From the viewpoint of design and analysis of pavement layered systems, the Mode I as well as mixed mode fractures have been found to be of great utilization. The Mode I fracture, or K-Theory, is primarily applicable to fatigue and fracture analysis of laboratory specimens as well as design of flexible layered systems. The Multi-Modal fracture, on the other hand, can be used to study the crack propagation in composite pavements, continuously reinforced concrete and development of overlay design strategies.

The opening mode (Mode I) or bending mode fracture has been used extensively to study the fatigue and fracture characterization of asphaltic mixtures. The research works at The Ohio State University, on the mechanistic modeling of fatigue process of flexible pavements, have been primarily concerned with the laboratory analysis of Mode I fracture involving the use of asphaltic beams or slabs resting on elastic foundation.

The basic step in such a method of analysis is the development of an interrelation between Irwin's local stress-intensity factor, K, and the crack size, c. A normalized (K/P - c/d) relation can then be used to investigate the crack propagation process of laboratory specimens subjected to bending mode fatigue loading.

Experimentally, the K-c relation can be determined for different types of loading and for any geometrical and crack patterns by a simple compliance measurement technique. According to this procedure, the compliance L, crack length c, and the rate of change of compliance with crack length ($\partial L / \partial c$ versus c) can be determined experimentally using prenotched specimens. Then the relation of the stress-intensity factor with the $\partial L/\partial c$ compliance can be represented by:

$$K/P = \sqrt{\frac{E}{2(1-\nu^2)} \cdot \frac{\partial L}{\partial c}} \qquad (2.35)$$

where P = applied load

E = Young's modulus

ν = Poisson's ratio

L = compliance or inverse slope up the load/deflection diagram

c = crack length

K = opening mode stress-intensity factor.

Such a procedure has been employed by Majidzadeh, et al., (33) (34) (35), for both beam on elastic foundation and slab supported on elastic foundation. In Figures (2.7) and (2.8), the normalized compliance L/L_o relations for asphaltic beams on elastic foundation and compliance L for pavement slabs resting on elastic support are presented. The comparisons of the K/P - c relations developed using experimental compliance procedures and numerical techniques, boundary collocation and finite elements for beam on elastic foundation, are presented in Figure (2.9).

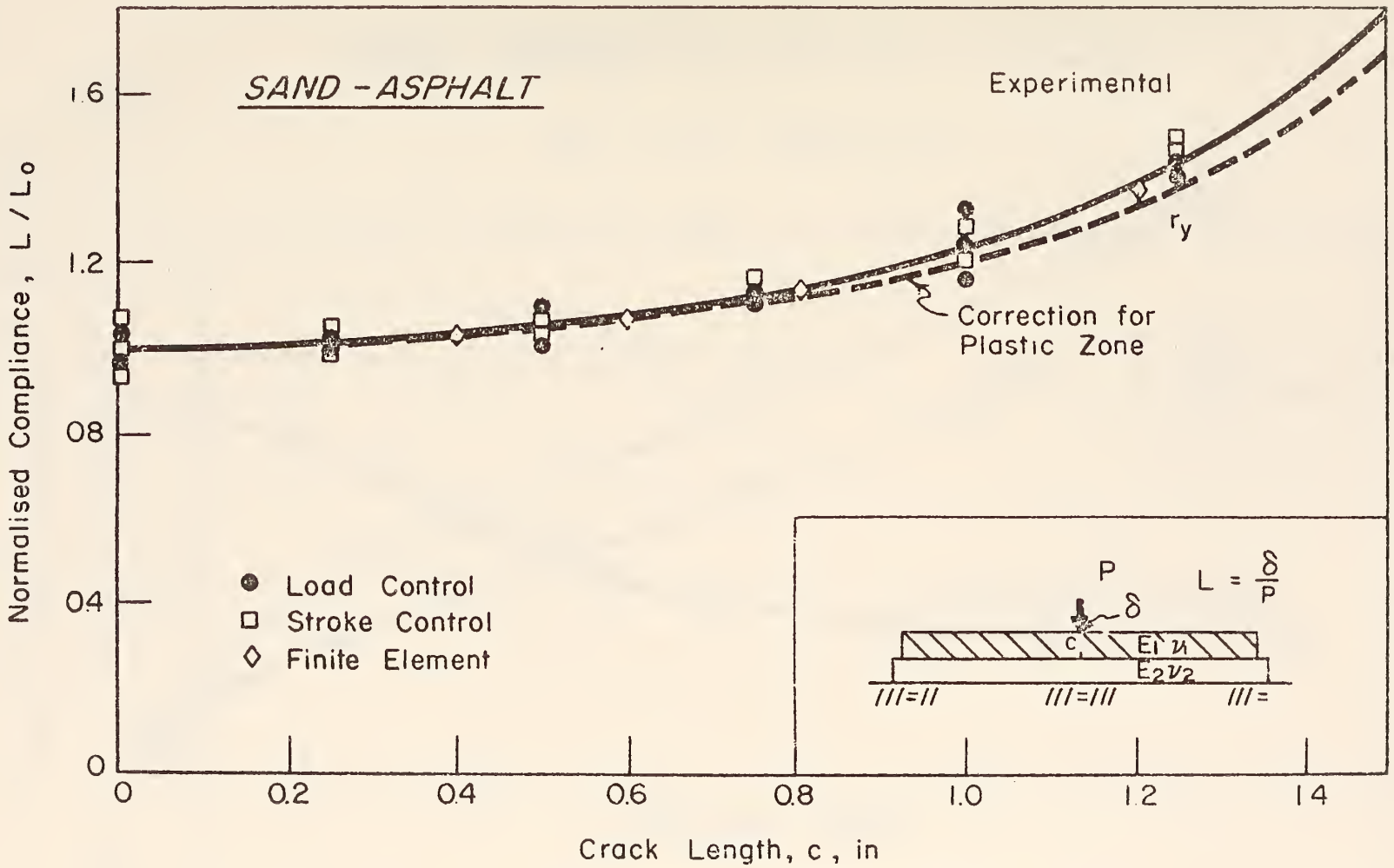

Figure 2.7 Normalized L/L_0 - c relation for Beams on Elastic Foundation Tests

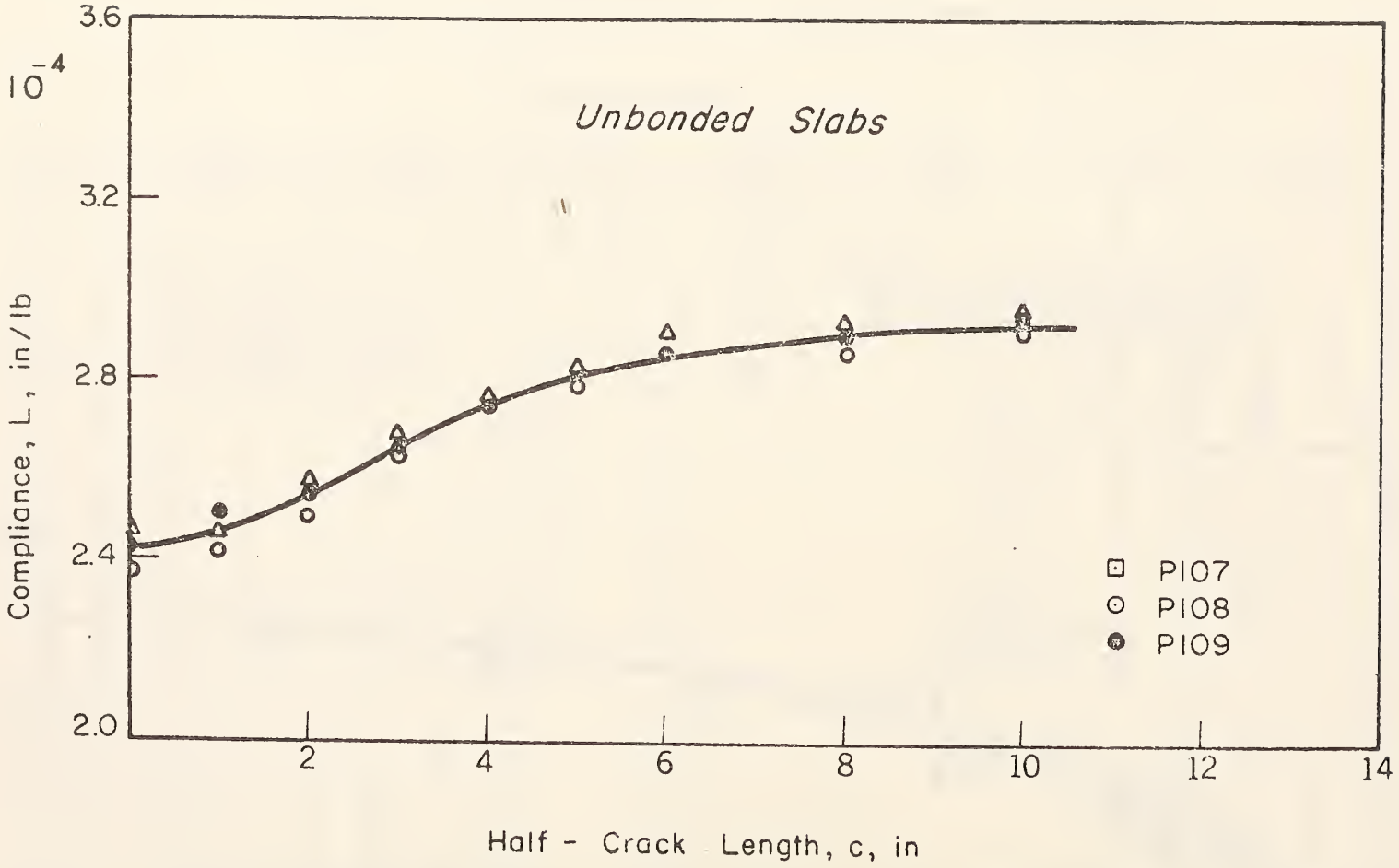

Figure 2.8 Compliance Versus Crack Length for Unbonded Slabs

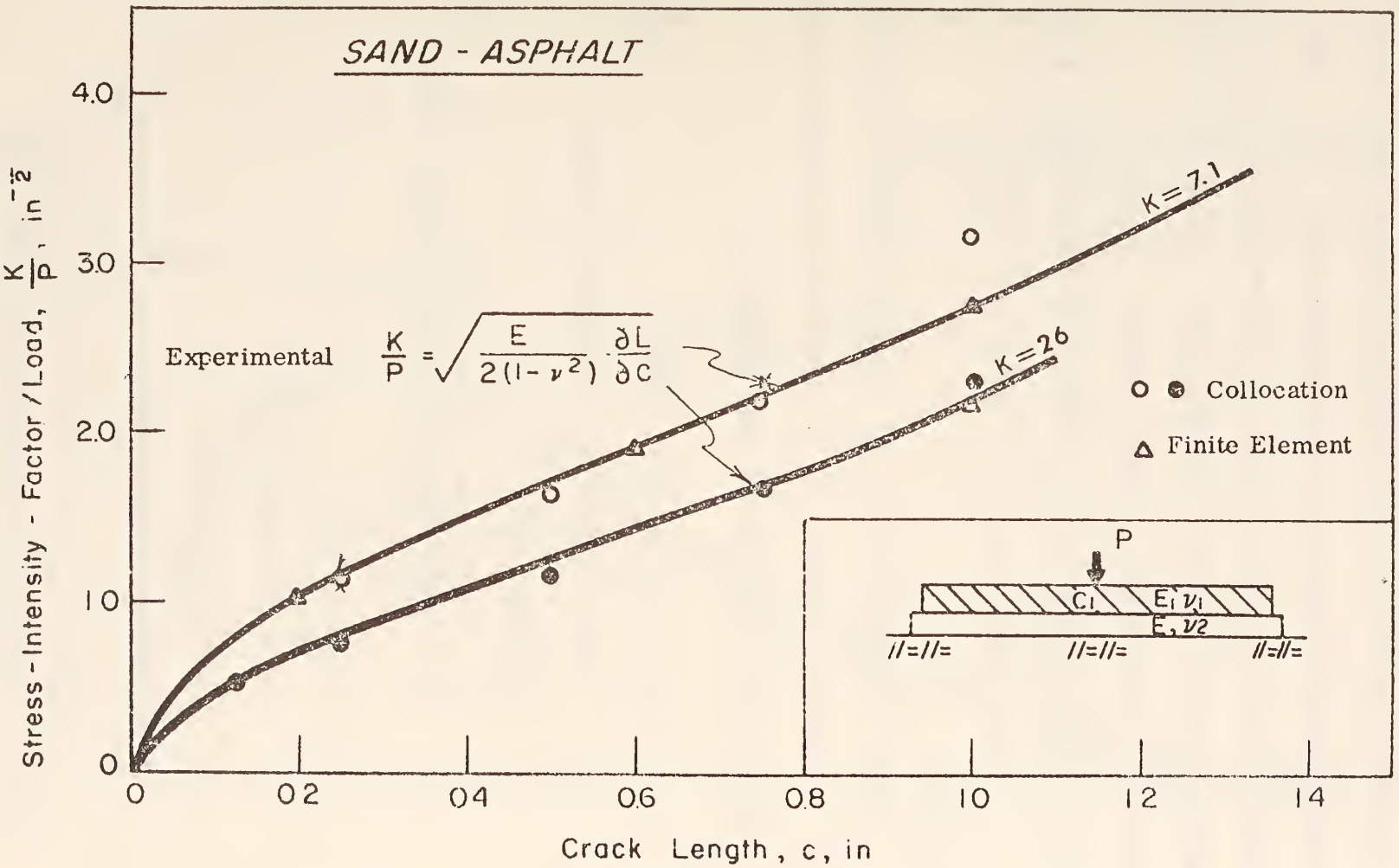

Figure 2.9 K/P - c Relation for Beams on Elastic Foundation Tests

As was indicated, the K/P - c relation can be obtained using such analytical procedures as finite element, boundary collocation, etc. The details of such programs have been presented in References (34) and (35). These analytical procedures include a method of analysis for slabs resting on elastic foundations, beams on elastic foundations, and a prismatic finite element program suitable for an overlay structural analysis. A typical K/P - c relation developed for slabs resting on elastic foundation is shown in Figure (2.10). In Part III of this report, further applications of such procedures are discussed.

A number of investigators (74,77) have utilized the K/P - c relations developed for simply supported beams. The most well-recognized form of such a relation is from the Winne and Wundt equation as:

$$K_I^2 = \sigma_n^2 (1 - \nu^2) h \, f(c/d) \qquad (2.36)$$

where σ_n = nominal bending stress at the root of the notch, psi

$$= \frac{6M}{b(d - c)^2}, \text{ where}$$

M = bending moment in psi. = Pl/4
P = applied concentrated load at midspan, pounds
l = span, inches

ν = Poisson's ratio

b = width of the beam, inches

c = crack depth , inches

d = depth of the beam, inches

h = d - c

f(c/d) = function of the geometry given in Figure 2.11.

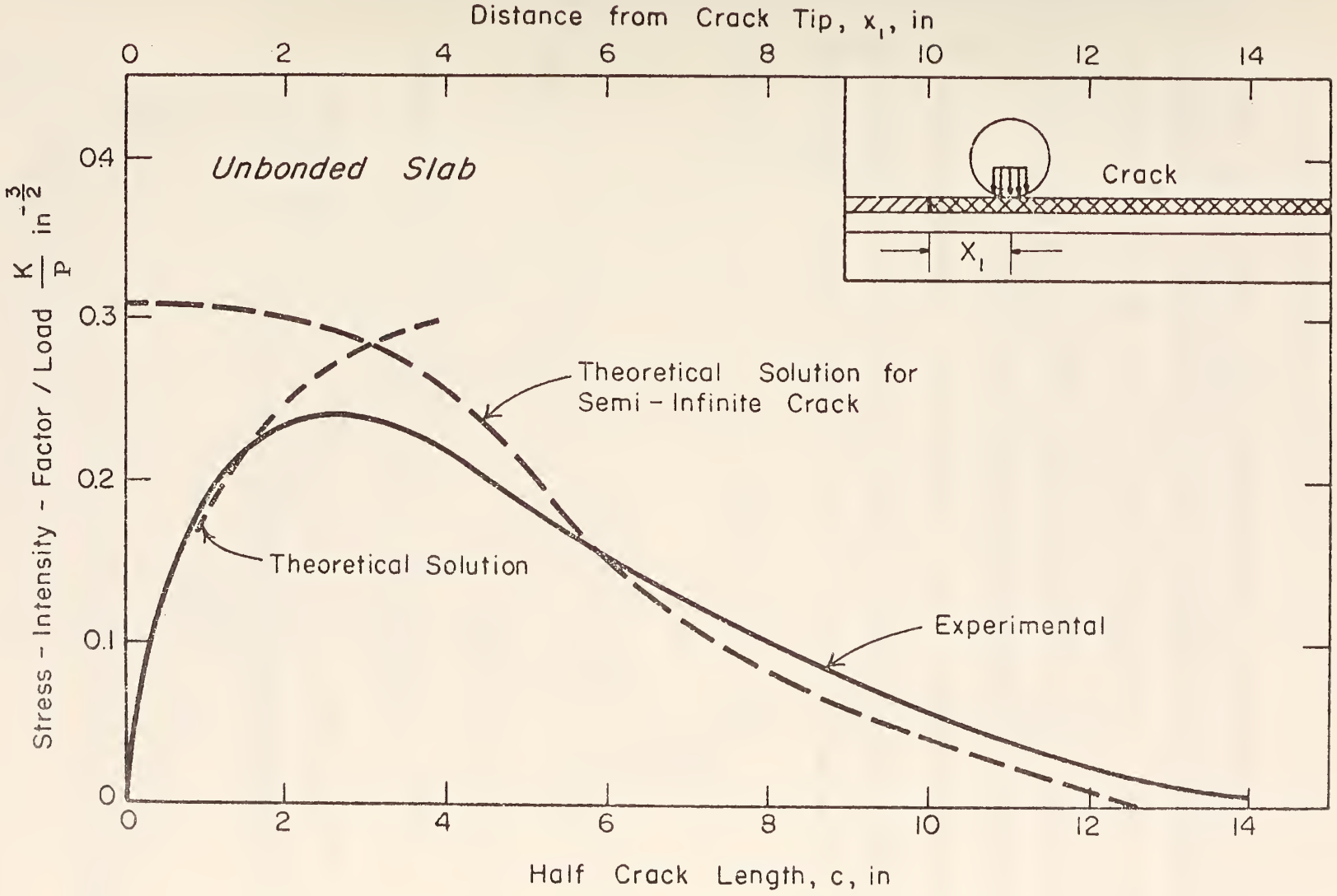

Figure 2.10 Comparison of the Theoretical and Experimental Stress-Intensity Factors for Unbonded Slabs

The f(c/d) can also be written as $f(c/d) = \frac{\pi c}{d} (1 - c/d)^3$. For deeply notched beams f(c/d) has a limiting value of 0.52 (see Fig. 2.11). An analytical formulation of K - c relation by Srawley (74) leads to a normalized relation between Y^2 and c/d as shown in Figure (2.12) from which the opening-mode stress-intensity factor for three-point bending beams can be evaluated.

Similarly, Gross et.al. (14), utilizing boundary collocation and Green's function methods, have developed a numerical function for stress-intensity factor for simply-supported, three-point bending beams with centrally located crack as:

$$K_I = \sigma \sqrt{c} \quad F(c/d) \tag{2.37}$$

where $\sigma = \frac{6M}{B d^2}$, $M = Pl/4$.

For l/d equal to 4 (see Figure 2.13),

$$F(c/d) = 1.090 - 1.735 (c/d) + 8.20 (c/d)^2 \tag{2.38}$$

and for l/d equal to 8 see Figure 2.13,

$$F(c/d) = 1.107 - 2.120 (c/d) + 7.71 (c/d)^2 - 13.55 (c/d)^3 + 14.25 (c/d)^4 \tag{2.39}$$

A fracture toughness K calibration curve has also been recommended by ASTM using Brown and Srawley's analysis (5), as given:

$$K_I = \frac{6M \, c^{\frac{1}{2}}}{B d^2} \quad Y$$

where, for a three-point bending,

$$Y = 1.96 - 2.75 (c/d) + 13.66 (c/d)^2 - 23.98 (c/d)^3 + 25.22 (c/d)^4 \tag{2.40}$$

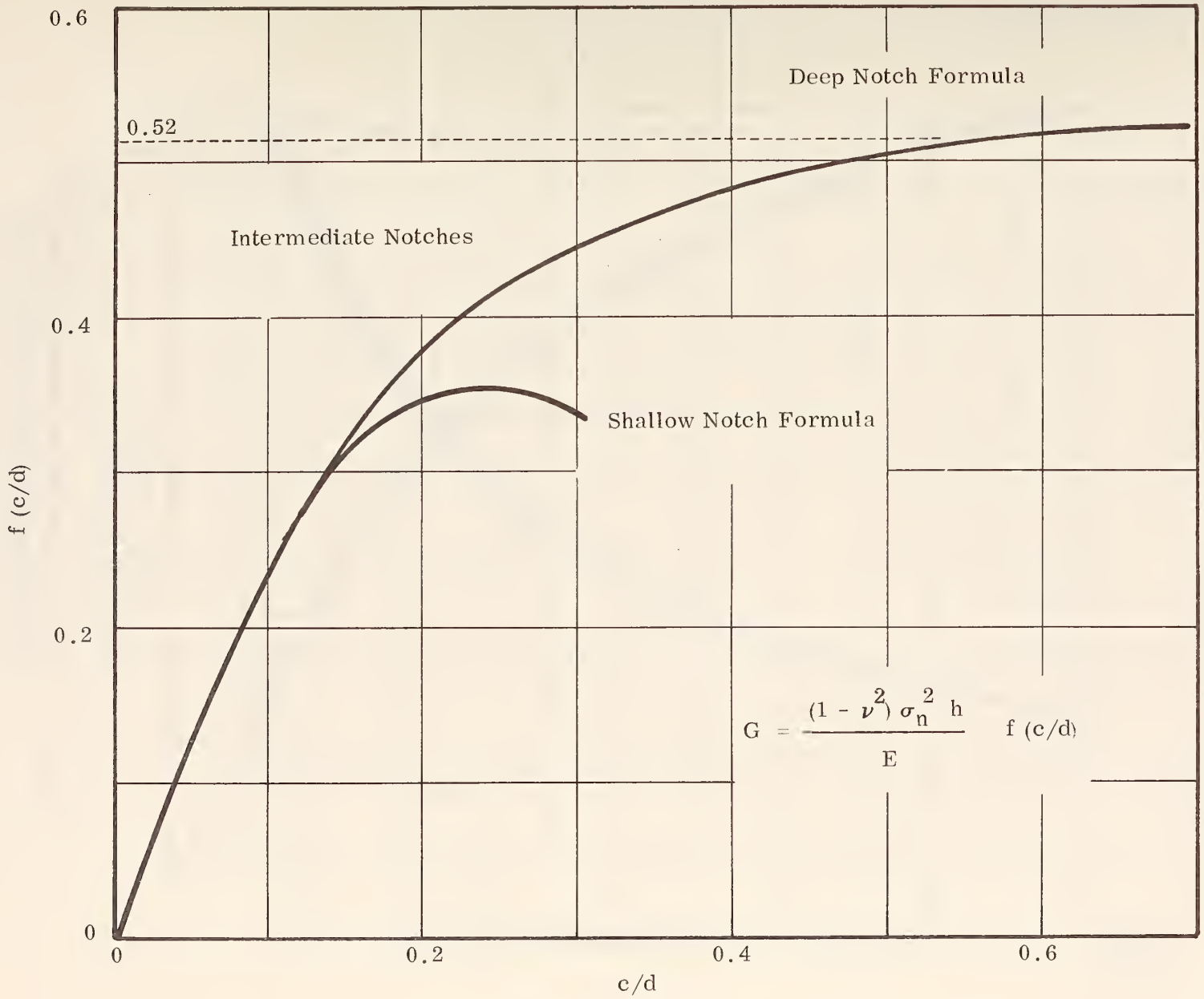

Figure 2.11. Values of f(c/d) for Different c/d Ratios

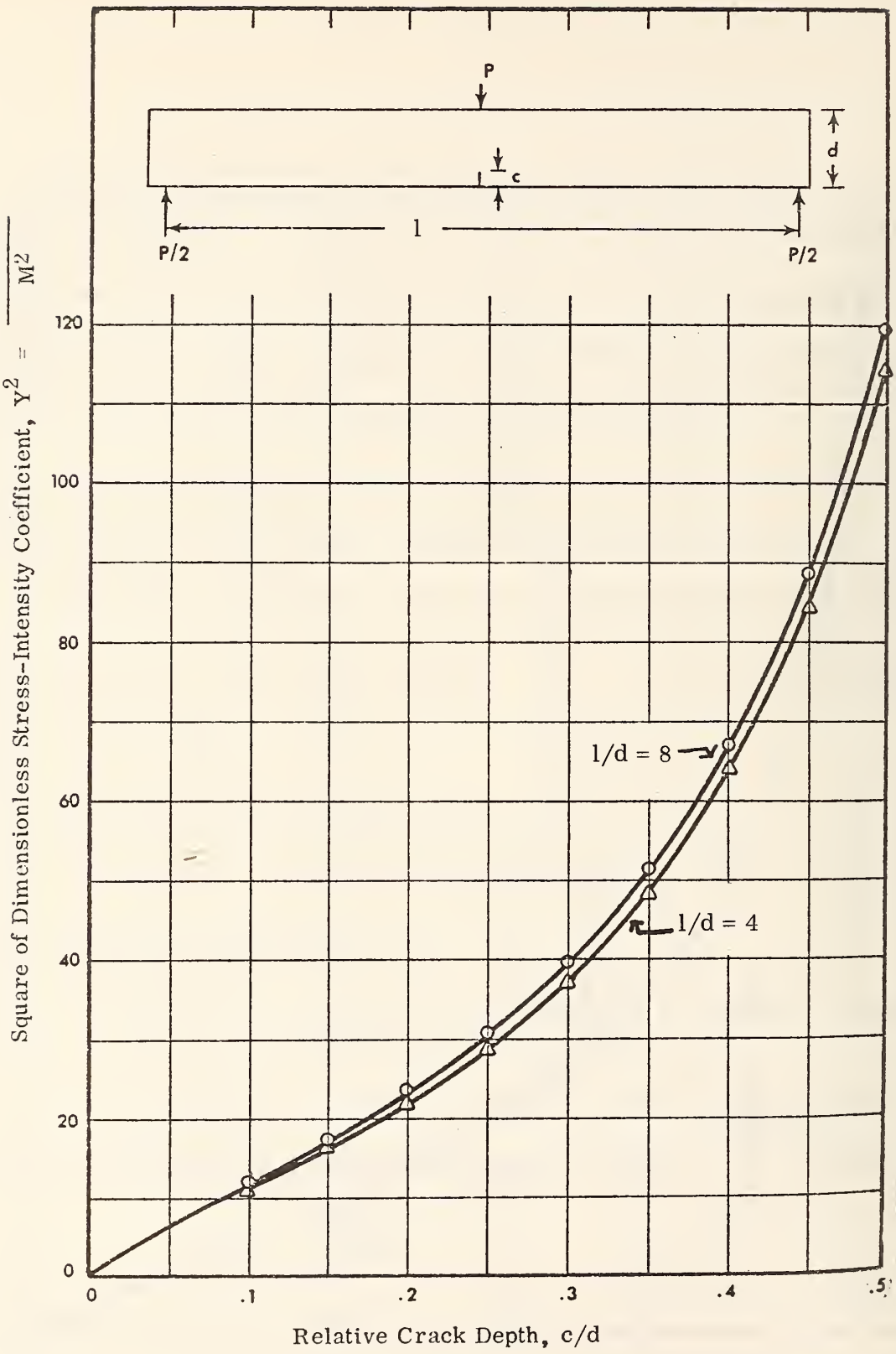

Figure 2.12 Dimensionless Stress-Intensity Factor for a Simply Supported Beam (from Ref. 14)

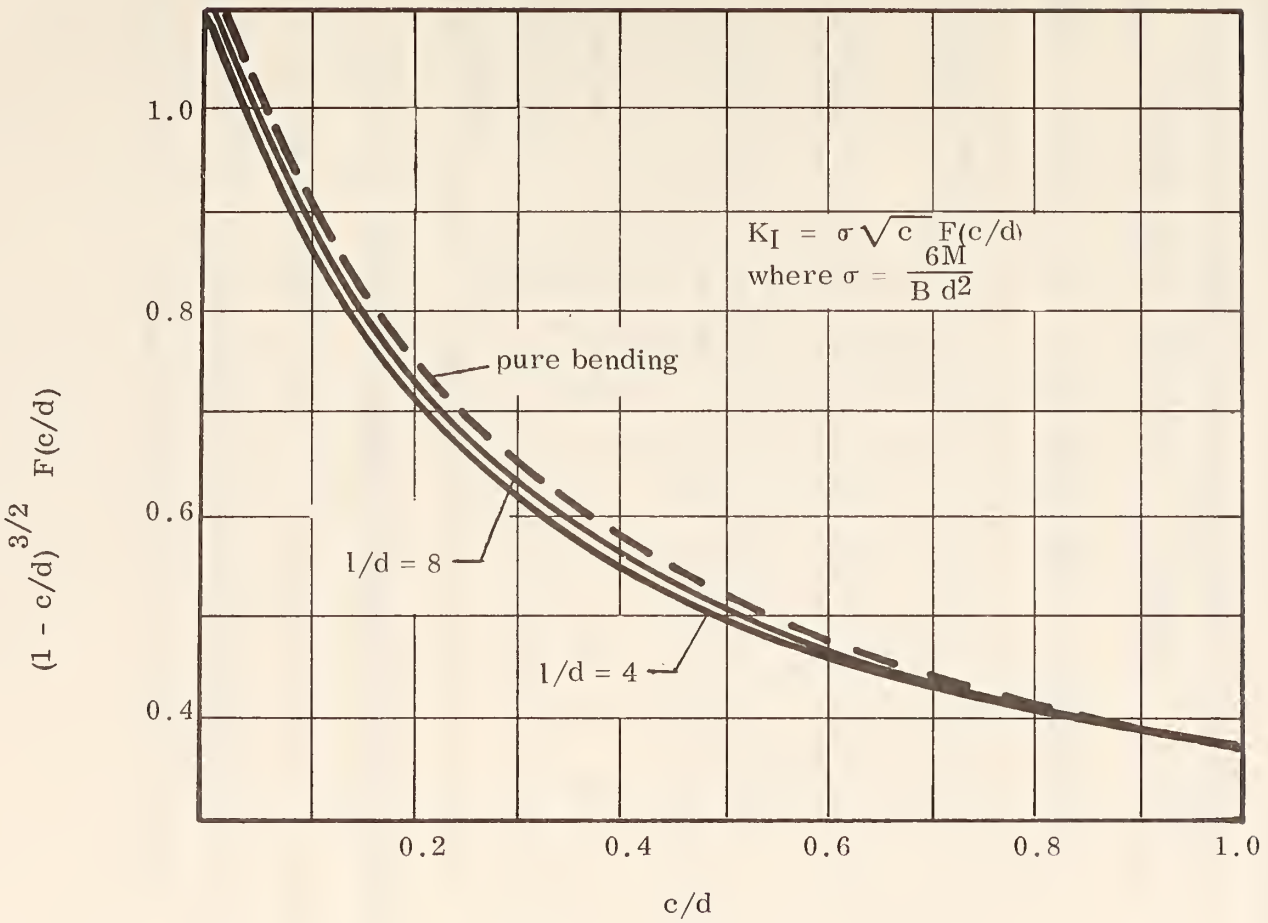

Figure 2.13. A Fracture Toughness K - Calibration Curve

Also c, d, B are crack length, beam depth and beam width respectively. M is the bending moment, either in 3-point or 4-point bending.

The K calibration in terms of c/d ratio and for 3-point bending, may also be written as:

$$K_I = \frac{P_Q l}{B\, d^{3/2}} \left[2.9(c/d)^{1/2} - 4.6(c/d)^{3/2} + 21.8(c/d)^{5/2} - 37.6(c/d)^{7/2} + 38.7(c/d)^{9/2} \right] \quad (2.41)$$

where P_Q is the applied load determined according to the procedure given on page 52, and l is the span of the 3-point bend specimen.

Among other important developments of the analytical and mechanistic aspects of the rational pavement design are the analysis of crack plate on elastic foundation (64), and the prismatic finite element with multi-modal fracture analysis (38). In either case, the multi-modal fracture analysis is carried out using finite element method and the strain energy density S and factors K_I - c and K_{II} - c relationships are calculated, relating the crack growth rate dc/dN to the stress-intensity factors.

II. FRACTURE TOUGHNESS

A. General Review

It was shown previously, as a result of flaws and imperfections in materials, that there exist local stress concentrations. The elevation of stress and its redistribution at crack tip positions are reflected by the stress intensity, K, and strain energy release rate, G. Physically, the parameters K_I, K_{II}, and K_{III}, related to the general state of local stress field, are intensities of load transmittal through the crack tip; similarly, the G_I, G_{II}, and G_{III} are strain energy release rates for three modes of fracture.

The interrelation between the stress intensity factor, K, and strain energy release rate, G, are written as:

For plane stress: $$K^2 = EG \tag{2.42}$$

For plane strain: $$K^2 = \frac{E}{(1-\nu^2)} G \tag{2.43}$$

In engineering analysis of fracture problems, it is preferred to work with the stress-intensity factor rather than the strain energy release rate. The reason is that the stress intensity K, due to the superimposed effects of various stress fields, are linear additions of corresponding K values, as given by:

$$K_I = K_I(1) + K_I(2) + K_I(3) + \ldots + K_I(n)$$

$$K_{II} = K_{II}(1) + K_{II}(2) + K_{II}(3) + \ldots + K_{II}(n) \qquad (2.44)$$

$$K_{III} = K_{III}(1) + K_{III}(2) + K_{III}(3) + \ldots + K_{III}(n)$$

On the other hand, in strain energy terms, the superimposed field is given by:

$$G_I = \left[G_I(1)^{\frac{1}{2}} + G_I(2)^{\frac{1}{2}} + \ldots + G_I(n)^{\frac{1}{2}} \right]^2$$

$$G_{II} = \left[G_{II}(1)^{\frac{1}{2}} + G_{II}(2)^{\frac{1}{2}} + \ldots + G_{II}(n)^{\frac{1}{2}} \right]^2 \qquad (2.45)$$

$$G_{III} = \left[G_{III}(1)^{\frac{1}{2}} + G_{III}(2)^{\frac{1}{2}} + \ldots + G_{III}(n)^{\frac{1}{2}} \right]^2$$

Secondly, in the analysis of fracture mechanics problems, consideration should be given to the definition of plane stress and plane strain conditions. In the field of mechanics, the plane stress condition is defined as:

$$\sigma_z = 0 , \quad \tau_{yz} = \tau_{xz} = 0$$

and the plane strain is defined as:

$$\sigma_z = \nu (\sigma_x + \sigma_y), \quad \tau_{xz} = \tau_{yz} = 0 , \quad \epsilon_z = 0$$

In constrast to general field of mechanics, the fracture mechanics definition of plane strain and stress conditions are more restrictive and are only applicable to crack tip locations. In such areas, the plastic zone ahead of the crack tip is constrained from elastic deformation by the presence of elastic material along the crack front. If the plastic zone is small as compared to the dimension and the length of the crack front, a plane strain condition prevails. The size of the plastic zone can be estimated for a plane strain

condition as:

$$r_y = \frac{1}{2\pi\sigma_y^2}\left\{ K_I^2 \cos^2\frac{\theta}{2}\left[(1-2\nu)^2 + 3\sin^2\frac{\theta}{2}\right] + K_I K_{II}\sin\theta\left[3\cos\theta - (1-2\nu)\right] + K_{II}^2\left[3 + \sin^2\frac{\theta}{2}\left((1-2\nu)^2 - 9\cos^2\frac{\theta}{2}\right)\right] + 3K_{III}^2\right\} \tag{2.46}$$

In the crack plane, where $\theta = 0$ and for a two-dimensional case:

$$r_y = \frac{1}{2\pi\sigma_y^2}\left(K_I^2 (1-2\nu)^2 + 3\left(K_{II}^2 + K_{III}^2\right)\right) \tag{2.47}$$

For Mode I fracture, this equation reduces to:

$$r_y = \frac{(1-2\nu)^2}{2\pi}\left(\frac{K_I}{\sigma_y}\right)^2 \quad \text{for plane strain.} \tag{2.48}$$

As the material body, with pre-existing flaws, are stressed to failure, the stress intensity factor K and strain energy release rate G are increased approaching their limiting values. These performance limiting parameters, for the plane strain condition are designated as K_{IC} and G_{IC} which have been shown that they can be taken as material constants, independent of geometry, crack size, and other boundary and loading conditions. The failure conditions for Mode I and II can be written as:

$$F \cdot \sigma\sqrt{c} \geq K_{IC} \tag{2.49}$$

and

$$F \cdot (\tau + f\sigma)\sqrt{c} \geq K_{IIC} \tag{2.50}$$

where σ = applied tensile stress

τ = shear stress

f = friction coefficient for the crack surface

F = a geometrical constant

As indicated previously, for multi-modal fracture, the Sih's strain energy density factor, S_C , can be related to fracture toughness as:

$$S_C = S\ (K_{IC}, K_{IIC}, K_{IIIC}) \tag{2.51}$$

The S_C is analogous to the K_C; where it measures the resistance of material to fracture under multi-modal conditions. Under normal tensile stress conditions where $K_{II} = K_{III} = 0$,

$$S_C = \frac{(1 - 2\nu)(1 + \nu)}{2\pi E} \cdot K_{IC}^2 \tag{2.52}$$

As it was shown previously, similar equations can be also developed for other fracture modes.

B. Fracture Toughness Measurement

As indicated previously the plane strain fracture toughness K_{IC} is a material constant which is a measure of the material's resistance to fracture. This material constant has been shown to be independent of geometry boundary and the mode of load application. The experimental procedures for fracture toughness measurement and evaluation are as follows:

1. Compliance Calibration

The presense of flaws and cracks within a body affect the load-deflection characteristics and can be evaluated using the material's modulus or its inverse, known as compliance. Irwin (19) has shown that the change in the spring constant, modulus or the compliance (inverse of modulus) can be used as a measure of crack extension and the release of excess elastic energy. For materials tested under a load control mode, i.e., "soft systems," the energy release rate is written as

$$G = \frac{1}{2B} \cdot P^2 \cdot \frac{\partial L}{\partial c} \tag{2.53}$$

For, stroke control testing, i.e., stiff machines , the energy release rate, however, is given by:

$$G = \frac{1}{2B} \cdot \Delta^2 \cdot \frac{\partial L}{\partial c} \tag{2.54}$$

where P, Δ, L, B are load, displacement, compliance and specimen width, respectively. The compliance procedures have been almost exclusively

applied to Mode I problems . The advantage of this method is that it only requires one size of prototype specimen. Furthermore, the material to be tested and the protype need not be the same. However, it is required that material to be homogenous, isotropic, having a well defined modulus of elasticity, as well as having dimensions proportional to the real specimens.

For analysis purposes, the compliance measurement is carried out on a specimen with an initial notch c_o, and then the notch is extended by a small increment Δc and the compliance is measured again. This procedure is continued until a compliance-crack length relation is resulted. The rate of change of compliance with crack length is then calculated from the shape of compliance-crack length as given by $\frac{\partial L}{\partial c}$. The strain energy release rate G and the strain intensity factor K ($K^2 = EG$) is then calculated using the equations given previously. The comparison of the K_{IC} results obtained by experimental compliance method and analytical procedures have been shown to be in excellent agreement.

2. Analytical Method

In this method, the strain analysis procedures are used to derive mathematical formulations between the strain-intensity or strain-energy release rate and the crack length and specimen geometry. One such procedure is the equation given by Winne and Wundt, as shown by

$$G_{IC} = \frac{(1 - \nu^2)}{E} \; h \; \sigma_n^2 \; f(c/d) \qquad (2.55)$$

As it was shown previously, for small crack $f(c/d) = \frac{\pi c}{d} (1 - c/d)^3$, whereas for deeply-notched beams, $f(c/d) = 0.52$.

Other analytical equations used for stress-intensity factor calculations were given by equations (2.37), (2.40) and (2.41) in Chapter I, Part II. In addition, numerous approximate analysis procedures have also been recommended by various researchers (2) (Figure 2.14).

Similarly, the use of the polynomial form of the K_{IC} equation has also been reported in studies of asphaltic concrete (16) and Portland cement concrete (20). One such equation (2.55) used for Portland cement concrete is written as:

$$K_{IC} = \frac{6M}{B d^2} \left[\frac{2c}{\pi} h(c/d) \right]^{1/2} \qquad (2.56)$$

where $h(c/d) = 10.08(c/d)^2 - 1.225(c/d) + 0.1917$

The detailed discussions of K_{IC} measurements for pertinent civil engineering materials will be discussed in a separate section. In all such analyses, the maximum load P_Q shall be calculated in accordance with the following specified procedures:

(i) Draw an initial tangent to the load-displacement curve (line OA) as shown in Figure (2.15).

(ii) Draw the second line O P_5 through the origin with slope less than the slope of initial tangent OA. P_5 is the load at intersection of O P_5 with the load-displacement

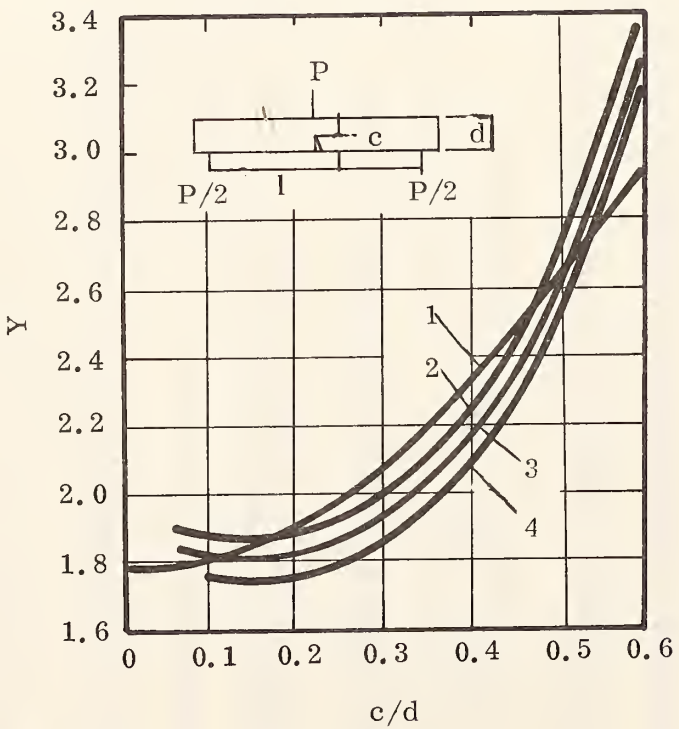

$$K_I = \frac{6 M c^{\frac{1}{2}}}{B d^2}$$

Where M is the bending moment in 3- or 4-point bending

For 3-point bending

$$Y = 1.96 - 2.75(c/d) + 13.66 (c/d)^2 - 23.98 (c/d)^3 + 25.22 (c/d)^4$$

1 = approximate method
2 = pure bending

3 = 3-point l/d = 8

4 = 3-point l/d = 4

Figure 2.14 K Calibrations for Bend Specimens

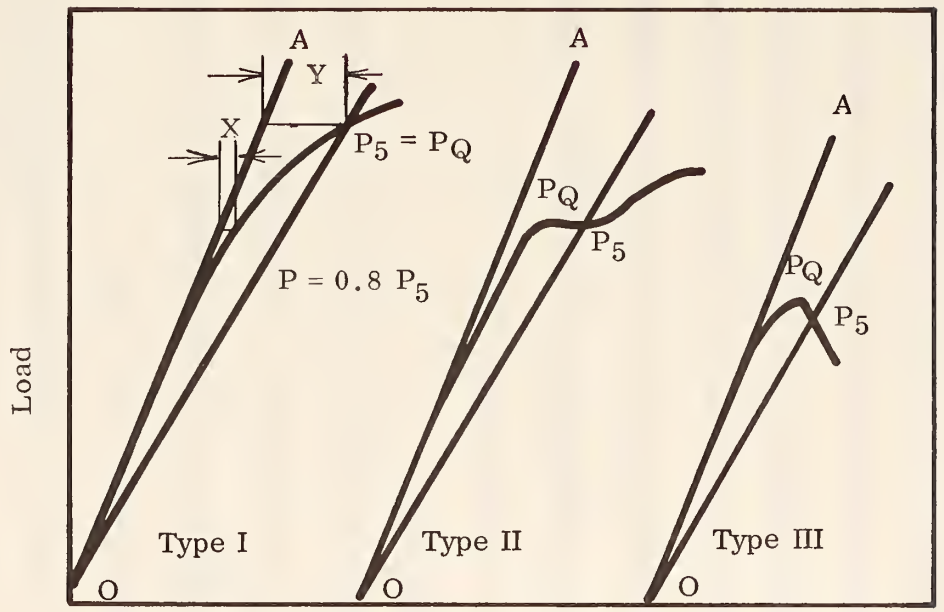

Figure 2.15 Principal Types of Load-Displacement Records

curve. To determine P_Q, if the load at every point on the curve which precedes P_5 is lower than P_5, then $P_Q = P_5$ (Type I). If, however, there is a maximum load preceding P_5, which exceeds it, then this maximum load is equal to P_Q. To check the validity of P_Q, select a point on the load-displacement such that $P = 0.8\ P_5$. Measure the distance X along the horizontal line from tangent OA to the curve. Similarly, measure the horizontal distance Y from OA to P_5. If the ratio of X to Y is greater than 0.25, then the K_{IC} is not a valid test and strain-intensity calculated is considered as a candid value of strain-intensity rather than as a true measurement of this material constant.

3. J-Integral Criterion

In the previous sections, the failure criterion for linear elastic mechanics with small scale yielding were presented. It was pointed out that the strength of crack tip singularity can be represented by the stress intensity factor, K, and its lower limiting critical value, K_{IC}.

For large scale yielding, Rice (68, 32) has proposed the path-independent J-Integral as a criterion for failure. For linear elastic material, J_{IC} is identical with G_{IC} parameter and can therefore be related to the fracture toughness, K_{IC}. For a general case, however, the J-Integral is interpreted as potential energy difference between two identically loaded and neighboring cracks; i.e.,

$$J = -\frac{dU}{dc} \text{ / unit thickness} \qquad (2.57)$$

where U = potential energy

c = crack length.

To evaluate the fracture criterion, the load-displacement is plotted for various crack sizes as used for compliance procedures. At a given total deflection, the area under the curve is measured using the planimeter. The energy represented by the area under the curves are plotted versus the crack length as shown in Figure 2.16. The slopes of the lines are given by Equation (2.57). It should be noted that load-displacement procedures used should measure the total energy input accurately. The use of crack opening displacement method for J-integral analysis is not satisfactory. Furthermore, the deflection at failure needs to be measured. In Figure (2.16), variations of U vs. c per unit thickness are shown. The slope of this diagram, i.e. dU/dc versus deflection is shown in Figure (2.17). The experimental observations would also provide an estimate of deflection at failure. As an example, considering that Δ_f, the deflection at failure, is 0.025 inch (Figure 2.18), then J at failure can easily be estimated.

C. Experimental Results

The critical toughness, K_C, is affected by the specimen's geometry as well as the boundary and loading conditions. In order to obtain a reproducible value for the lower limiting critical toughness K_{IC}, which can be considered

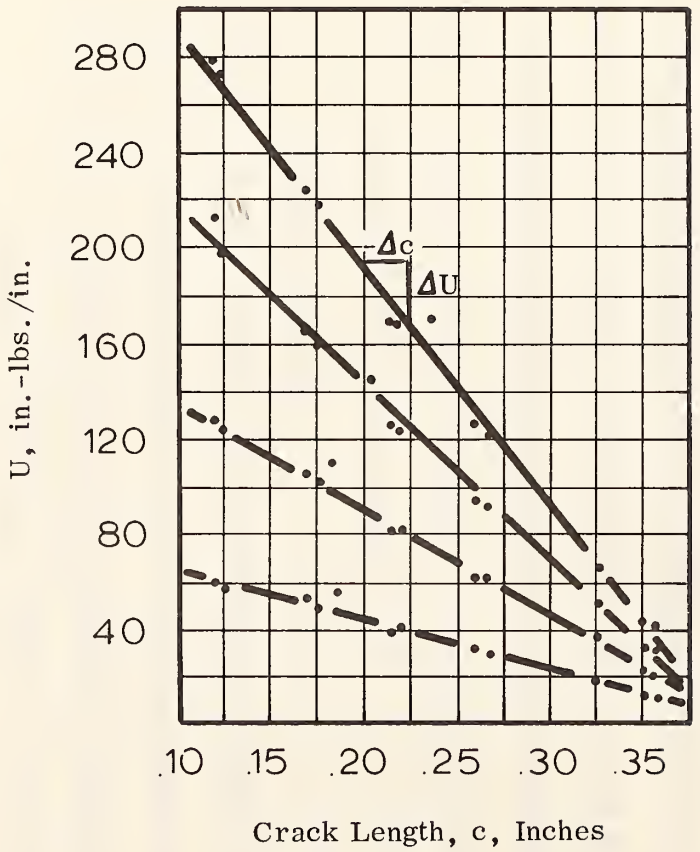

Figure 2.16. Energy Absorbed at a Given Deflection Versus Crack Length

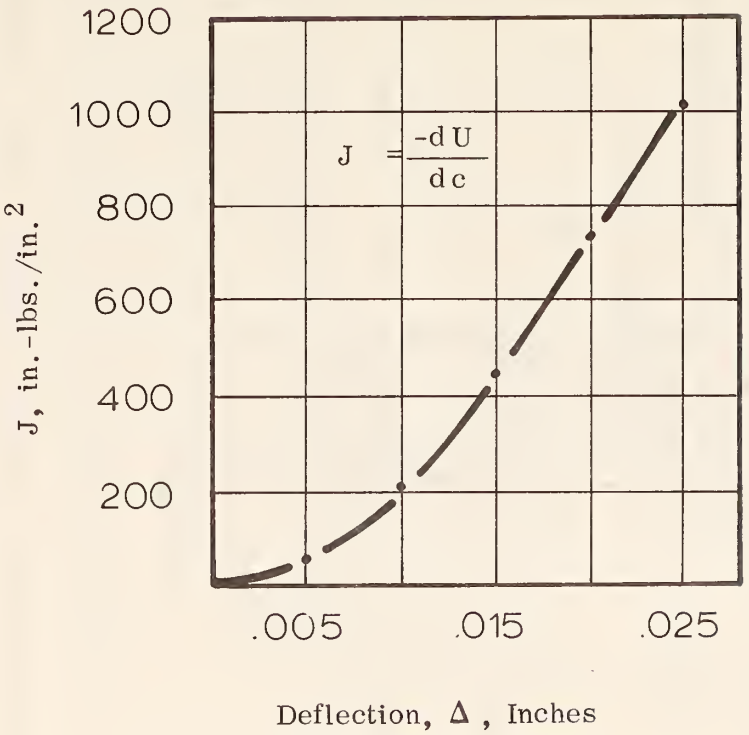

Figure 2.17. J Value as a Function of Deflection

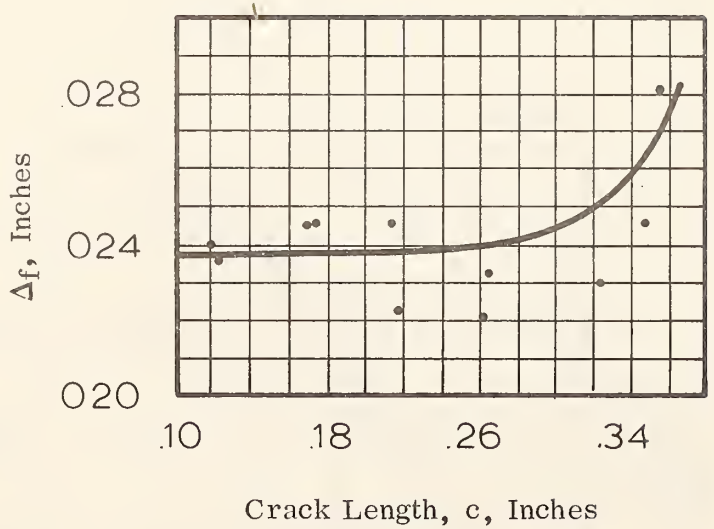

Figure 2.18. Deflection at Failure as Related to Crack Size

as a material constant, the state of stresses should closely approximate a plane strain condition. This requirement and restriction on the stress state implies that the size of plastic zone must be small as in comparison with the dimensions of the specimen. The radius of the plastic zone is given by an approximate relation:

$$r = 0.05 \left(\frac{K_{IC}}{\sigma_y}\right)^2 \tag{2.58}$$

where K_{IC} is fracture toughness and σ_y is the material yield strength in tension. To meet the plane strain condition, ASTM has established a minimum requirement for the plate thickness B and crack length c as given by:

$$B \geq 2.5 \left(\frac{K_{IC}}{\sigma_y}\right)^2 \tag{2.59a}$$

and

$$c \geq 2.5 \left(\frac{K_{IC}}{\sigma_y}\right)^2 \quad \text{and specimen depth } d \geq 2B. \tag{2.59b}$$

The deviations from such a size requirement will result in higher values of K_{IC} or plane stress representation of fracture toughness, as shown in Figure (2.19). It should be noted that as the specimen's thickness increases, the stresses acting on the crack front also increase, leading to more triaxial state of stresses at the crack front. Such a condition corresponds to a plane strain state. In Figure (2.20), a schematic view of the effect of specimen size on fracture toughness and the test results on metals is shown.

Another important variable is the mode of load application and the so-called soft-hard characteristics of the testing machine. The load-controlled

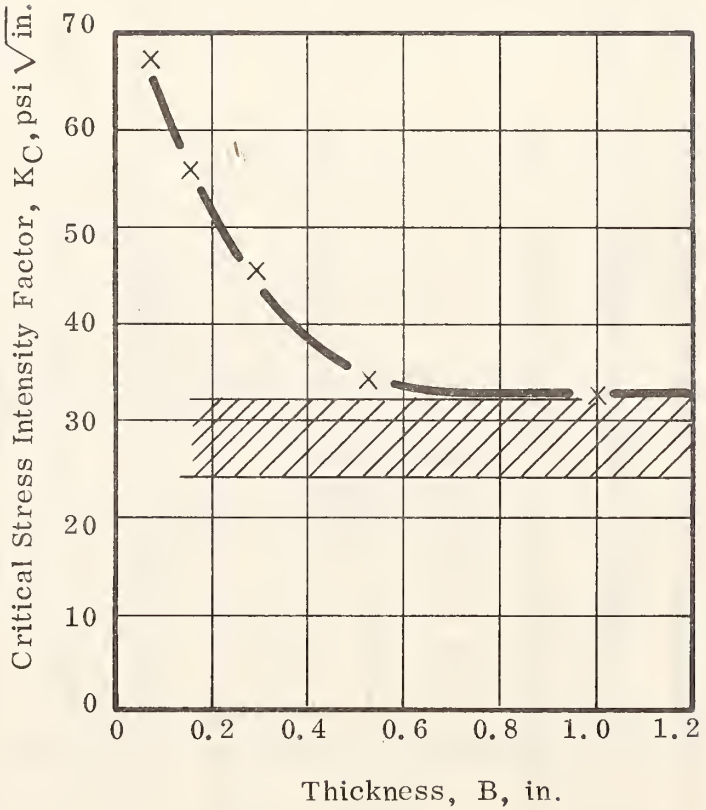

Figure 2.19. Effect of Plate Thickness on Fracture Toughness

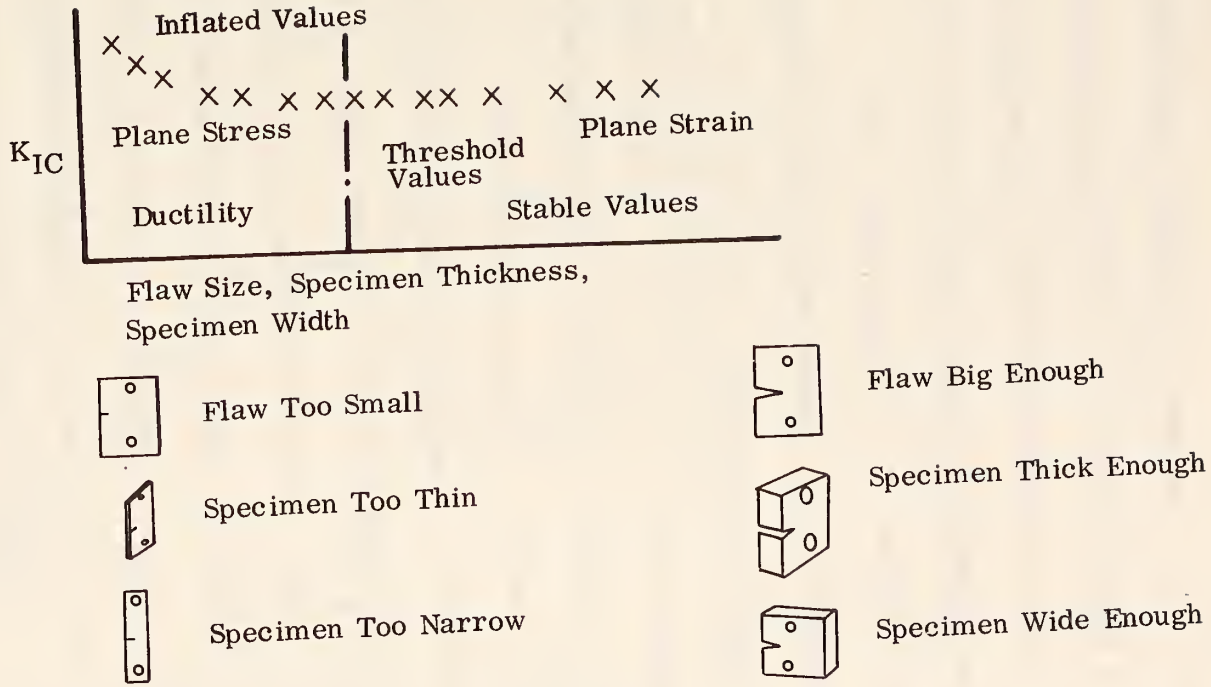

Figure 2.20. Size Effect in K_{IC} Measurements

testing systems are generally considered as soft machines. A typical load-deformation characteristic of specimens tested under a soft machine is shown in Figure (2.21). It should be noted on the machine-specimen instability path as shown in Figure (2.21), a plane stress failure condition might occur. On the other hand, stroke-controlled testing systems are ideally stiff machines in which fracture occurs in plane strain condition (Figure 2.22).

The fracture toughness K_{IC} has also been shown to be affected by temperature as well as rate of load application. In Figure (2.23), the variation of K_{IC} with temperature is shown. It is also noted that yield strength σ_y is also influenced by temperature. Generally, at high temperatures, σ_y decreases, whereas K_{IC} exhibits an increase with temperature.

The experimental data on metals also show that there is an interrelation between tensile strength and fracture toughness, K_{IC}. It is generally observed that K_{IC} and σ_y are inversely interrelated. Although there is no basic reason why one should expect a simple relation between K_{IC} and σ_y however, such a relation can be a useful approximation for K_{IC} calculation. Experimental data on metals have shown such a relation can often be approximated by $K_{IC} = \sigma_y^{-3}$. Similarly, an empirical formula relating K_{IC} and σ_y has been presented as follows (Figure 2.24):

$$K_{IC} = \frac{2}{3}\left[E \cdot \sigma_y \cdot n^2 \cdot \xi_f\right]^{\frac{1}{2}} \tag{2.60}$$

where σ_y = yield strength

n = strain hardening exponent $\sigma = C\,\xi^n$

C = a constant

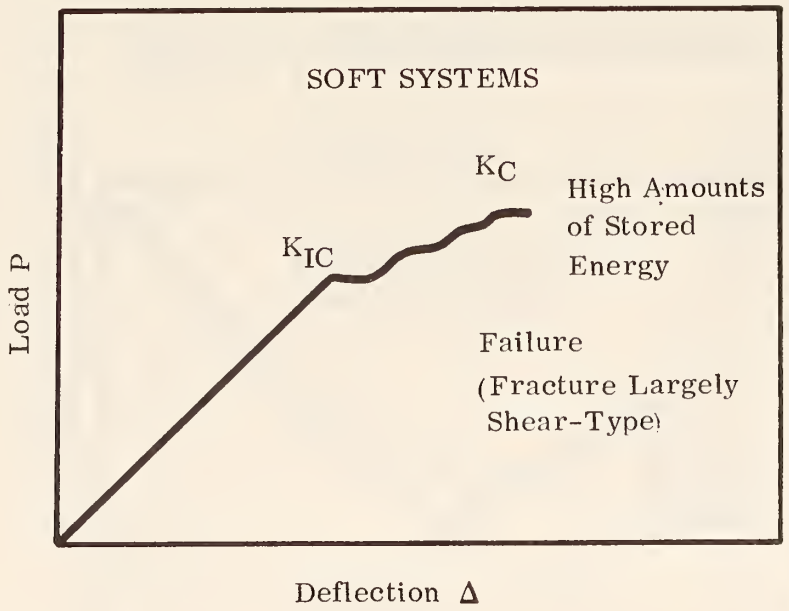

Figure 2.21. Soft-System Characteristics

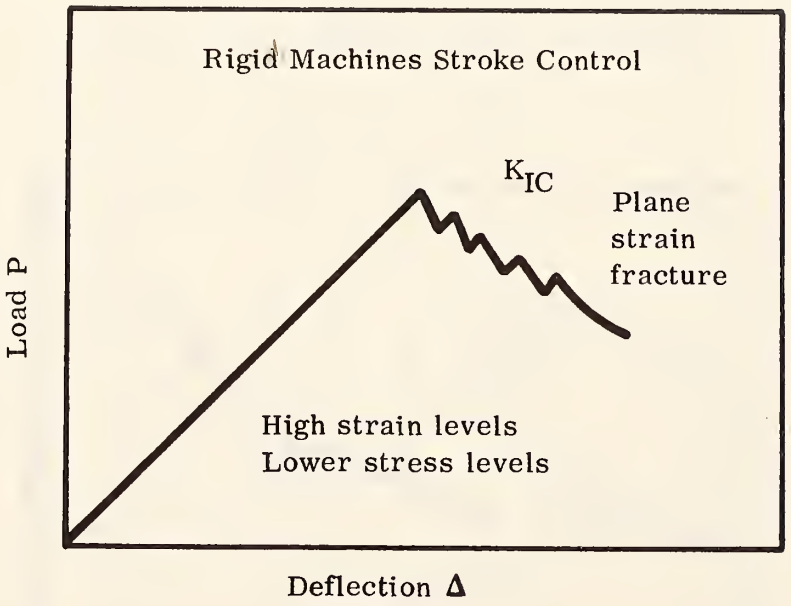

Figure 2.22. Stiff-System Characteristics

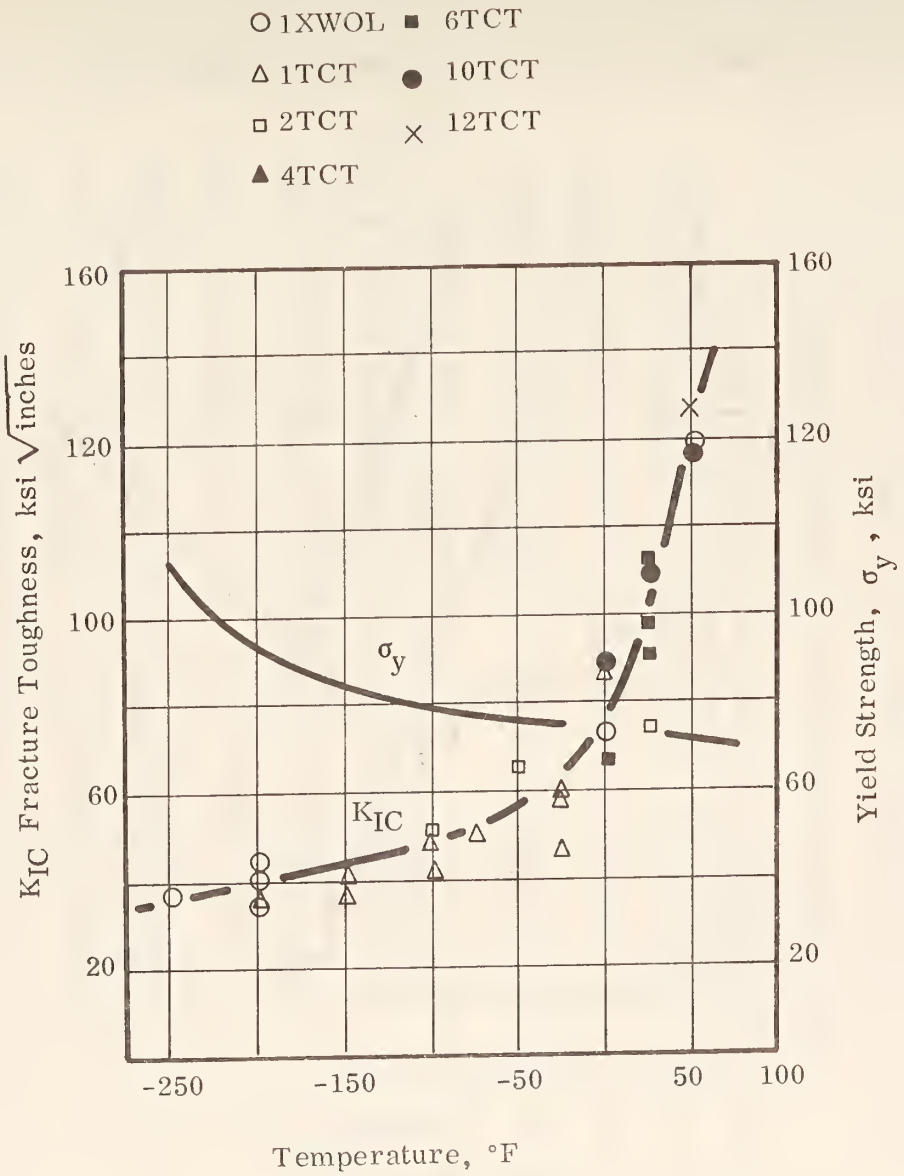

Figure 2.23 Temperature Dependence of K_{IC}

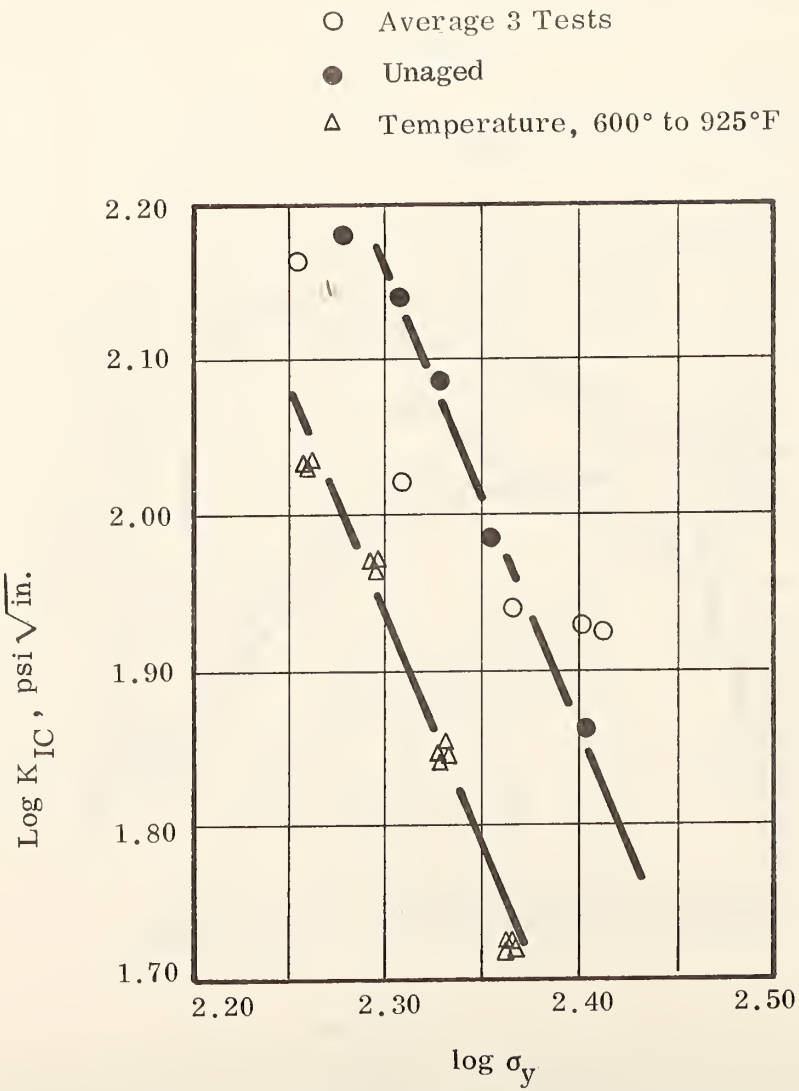

Figure 2.24. Relation Between Plane Strain Fracture Toughness and Yield Strength

E = modulus of elasticity

ξ_f = true strain at fracture.

It should be noted that all material would not necessarily satisfy such an interrelation between σ_y and K_{IC}.

In Tables 2.1 and 2.2, the available K_{IC} and G_{IC} data on numerous engineering materials are shown. The fracture toughness data on concrete, asphalt and other paving materials are also available on a limited basis.

The fracture analysis on concrete was carried out in the early sixties by M. F. Kaplan (37) who performed tests on concrete beams with crack simulating notches. The critical strain-energy-release rate, G_C, associated with the rapid extension of the crack, was determined by two methods: the analytic method and the direct experimental method. Similar beams with different depths of notch gave G_C values which are in close agreement. However, G_C, values of beams of larger dimensions were higher than those of smaller dimensions. Some differences in G_C values were reported; the discrepancy is possibly due to the method of G_C determination. Kaplan's conclusion was that the critical strain-energy-release rate may be ascertained by suitable analytical and experimental methods, and the fracture strength of concrete containing cracks can thereby be predicted.

Moavenzadeh and Kuguel (45) also used notched-beam specimens of cement paste, mortar and concrete to study their fracture properties. They found out that the fracture work of the paste increases by the introduction of solid particles. This is due to the multiplicity of the crack growth during the

TABLE 2.1 FRACTURE-TOUGHNESS VALUES*

Material	Ultimate Strength σ_u - ksi	Critical Stress-Intensity Factor K_C - ksi $\sqrt{in}$
A517 F Steel (AM)	120	170
AISI 4130 Steel (AM)	170	100
AISI 4340 Steel (VAR)	300	40
AISI 4340 Steel (VAR)	280	40
AISI 4340 Steel (VAR)	260	45
AISI 4340 Steel (VAR)	240	60
AISI 4340 Steel (VAR)	220	75
300M Steel (VAR)	300	40
300M Steel (VAR)	280	40
300M Steel (VAR)	260	45
300M Steel (VAR)	240	60
300M Steel (VAR)	220	75
D6AC Steel (VAR)	240	40-90
H-11 Steel (VAR)	320	30
H-11 Steel (VAR)	300	40
H-11 Steel (VAR)	280	45
12Ni-5Cr-3Mo Steel (VAR)	190	220
18Ni (300) Maraging Steel (VAR)	290	50
18Ni (250) Maraging Steel (VAR)	260	85
18Ni (200) Maraging Steel (VAR)	210	120
18Ni (180) Maraging Steel (VAR)	195	160
9Ni-4Co-0.3C Steel (VAR)	260	60
A1 2014-T651	70	23
A1 2024-T851	65	23
A1 2219-T851	66	33
A1 2618-T651	64	32
A1 7001-T75	90	25
A1 7075-T651	83	26
A1 7079-T651	78	29
A1 7178-T651	83	24

* These values are taken from References (73)(74) and (75) and are to be considered as nominal values only.

TABLE 2.2 CRITICAL STRAIN ENERGY RELEASE RATE VALUES *

Material	Critical Energy Release Rate G_{IC}-lb/in
Dural	1.60×10^{3}
Key Steel	5.71×10^{2}
Brass	3.43×10^{2}
Teak Wood	6.85×10
Cast Iron	4.57×10
Cellulose	2.28×10
Polystyrene	1.14×10
Polymethylmethacrylate	5.71
Epoxide Resin	3.77
Polyester Resin	2.51
Graphite	5.71×10^{-1} - 1.14
Alumina	4.57×10^{-1}
Magnesia	1.14×10^{-1}
Glass	4.57×10^{-2}

* Most of these data were obtained from a notched bar under three-point bending (73)

fracture process in the specimens. The extent of the internal cracking was measured using a quantitative microscopy technique. The result of such crack measurements indicated that the true fracture work of concrete (determined by accounting for multiplicity of cracks in the specimen) is lower than that of cement paste. This is attributed to the preference of cracks to propagate through the interface of paste and aggregate, which in general is of lower bond strength than the paste matrix.

Naus and Lott (50) defined an effective fracture toughness for concrete, assuming that it is a homogeneous material. The conclusions of his studies were as follows: The effective fracture toughness of concrete increases with age of concrete, increase of maximum size of coarse aggregate and increase of gravel-cement ratio. There is no apparent effect of varying the water-cement ratio on the effective fracture toughness of the concrete. However, a decrease of effective fracture toughness was observed with increase of air content in the concrete.

K. P. George (10) has also studied the applicability of the Griffith theory of brittle fracture to the fracture of soil-cement material. He has investigated the possibility of using the concept of a critical strain-energy-release rate G_C, or the fracture toughness K_C, determined from G_C, in predicting the crack propagation rate in soil-cement base. Critical strain-energy-release rate, G_C, and the fracture toughness, K_C, of five different

soil-cement mixtures were experimentally determined on notched beams and their variations with respect to several parameters were investigated. Some relevant conclusions were drawn:

1. The value of the critical strain-energy-release rate, G_C, is more or less independent of the notch depth.
2. G_C increases as the clay content of the soil becomes greater.
3. G_C increases slightly as temperature is lowered to the freezing point of water and thereafter increases rapidly as temperature drops below the freezing point.
4. G_C increases slightly with the rate of loading.

The variations of G_C according to soil texture and the rate of loading as well as its independence of notch geometry indicate that G_C is truly a measure of physical properties of the materials. He also examined the crack propagation in model base slabs constructed to simulate field conditions. It has been shown that the critical stress intensity factor, K_C, computed from G_C, tends to be related to the crack propagation rate.

The application of fracture mechanics principles to analysis and evaluation of asphaltic systems has been carried out by Moavenzadeh (44), Herrin (16), Majidzadeh et al. (33-41), Monismith (46), and Blight (3). Moavenzadeh investigated the application of Griffith theory to fracture analysis of asphalt cements tested at low temparatures. Utilizing the Winne and Wundt

equation presented previously, the critical strain-energy-release rate G_{IC} was calculated for three asphalt cements. It was concluded that at sufficiently low temperatures, the asphalt cement behaved as a brittle, amorphous material satisfying the requirements of Griffith theory. It was pointed out, as shown in Figures (2.25) and (2.26) that G_{IC} for asphalt cement is a rate and temperature dependent parameter. The degree of aging and the asphalt type also influence the critical strain-energy-release rate (Figure 2.27).

Majidzadeh, Kauffmann and Ramsamooj (35)(36)(37), have also investigated the fracture characteristics of asphaltic materials at various temperatures and rates of loading. Kauffmann (38) studied the variations of fracture toughness K_{IC} with rate of loading and temperature (Figure 2.28). For sand-asphalt mixtures tested at 14, 73 and 32°F, it was reported that the critical stress intensity factor increased with the rate of load application. Similarly, the fracture toughness, K_{IC}, increased with the test temperatures. A series of 1" x 1" x 12" beam specimens were prenotched with notch sizes varying from 3/32" to 12/32" in depth before testing. The experimental results indicated that for such geometrical conditions, the K_{IC} is independent of c/d ratio and remains as a material constant.

Monismith and Salam (46), in their investigation of asphalt mixture behavior, conducted two types of fracture tests:

(i) Single-edge-notched bend specimens of 1.5" x 2.0" x 15" tested in four-point bending,

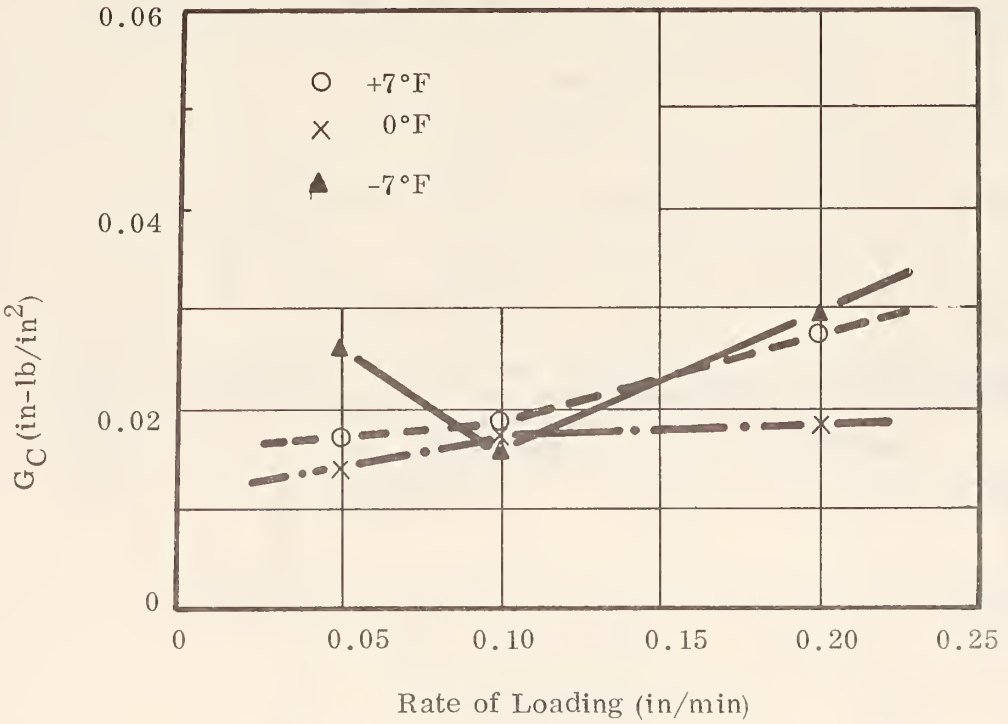

Figure 2.25. G_C versus the Rate of Loading for the Unaged 60-70 Asphalt

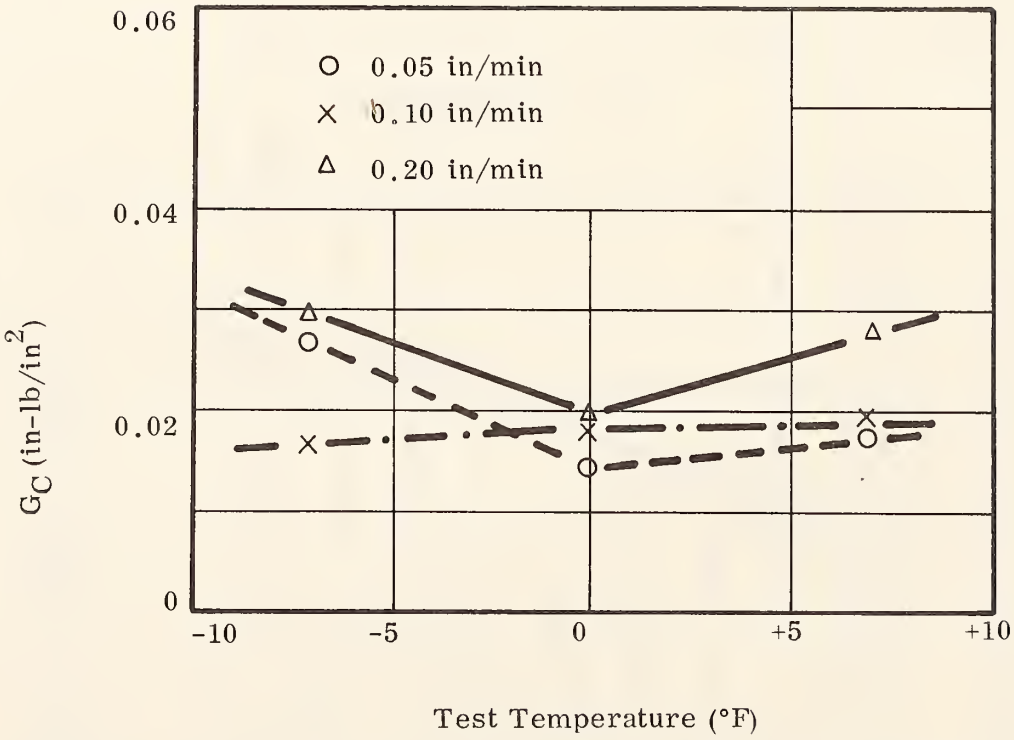

Figure 2.26. G_C versus the Test Temperature for the Unaged 60-70 Asphalt

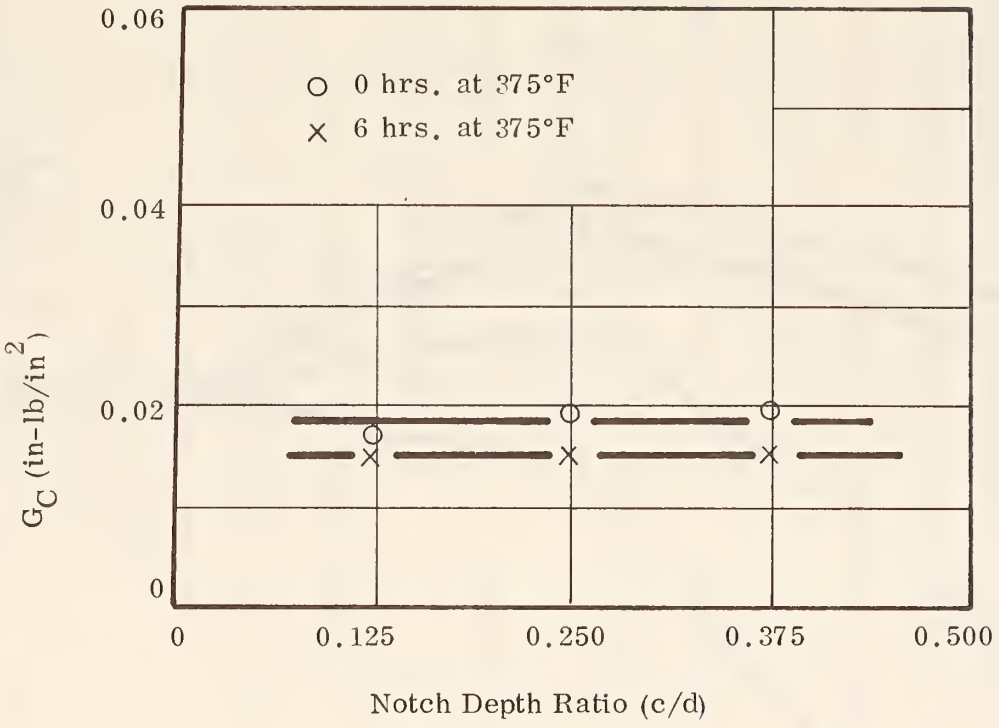

Figure 2.27. G_C versus c/d for the B-3056 Asphalt, Loaded at 0.10 Inches/Minute, Tested at 0°F

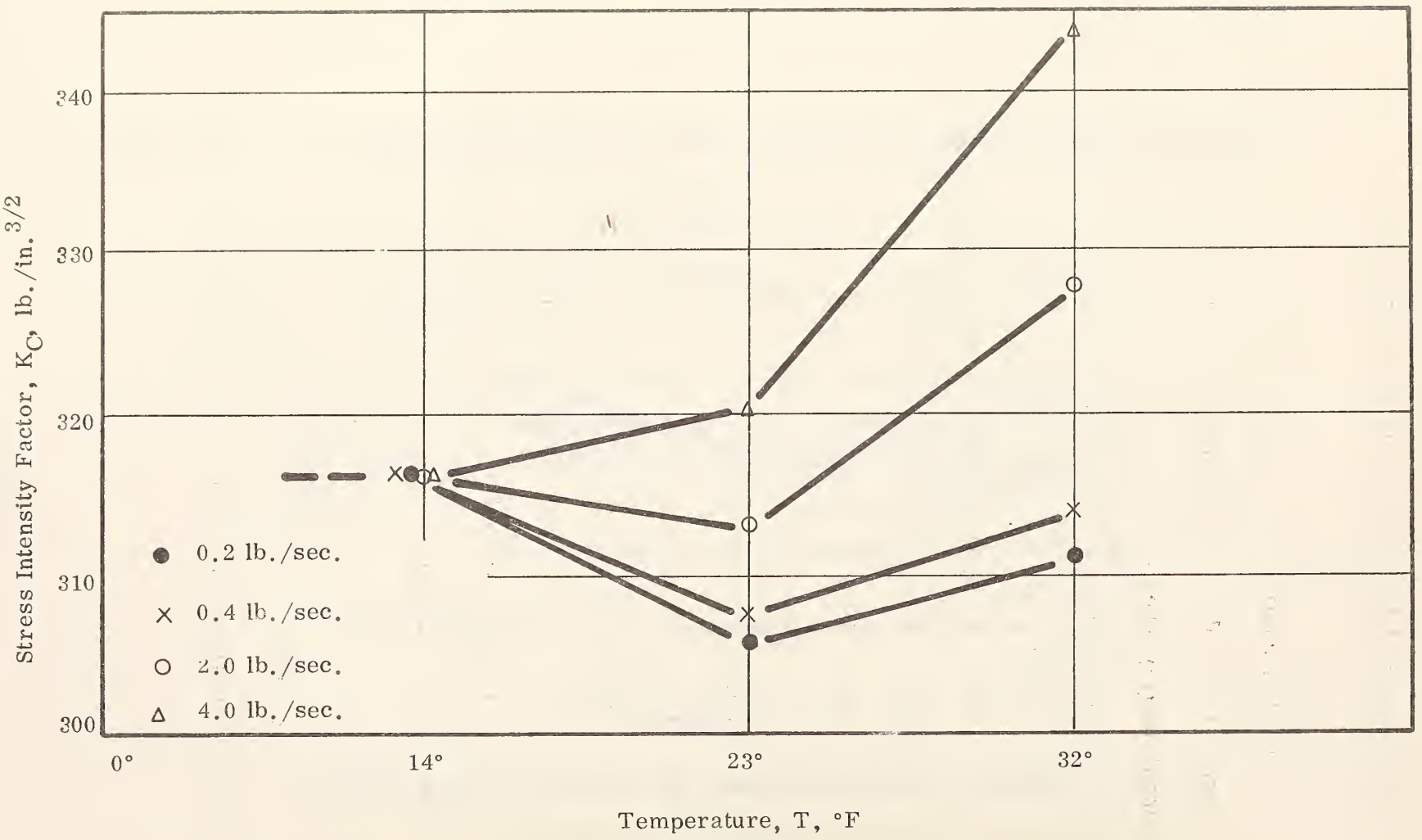

Figure 2.28. Stress Intensity Factor Versus Temperature for Sand Asphalt Mixes at Different Rates of Loading

(ii) Single-edge-notched tension tests on specimens of 1.5 x 1.5 x 4.5".

To maintain a constant loading condition, all specimens were tested at a loading time of about 0.5 seconds. The experimental results presented by Monismith and Salam(46) indicate that at low temperatures (less than 10°F) K_{IC} increases with asphalt content up to 8% level. At higher temperatures, the measured K_{IC} indicated a decrease with asphalt content. It has been postulated that an increase in the plastic flow and crack tip blunting might have been responsible for the reduction in K_{IC} parameter.

The effect of aggregate gradation, asphalt hardness (Figs. 2.29-2.32), and void content has been reported to be of lesser importance when specimens are tested at temperatures of 40°F or higher.

The aggregate type, on the other hand, were reported to have a significant influence on the fracture toughness.

Blight (3) has also investigated the fracture properties of paving materials. Utilizing the modified Griffith equation, the effective fracture surface-energy $\overline{\gamma}$ is given by

$$\sigma = \text{constant}\left(\frac{E\ \overline{\gamma}}{c}\right)^{\frac{1}{2}} \qquad (2.61)$$

where $\overline{\gamma}$ is the effective fracture surface-energy or the sum of the true surface-energy γ, and the plastic work, γ_p. The experimental results

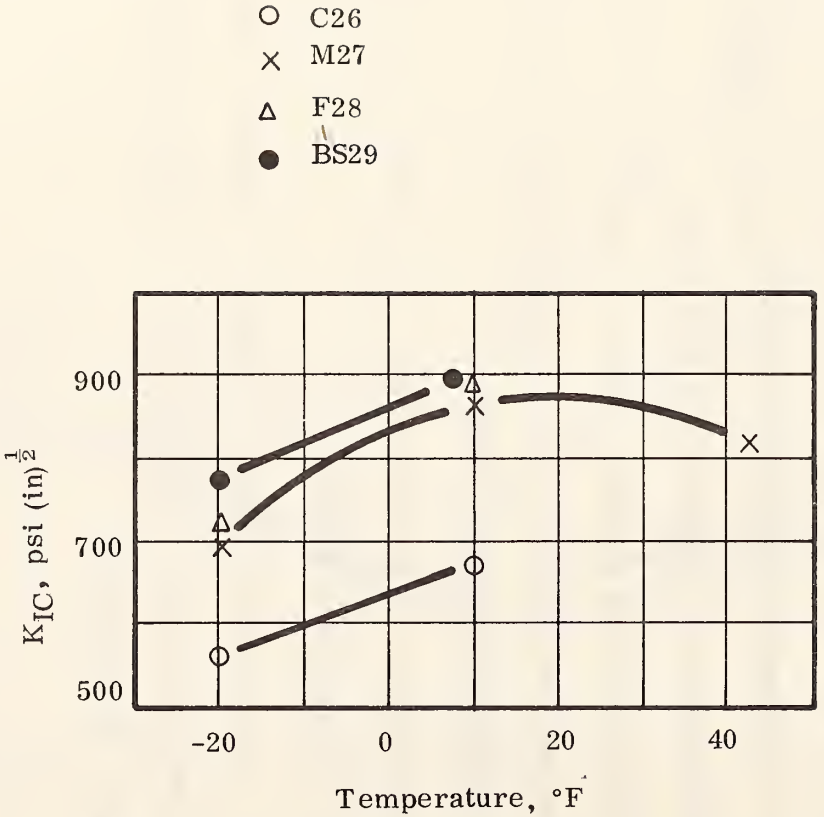

Figure 2.29. Influence of Aggregate Grading on Fracture Toughness - Tension Tests

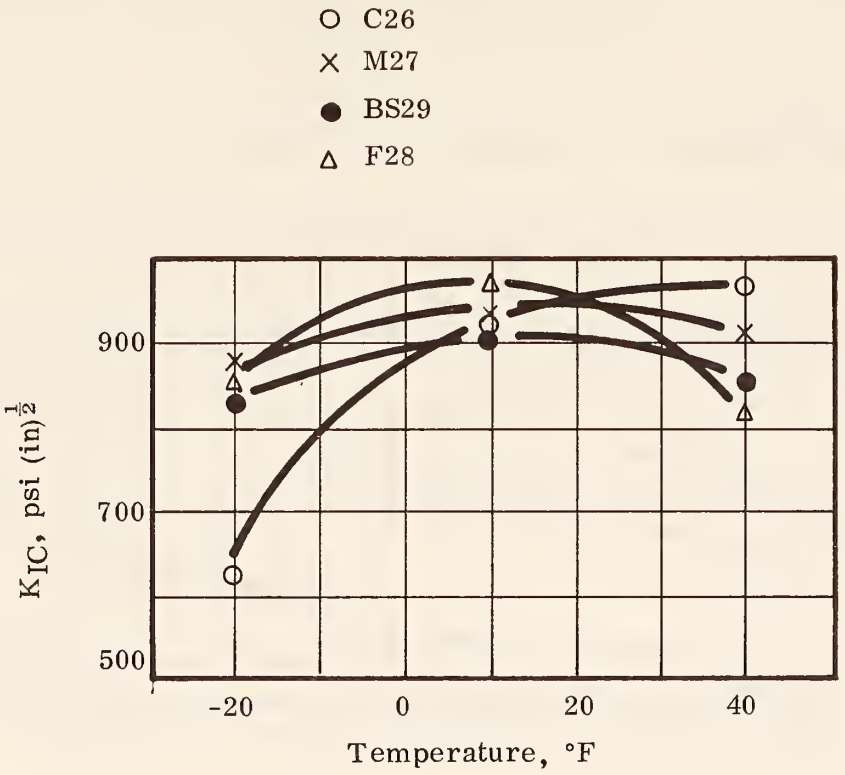

Figure 2.30. Influence of Aggregate Grading on Fracture Toughness-Bend Tests

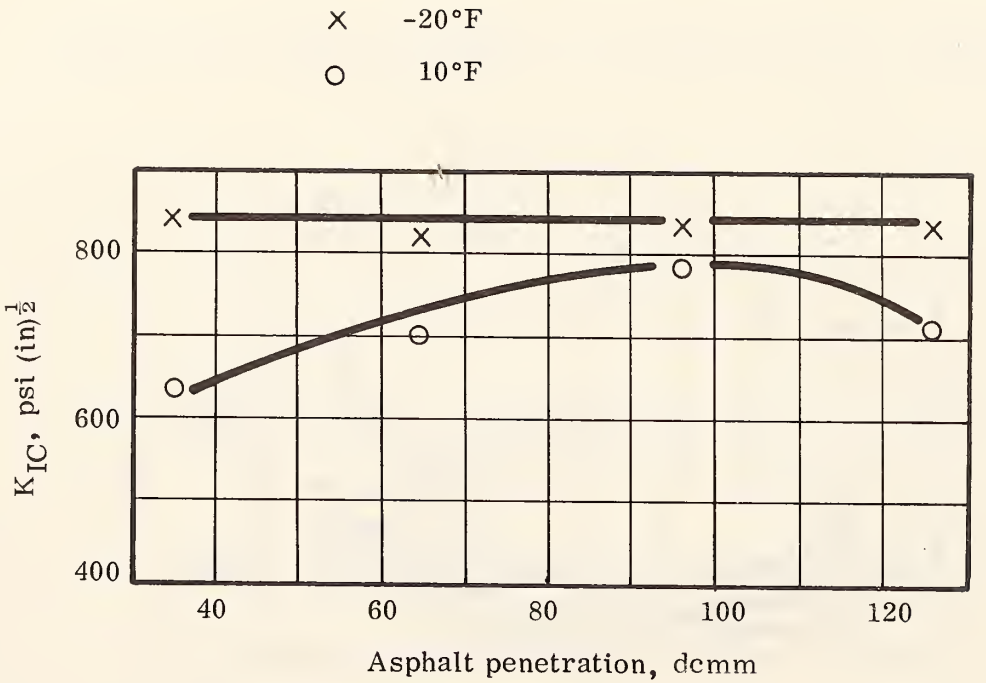

Figure 2.31. Fracture Toughness as a Function of Asphalt Penetation - Tension Tests

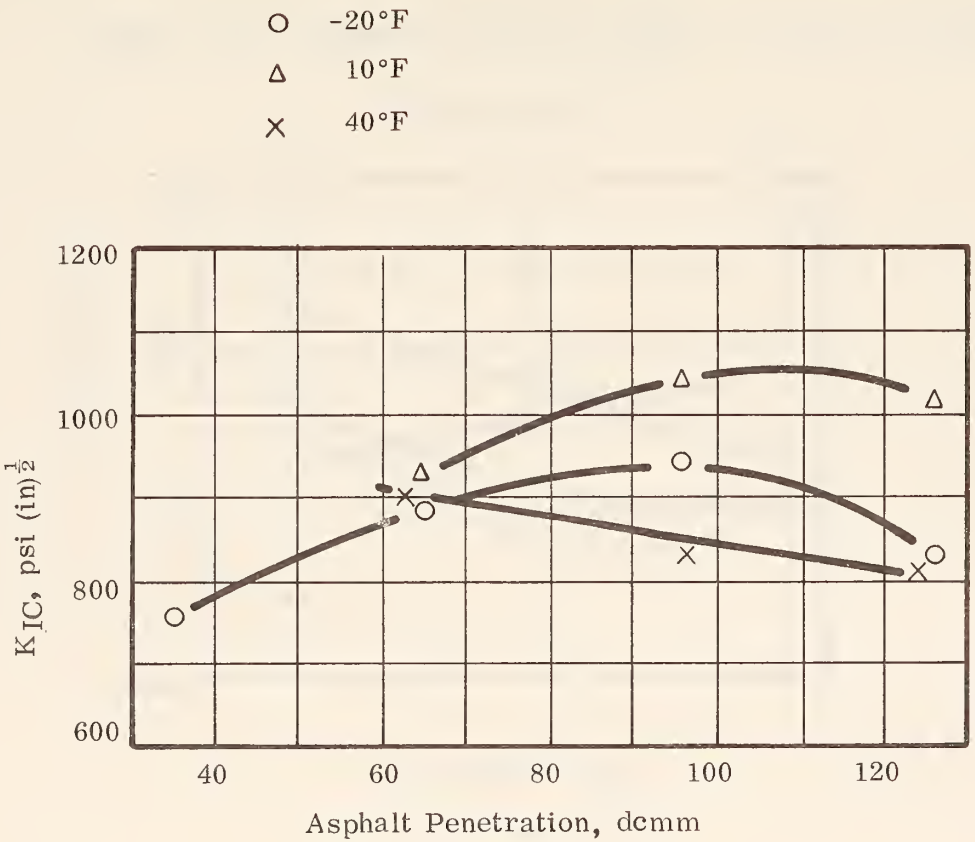

Figure 2.32. Fracture Toughness as a Function of Asphalt Penetration - Bend Tests

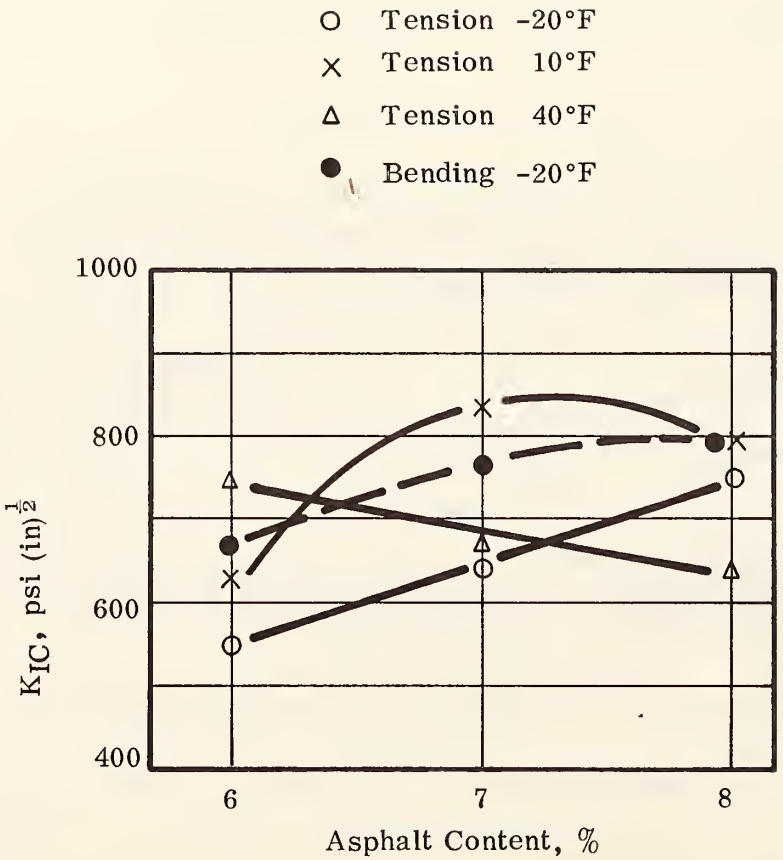

Figure 2.33. Influence of Asphalt Content on Fracture Toughness

presented indicate that the effective fracture surface-energy $\overline{\gamma}_p$ of asphaltic material is related to strain at failure and its value differs for various materials. However, it is noted that fracture surface-energy is independent of the method of testing employed.

III. MECHANISTIC MODELS FOR FATIGUE

A. Review

The "fatigue" is considered as a process of progressive damage or deterioration under repeated or cyclic loading which eventually leads to failure of the structural system. As a phenomenon of a highly complex nature, it involves a localized progressive structural change within the material, which can be subdivided into three stages: crack initiation, crack growth and terminal state of fracture. The occurrance of these processes in a material system result in a gradual weakening of the structural component. During the stage of crack initiation, microcracks are originated at centers of inpurities, flaws, and microstructural defects. These centers of strain-incompatibility, when subjected to reversed cyclic strain, are believed to be responsible for crack initiation process. The second stage of fatigue process is the crack propagation which at first is preceded by a zone during which micro-macro crack transitions occur.

The process of crack propagation and the terminal state of fracture have been treated by numerous theories. The introduction of fracture mechanics principle into analysis of fatigue of material systems has provided an analytical method of classifying the crack severity. It has also presented a rational scheme for the life expectancy calculations of structural systems.

In such a mechanistic approach it is postulated that the crack growth

is a consequence of the changing of the crack tip profile. During a cyclic deformation, a crack will undergo a phenomenon of blunting and resharpening. In tensile loading cycles, the crack tip tends to open first and then becomes blunted as the plastic zone forms and spreads ahead of the crack tip. During the unloading cycle, the elastic contraction of the material surrounding the crack imposes a residual compressive stress on the plastically-deformed material at the crack tip. This reduces ductility and resharpens the crack which aids the growth of the crack in the next loading cycle. This process leads to slow crack growth until the crack reaches a critical size, where unstable fracture occurs. The factors affecting the rate of crack growth are stress or strain amplitude and the defect size which determine the stress intensity at the crack tip.

The mechanism of the fatigue crack growth can be explained in classical terms of the energy balance at the crack tip. The work of the external force at the crack tip is divided into stored elastic energy, surface energy required to form cracks, and deformation energy required for some irreversible structural distortions. The rate at which a crack may propagate and the path it follows depends entirely on this energy balance at the crack tip. When there is a large amount of plastic deformation, the crack may become blunted and does not propagate or propagates very slowly. On the other hand, when the elastic energy released exceeds the energy demanded for creating new surfaces, the crack will propagate along the path which requires the

minimum amount of energy to create new surfaces.

The mechanistic formulation of the fatigue process is credited to Paris, Gomez and Anderson (59) who first introduced the application of the stress-intensity factor to fatigue crack propagation rates. In 1963, Paris and Erdogan found from experimental data that the crack propagation rate, $\frac{dc}{dN}$, was proportional to the fourth power of ΔK for a number of materials. This law of crack growth is expressed as $\frac{dc}{dN} = A K^n$, where A and n are material constant (n = 4.0).

The fourth power relation has been justified by consideration of the energy absorption within the entire plastic zone ahead of the crack tip (6). However, experimental data available on many engineering materials indicate that n might be smaller than four. In Figures (2.34 - 2.36), typical $\frac{dc}{dN}$ vs.K relations for metals are provided.As it is noted, the power constant n varies over a wide range depending on material characteristics and testing conditions.

The data available for asphaltic mixtures also indicate that constant n varies depending on asphaltic mixture characteristics. For fine grained asphaltic mixtures, as sand asphalt and surface course asphaltic concrete with small size aggregate, a more rapid crack propagation has been reported (33), (34), (35). The n = 4 condition has been also reported by Majidzadeh, et. al., (40), (36), (37), as valid for sand-asphalt mixtures tested under monotonic loading conditions. The random or block loading condition also has been found to be affecting the crack propagation process.

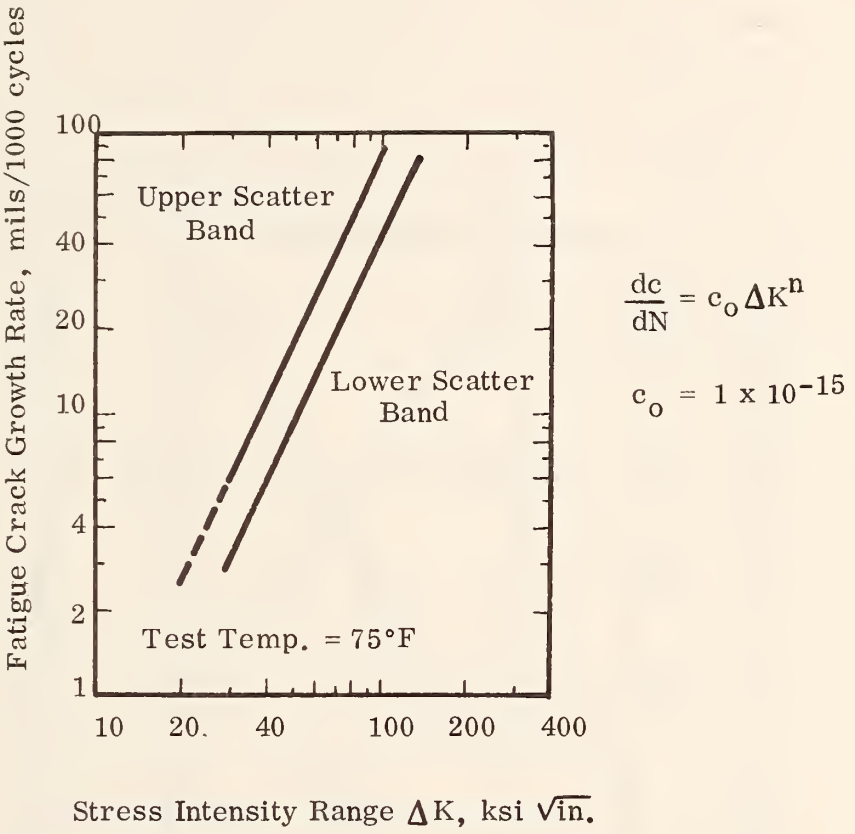

Figure 2.34. Fatigue Crack Growth Rate as a Function of ΔK

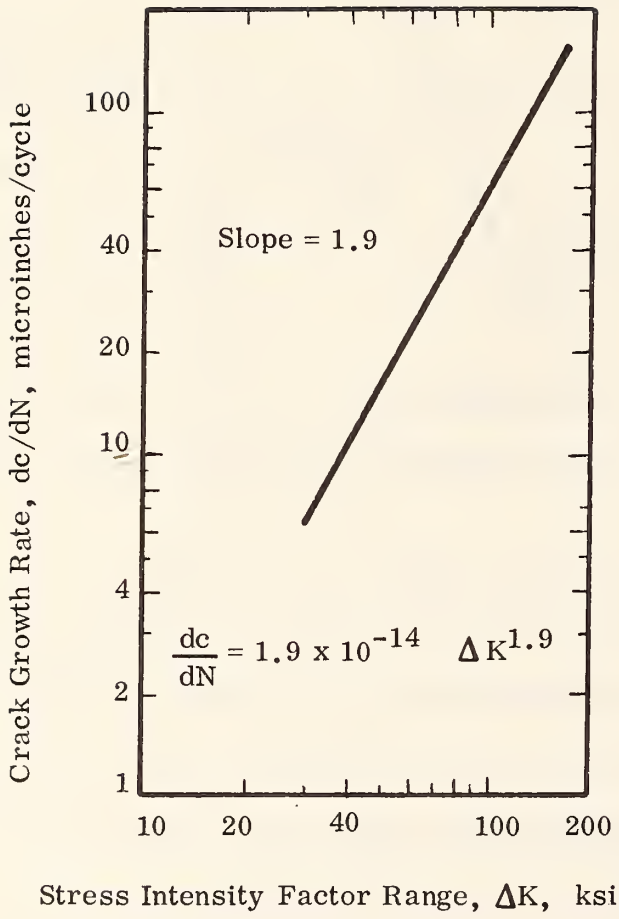

Figure 2.35. Fatigue Crack Growth Rate as a Function of ΔK

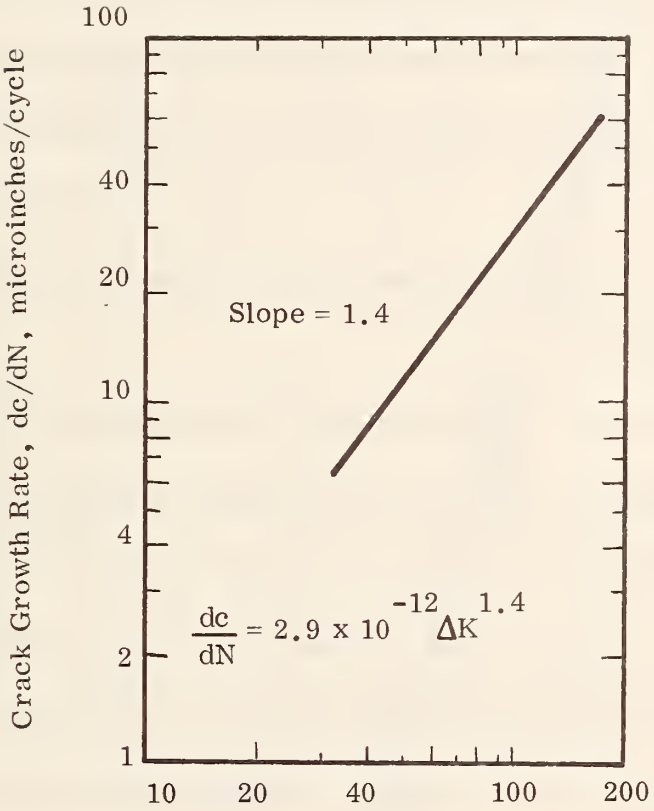

Figure 2.36. Fatigue Crack Growth Rate as a Function of ΔK

To incorporate the effect of other test variables, such as frequency, mean load and load range, a number of empirical equations have also been proposed in the literature. As an example, Mukherejee (49) has presented the following equation:

$$\frac{dc}{dN} = A\,(f)^{-0.43}\,(K_{max})^{3.37}\,(\Delta K)^{1.16} \qquad (2.63)$$

where f is frequency, K_{max} and ΔK are maximum stress intensity factor and $K_{max} - K_{min}$ respectively. This equation indicates that frequency of loading influences the crack growth rate. The effect of rest period has also been investigated by a number of researchers. It has been argued that the mechanism of crack propagation under dynamic loading and static conditions are similar except for the rest period effect.

The experimental results by Kauffmann (28) indicate that the fatigue crack growth process in asphaltic mixtures is considered as a stress-independent, stress-interaction type phenomena. It has been observed that for the range of variables investigated, the rest period does not significantly affect the fatigue life. The available data also indicate that load sequence has a significant effect on the fatigue life. The delay in the rate of crack propagation due to loads of variable amplitude in the loading sequence is attributed to the beneficial effects of residual stresses at the crack tip. Although the mathematical formulation of the delay phenomena has not yet been fully developed, the reduction in the crack growth rate can be evaluated experimentally (Figures 2.37 and 2.38).

The crack growth model has been, in recent years, subject to numerous

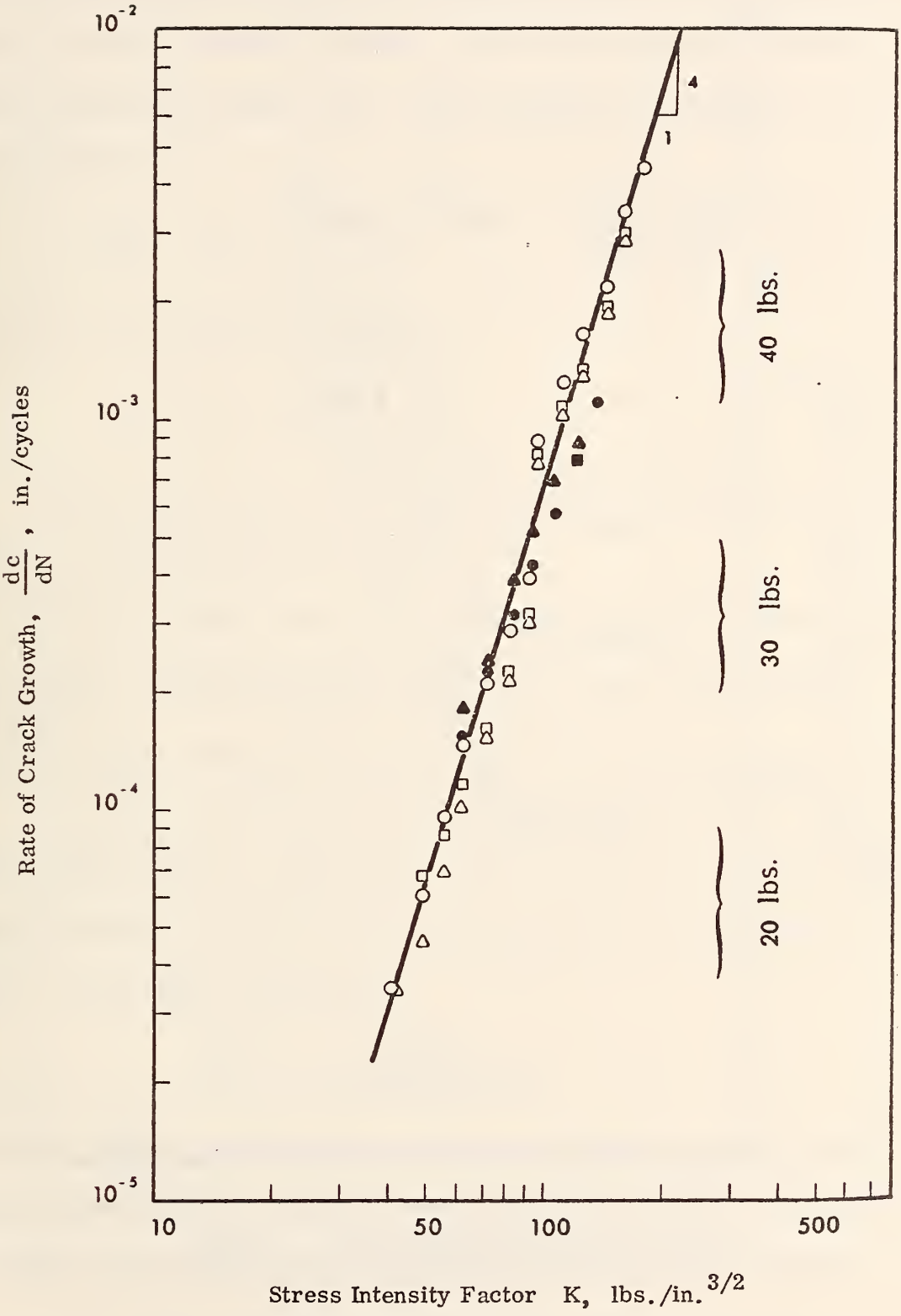

Figure 2.37 K versus $\frac{dc}{dN}$ for Monotonic Loading with Different Amplitudes

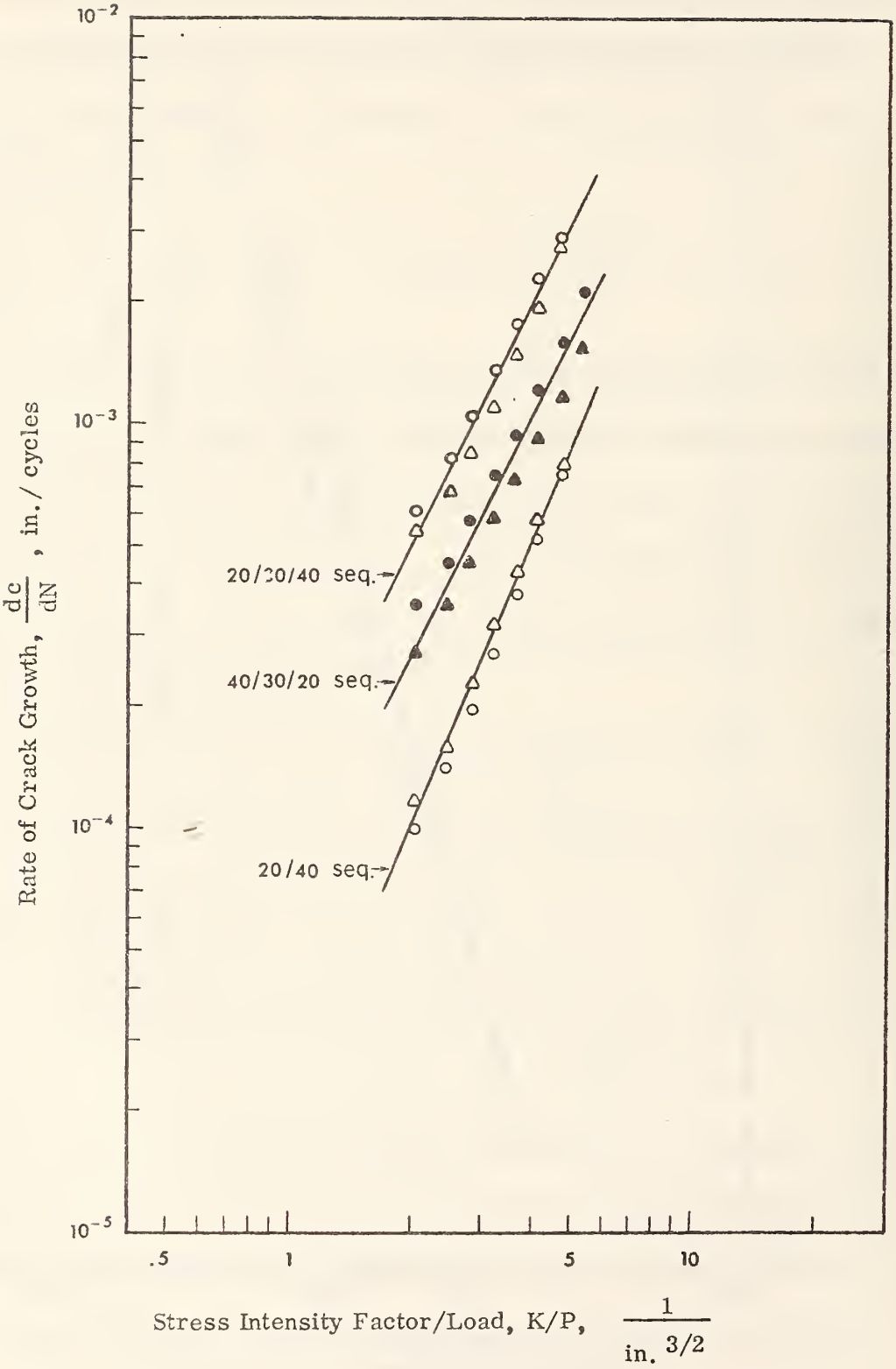

Figure 2.38 $\frac{dc}{dN}$ versus $\frac{K}{P}$ for Sequential Loads

100

modifications. One such analysis is the work of Cherepanov (6) who utilized the plastic work at the crack tip to develop a relationship between total plastic work and the stress-intensity factor. This development is presented by an equation given by:

$$\frac{dc}{dN} = \beta \left(\frac{(K^2_{max} - K^2_{min})}{K_C^2} + \ln\left(\frac{K_C^2 - K^2_{max}}{K_C^2 - K^2_{min}} \right) \right) \qquad (2.64)$$

where β is a material constant given by:

$$\beta = a_4 \frac{E K_c^2}{2 \sigma_y^2} \qquad (2.65)$$

In this equation, a_4 is a dimensionless parameter related to σ_y / E and ν where σ_y is the yield stress of the material.

The crack growth models are in general incorporated into three loading variables: mean stress-intensity factor K_{max}, cyclic stress-intensity factor $\Delta K = K_{max} - K_{min}$, and stress ratio given by $R = K_{min}/K_{max}$.

The effect of mean load and load range has also been incorporated in Pearson (62) and Porter (63) models of crack propagation. The Pearson (62) model is expressed in terms of R, load ratio and critical stress intensity factor. This model can be written as:

$$\frac{dc}{dN} = \frac{A (\Delta K)^n}{(1 - R) K_C - \Delta K} \qquad (2.65)$$

where $R = \frac{K_{min}}{K_{max}}$, and K_C is the critical stress intensity factor. Pearson (62) has indicated that for materials with relatively high critical stress intensity factor, the load ratio R does not significantly affect the crack growth

rate. However, for conditions where K_{max} approaches K_{IC}, the crack growth data should be modified as follows:

$$\frac{dc}{dN} = \frac{A K_C (\Delta K)^n}{(1-R) K_C - \Delta K^m} \qquad (2.66)$$

where m and n are constants.

In a more recent study, Majidzadeh et al. (41) have used the results of linear elastic fracture mechanics to study the fatigue of field asphaltic specimens. The analysis of fatigue and fracture of field specimens has indicated that the power n may not always be 4 and might vary with material characteristics and test conditions. There are indications that the conditions of the testing and the properties of the asphaltic mixtures may influence this power law. As an example, in this study, a power law of the second degree in K has proved to be of the highest correlation.

This observed difference in the exponent of the power law suggests that it might be desirable to review the models and recent advancements in the theory underlying the crack propagation process. This was done in the hope that the variables such as the power and material constants could be related to the fundamental properties of asphaltic concrete and the testing procedure.

It is well known that asphaltic concrete displays a delayed response due to loading. This rheological response depends on the environment and the rate of loading. It could be linear or non-linear, depending upon those conditions and the intensity of the load. Because of the complexity of this problem, linearity of the material will be assumed. It is realized that this assumption

may not hold under actual conditions, but with the present state of knowledge it is necessary.

This literature review will not be concerned with the micro-mechanics aspect of fracture or the fatigue problem. It will concentrate on the continuum mechanics perspective. Asphaltic concrete is assumed to be linearly viscoelastic, so that concepts from linear elastic fracture mechanics can be used.

It is not possible to discuss in detail the vast volume of research that has accumulated in recent years concerning the crack propagation problem. The work of some researchers will be reviewed briefly in preparation for certain applications.

B. Viscoelastic Fatigue Damage Modeling

The review of literature indicates that theoretical approach to analysis of generalized crack propagation problems involve consideration to three stages. The first stage is to obtain a solution for the boundary value problem, using the material constitutive equation which is, in this case, considered as a linearly viscoelastic material. The second stage is the use of a failure criterion and , lastly, a crack model assumption is needed.

1. Viscoelastic Boundary-Value Problem

Usually the solutions to viscoelastic boundary-value problems can be obtained by applying the classical correspondence principle. This is convenient as the solutions to elastic boundary value problems are readily

available and can be transformed to obtain the solution to the viscoelastic case. However, it should be noted that this simple correspondence principle cannot be applied to fracture problems since these problems involve moving boundaries (cracks). Graham (11) established a useful extension for crack problems. This extended correspondence principle applies with certain restrictions, as: the crack size should increase monotonically with time; the stresses are independent of elastic constants and finally these elastic constants appear in a separate factor in the displacement expression. The crack closure case does not satisfy the first restriction. All three restrictions are satisfied for all quasi-static problems if tractions are specified on the boundaries, tractions on crack surfaces are self-equilibrating and there are no body forces.

To obtain the solution to the viscoelastic BVP, the Laplace transform of the elastic solution for the same BVP is taken. Next, the elastic constants are replaced by the transformed viscoelastic expressions. Finally, the expressions are inverted back to the time domain. In the case of a crack with the above restrictions, the stresses will be the same for the elastic and the viscoelastic cases. The displacement, however, will be rather complicated for the viscoelastic case and will involve convolution integrals. The complexity of the displacement expression is the reason for the lengthy mathematics and some of the simplifying assumptions involved.

2. Fracture Criteria

The fracture criteria used by most investigators are modifications of the Griffith energy balance formulation. Consider the energy balance equation:

$$\dot{U} = \dot{V} + \dot{T} + \dot{D} \tag{2.67}$$

where U = the work done by the external loads
V = the elastic stored energy
T = the kinetic energy
D = irreversible energy such as surface energy, plastic work, and viscous dissipation.

The dot indicates differentiation with respect to time. Theoretically, these energies can be evaluated for the particular boundary value problem. They can be used in conjunction with the equation of motion to obtain a solution for the rate of crack extension (Erdogan, 8). In practice, this is very difficult to apply. Simplifications in analysis lead to the assumption of a plane symmetric problem with no body forces, and neglecting kinetic energy. The energy balance will then become:

$$\iint_S T_i^{\nu} \dot{u}_i \, ds = \iiint_R \sigma_{ij} \dot{\epsilon}_{ij} \, dR + 4\Gamma_f \dot{a} \tag{2.68}$$

Γ_f being the specific fracture energy.

To simplify this quasi-static problem considerably, a local energy balance can be used in a region surrounding the crack tip. The assumption implied here is that the size of the plastic zone is small compared to the region where the energy balance is applied. Consider the following two figures (Knauss, 29):

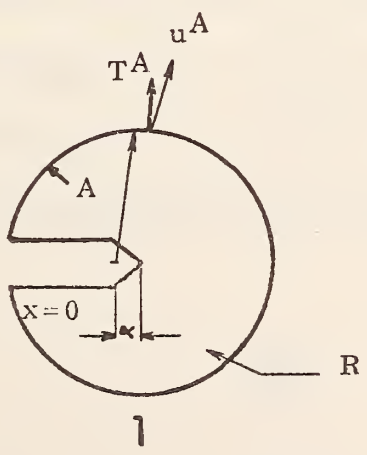

1

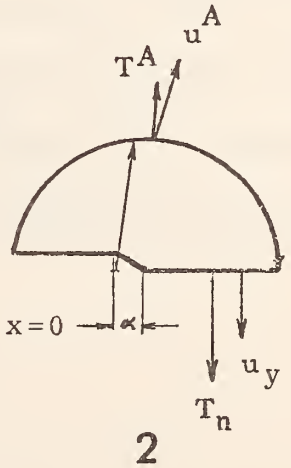

2

For Figure 1, the energy balance is:

$$\dot{U} = \dot{V} + \dot{D} + 2\ \dot{S} \tag{2.69}$$

$\dot{D}$ = rate of change of dissipated energy; $\dot{S}$ = rate of change of surface energy.

For Figure 2, there is no S since there is no crack:

$$\tfrac{1}{2}\dot{U} = \tfrac{1}{2}\dot{V} + \int T_n\ ,\ \dot{U}_y\ dx + \tfrac{1}{2}\dot{D} \tag{2.70}$$

Comparing the two, it is evident that:

$$\int T_n\ \ \dot{U}_y\ dx = \dot{S} = \Gamma_f\ \ \dot{a} \tag{2.71}$$

This is for a traction-free crack. This local energy principle applies to many BVP's as was used by various investigators (29,31,47,69,79). It can be stated simply as with crack advancement the work of the released tractions goes into creating new surfaces.

3. Crack Model Assumption

The crack models presented in the literature are primarily those of Griffith, Barenblatt, Dugdale, etc. The Griffith model is the oldest and simplest. It considers the crack to be in a perfectly brittle material. There is no yielding at the crack tip although the stresses can be very high. The resulting equation is:

$$\sigma\ a^{\frac{1}{2}} = K \tag{2.72}$$

where σ is the stress applied at the boundaries of the infinite plate, a is half the crack length and K is the stress intensity factor.

The Dugdale model assumes a thin plastic zone at the tip of the crack. This special configuration yields an estimate of the plastic zone size as:

$$\frac{\alpha}{a} = 2 \sin^2 \frac{\pi}{4} \frac{\sigma}{Y} \approx \frac{\pi^2}{8} \frac{\sigma^2}{Y^2} \quad \left(\text{for } \frac{\sigma}{Y} << 1\right) \tag{2.73}$$

where α is the size of the plastic zone, Y is the yield stress, σ and a as above.

The Barenblatt model (4) proposes the addition of cohesive forces along the faces of the crack that resist the opening of the crack. This model is advantageous in getting rid of the singular solution at the tip of the crack inherent in the above models:

$$N_o = \sqrt{\frac{\alpha}{\pi}}\, \sigma_m I_1 \tag{2.74}$$

where $N_o = \frac{K_I}{\sqrt{2\pi}}$, I_1 is some integral depending upon the assumed stress distribution, σ_m is the maximum stress in the cohesive zone. The Barenblatt model includes the Dugdale model as a special case.

It is possible now to combine the results of the boundary-value problem solution, the crack model, and the failure criterion to obtain a solution for the crack problem in viscoelastic media. This can be quite involved due to the presence of convolution integrals in the expressions written for the displacement. To get rid of the complexities of this problem, Williams (76) studied

the simple geometry of a spherical cavity in a body under all-around tension. Since variations in the crack shape result only in the change of a constant in the criticality condition, the study of a simple geometry will still reflect the viscoelastic character of fracture. In this manner Williams did not have to assume a crack model, he used a simple cavity for which the BVP solution is simple. In this manner the calculations become simpler. He applied a global energy balance, and for the case of a step load, he obtained:

$$\frac{\sigma_{oc}}{1 - \left(\frac{a_o}{b}\right)^3} = \frac{4}{3}\sqrt{\frac{T/a_o}{2\ J(t_o) - J_g}} \qquad (2.75)$$

where a_o = cavity radius

b = the radius of body

T = the fracture energy

J = the creep compliance

J_g = the glassy compliance

The Griffith solution can be retrieved from the above formula for the glassy case by putting $J(t_o) = J_g$.

Other investigators assumed actual crack models rather than a simple cavity. The work of these investigators will be grouped according to the models they assumed and are presented in the following sections of this chapter.

4. Analysis Procedure

a. Griffith Geometry

Knauss (30) studied the Griffith geometry for the case of a linear viscoelastic material. Using a local energy balance equation and assuming the stress distribution at the top of the crack to be given by the linearly viscoelastic solution, he obtained:

$$\sigma_{oc} = k \sqrt{\frac{T/a(t)}{J\left(\frac{\alpha}{\dot{a}}\right)}} \tag{2.76}$$

where $a(t)$ = half of crack length

α = the size of the crack failure zone.

It is noted that this equation is more complicated than Williams' result because of the more complex geometry. Since the crack length depends on time and its first derivative is in the argument of the creep function, the resulting equation is a nonlinear first order differential equation. Its solution depends on some approximations and whatever creep function is assumed.

Mueller (47) studied the problem of a large crack in an infinitely long strip under a prescribed strain in the lateral direction. Superposition of two simple problems was used to obtain a nondimensional stress intensity factor and the size of the crack opening. The solution was obtained assuming a stationary crack with a sudden application of the prescribed strain. This same problem was extended to study crack propagation by applying a local energy balance (48). It was found that the crack tip velocity depends on geo-

metry, applied load and its history, and material properties as follows:

$$\epsilon_o E_r = \sqrt{\frac{3}{2} \frac{T/b}{G\left(\frac{\alpha}{a}\right)}} \tag{2.77}$$

where ϵ_o = the prescribed step strain

E_r = the long time relaxation modulus

b = half width of the strip

G = some function of the creep compliance

If $\epsilon_o E_r$ is thought of as the stress, the similarity of this result to the previous ones is immediately obvious.

For crack propagation under variable load histories, Knauss and Dietmann (31) used the local energy balance approach, assuming the distribution of the stresses ahead of the crack to be of a singular form and of a certain variation. The displacement corresponding to this stress distribution is obtained by using the extended correspondence principle. The power equation is applied and a differential equation for the crack tip velocity as a function of the time history of the stress intensity factor is obtained. The equation is a complicated nonlinear differential equation and for specific stress histories, might be simplified. If the stress intensity factor does not change rapidly, then the result is the same as in Reference (48). The case for a cyclic strain input was also examined and some graphic results were given. It is pointed out that the complexity of the differential equation makes it of little practical interest in its present form.

It is noted that in all of the above work, no special consideration of the character of the material at the crack tip was made. This zone is usually very highly stressed; it is probably in a plastic state or might even be in a disintegrated state though not yet cracked. Although the behavior of the material in this zone is not well understood, one might be able to make some assumptions that will simplify the calculations. The material around the crack tip is probably highly nonlinear and therefore making such assumptions will not necessarily lead to less exact results than the linearity assumption that is implied in the previously discussed literature.

It has been shown by some investigators that the material at the tip of the crack is crazed and of a lower density than the rest of the material. The material behavior here is very similar to metal yield and is in a wedge-like shape. Wnuk and Knauss (81) used these observations to assume the viscoplastic model of Crochet for the tip of the crack while the bulk material is linearly viscoelastic. A solution by Graham (11) for a crack opened by a normal pressure acting on its surface was used along with the assumed yield model. With some assumptions, the final nonlinear differential equation will be:

$$\dot{y}^2 - y\ddot{y} = y^2 \left(P(t)\,\dot{y} + Q(t) \right) \tag{2.78}$$

where $y(t) = Y(t) - A$, $Y(t)$ is the time dependent yield and A is a material constant from Crochet model.

$P(t) = \frac{\sqrt{2}\,\chi\, C}{E_g}\,\dot{\psi}(t)$ where $\chi = 1/2\,(1-\nu)\,(1+\nu)$, C is a material constant from the Crochet model, E_g is glassy modulus, and $\dot{\psi}(t)$ is the slope

of nondimensional creep compliance J(t)/J(o) and finally $Q(t) = \frac{2}{\sqrt{2}} \frac{\chi C}{Eg} (A+B) \ddot{\psi}$ where B is also a material constant in the Crochet model. This differential equation is also very difficult to solve in general. A simple case of a Maxwell model is solved in (81). Another possibility is to assume a time independent yield and the result will be simpler (81).

b. Dugdale Crack Model

This model was used by many workers in the field of fracture because of its simplicity. Wnuk (78), (79), (80) used it to simplify his mathematical derivations. Wnuk proposed a nonlinear differential equation to describe the quasi-static subcritical growth of a crack. He derived this equation in a simple way by applying a local energy balance:

(a) Amount of energy supplied during a δ L advance of the crack is:

$$\Delta U = \left.\frac{\delta U}{\delta L}\right)_{\sigma} \delta L + \left.\frac{\delta U}{\delta \sigma}\right)_{L} \frac{d\sigma}{dL} \quad \delta L \tag{2.79}$$

The first term is for creation of new surfaces and the second is for strain redistribution.

(b) Amount of energy demand is: $\Phi_c \quad \delta L$

$$\therefore \quad \left.\frac{\delta U}{\delta L}\right)_{\sigma} + \left.\frac{\delta U}{\delta \sigma}\right)_{L} \frac{d\sigma}{dL} = \Phi_c \tag{2.80}$$

This equation can be put in a simpler form:

$$G + M = G_C \tag{2.81}$$

where G = the energy release rate

M = the slow growth operator

G_C = the critical energy for onset of rapid fracture.

For the case of an elastic solid with a plastic region surrounding the crack tip the G and M operators are (78):

$$G = 2\,Y\,u_{tip} + 2\,Y\,\frac{\delta}{\delta l}\int_{l}^{a} u\,(x)\,dx \qquad \text{and}$$

$$M = 2\,Y\,\frac{d\sigma}{dl}\,\frac{\delta}{\delta \sigma}\int_{l}^{a} u\,(x)\,dx \tag{2.82}$$

where Y = the constant yield stress in the plastic zone

σ = the applied stress

l = half the crack length

a = half the crack length plus the yield zone length

$u(x)$ = the displacement normal to the crack plane.

For the viscoelastic case with a plastic yield zone the differential equation can be extended as simply (78):

$$(G + M)\,\Psi\left(\frac{\Delta}{L}\right) = G \tag{2.83}$$

where Ψ = the normalized creep compliance function, and

Δ = the inherent opening distances.

This differential equation can be simplified by (78):

(a) Assume linear range $\frac{\sigma}{Y} \ll 1$ and, therefore, $\frac{\Delta}{L} << 1$, then

$$G = 2\,Y\,u_{tip}$$

$$M \cong 2\,Y\,\frac{do}{dl}\,\frac{\delta}{2\sigma}\left(\frac{\Delta}{3}\,U_{tip}\right) \tag{2.84}$$

$$U_{tip} = \frac{G}{2Y} \qquad \text{and} \qquad \Delta = \frac{\pi E}{8\eta Y^2}\,G$$

and so M becomes:

$$M \cong \frac{\pi E G}{12 \eta Y^2} \frac{dG}{d\sigma} \frac{d\sigma}{dl} \quad \text{where } \eta = \begin{cases} 1 & \text{plane stress} \\ 1-\nu^2 & \text{plane strain} \end{cases} \tag{2.85}$$

and the differential equation becomes:

$$\left[1 + \frac{\pi^2 l \sigma}{6Y^2} \cdot \frac{d\sigma}{dl}\right] G \Psi\left(\frac{\Delta}{l}\right) = G_C \tag{2.86}$$

(b) Assume a Dugdale model for the crack tip shape. Using a solution for the displacement normal to the crack, Wnuk finally puts the differential equation for the elastic case in the form:

$$\frac{d\beta}{d\zeta} = \frac{3}{2}\frac{2-\zeta\beta^2}{\zeta^2\beta^3} \quad \text{for plane crack}$$

$$\frac{d\lambda}{d\zeta} = \frac{3}{2}\frac{2-\zeta\lambda^2}{\zeta^2\lambda^3} \quad \text{for penny-shaped crack} \tag{2.87}$$

where $\beta = \frac{\pi\sigma}{2y}$, $\lambda = \frac{\sigma}{y}$

$$\zeta = \frac{l}{l_*} \quad \& \quad l_* = \frac{\pi K_c^2}{8 y^2}$$

For the viscoelastic case, the differential equation is:

$$\left(\frac{2}{3}\zeta\beta + \frac{C}{\dot{\beta}}\right)\frac{d\beta}{d\zeta} = \frac{2-\zeta\beta^2}{\zeta\beta^2} \quad \text{plane crack}$$

$$\left(\frac{2}{3}\zeta\lambda + \frac{C}{\dot{\lambda}}\right)\frac{d\lambda}{d\zeta} = \frac{2-\zeta\lambda^2}{\zeta\lambda^2} \quad \text{penny-shaped crack} \tag{2.88}$$

where $C = \dot{\psi}\Big|_{\dot{l}=0} \frac{\Delta}{l}$

Though these differential equations have no closed form solutions, it will be seen later how they can be of help in determining the form of the crack propagation law with some approximations.

c. Barenblatt Crack Model

In the above Dugdale model and the previous modified Griffith model, assumptions were made regarding the failure zone behavior. In the Barenblatt equilibrium model, the behavior of the failure zone is arbitrary. This is much more general and covers the others as special cases.

Schapery (69) utilized the Barenblatt equilibrium model, a local energy criterion, and the elastic solutions of Williams and Barenblatt. By superposing the elastic solution of Williams for a crack in a plane strain due to external loading and the solution of Barenblatt for a crack with a stress of σ_f in the failure zone with no external loading, one obtains an expression for the stress intensity factor and the displacement (69):

$$N_0 = \sqrt{\frac{a}{\pi}}\ \sigma_M\ I_1 \tag{2.89}$$

where $$I_1 = \int_0^1 \frac{f(a\eta)\, d\eta}{\sqrt{\eta}}$$

$\eta = \frac{\xi}{a}$ and

$f = \frac{\sigma_f}{\sigma_m}$ is the distribution of σ_f in terms of maximum stress.

N_0 is the stress intensity factor of Barenblatt and is:

$$N_0 = \frac{K_I}{\sqrt{2\pi}} \tag{2.90}$$

The expression for N_0 can be thought of as a relation for the size and nature of the failure zone. The displacement expression is:

$$v = -\frac{2Ce}{3\pi}\frac{\sigma_m}{\alpha} I_2 \xi^{3/2} H(\xi) \quad \text{, where} \tag{2.91}$$

$$Ce = \begin{cases} \frac{4(1-\nu^2)}{E} & \text{, plane strain} \\ 4/E & \text{, plane stress} \end{cases}$$

$$I_2 = \int_0^1 \frac{df}{d\eta}\frac{d\eta}{\sqrt{\eta}}$$

and H = Heaviside function.

Now that the elastic stress and displacement expressions are available, the extended correspondence principle can be utilized to get the viscoelastic counterparts. Here, an assumption of a constant Poisson's ratio will simplify matters and only the uniaxial creep will enter the equations.

When the displacement expression is transformed to the viscoelastic case, a convolution integral arises. The assumption of small curvature on a log-log plot of the creep compliance is used to reduce the convolution integral for displacement to a simple product form by using a power law representation for the creep compliance. The final step is applying the local energy balance and Schapery obtains:

$$C_V(\tilde{t}_\alpha) = \frac{4\Gamma}{\pi N_o^2} \quad \text{where} \tag{2.92}$$

$C_V(\tilde{t}_\alpha)$ is the creep compliance with the argument, $\tilde{t}_\alpha = \lambda_n^{1/n}\frac{\alpha}{\dot{a}}$, and is some function of n which arises in using the power creep curve; α is the failure zone size and can be found from:

$$\alpha = \frac{\pi^2 N_o^2}{\sigma_m^2 I_1^2} \quad ,$$

Γ is the fracture energy, N_0 is the stress intensity factor of Barenblatt, and for the opening mode is equal to $\frac{K_I}{\sqrt{2\pi}}$, σ_m is the maximum of the failure zone stress distribution and I_1 is some integral which depends on the assumed stress distribution. Γ, σ_m and I_1 are considered fracture properties and experiments should help in their determination.

Knauss (29) also used the Barenblatt equilibrium model because of its generality and the finiteness of stresses at the crack tip. He points out that the Dugdale Model is a special case of the Barenblatt model. He uses two criteria for crack propagation: the energy criterion and the maximum strain criterion. His final results have a convolution integral in the expressions written for the crack propagation rate. It is pointed out that this work is very similar to the above work by Schapery, except that no approximation was used by Knauss to eliminate the convolution integral.

5. Theoretical Models For Fatigue Process

The next logical step is to extend the above concepts and methods of solution to problems involving repeated loads. This is not as straightforward as it might appear and further mathematical simplification and assumptions will be needed. Only the procedures which result in an explicit relation for the crack propagation law will be considered here. The others which can be solved by other techniques but for which an explicit form is not readily available will not be considered further.

Wnuk (80) uses his resulting differential equation to study the case for repeated loads. Fatigue is viewed as a sequence of extensions. Consider the case for the plane crack:

$$\left(\frac{2}{3}\,\xi\beta + \frac{C}{\beta}\right)\frac{d\beta}{d\xi} = \frac{2-\xi\beta^2}{\xi\beta^2} \tag{2.93}$$

Assuming crack length constant in a cycle, it can be shown that:

$$\frac{d\beta}{dn} = \frac{1}{12}\,\xi^2\left(\beta_{max}^4 - \beta_0^4\right) + \frac{c\,\xi}{6<\beta>}\left(\beta^3 - \beta_0^3\right) \tag{2.94}$$

If β_0 is assumed to be above the minimum cycle stress and $<\beta> = 2f$, where f is the frequency, the final result will be after changing to dimensional quantities:

$$\frac{dl}{dn} = \frac{l_*}{3}\left(\frac{\Delta K}{K_C}\right)^4 + \frac{c\,l_*}{12f}\left(\frac{\Delta K}{K_C}\right)^2 \tag{2.95}$$

The first term being the familiar Paris law, the second term is due to the rate dependency of the material. Another similar result was obtained by Wnuk but with slightly different assumptions, such as the possibility of extension during unloading:

$$dl/dn = \frac{l_* a^2}{12}\left\{4a^2\left(\frac{\Delta K}{K}\right)^4 + 9C f^{-1}\left(\frac{\Delta K}{K}\right)^2\right\} \tag{2.96}$$

where $a = \frac{\Delta K_{eff}}{\Delta K}$ $\qquad$ $K_{eff} = K\Psi^{1/2}\{\frac{\Delta}{l}\}$

Schapery's (69) analytical approach can be solved to get an explicit relation for the tip velocity:

$$C_v(\tilde{t}_\alpha) = \frac{4\Gamma}{\pi N_0^2} \tag{2.97}$$

or

$$C_v\left(\lambda_n^{1/n}\,\frac{a}{\dot{a}}\right) = \frac{4\Gamma}{\pi N_0^2}$$

Putting in the power creep law, $C_v(t) = C_1 t^n$:

$$C_1 \left(\lambda_n^{1/n} \frac{a}{\dot{a}} \right)^n = \frac{4\Gamma}{\pi N_0^2}$$

$$C_1 \lambda_n \frac{a^n}{\dot{a}^n} = \frac{4\Gamma}{\pi N_0^2} \tag{2.98}$$

but $$a = \frac{2 N_0^2}{\sigma_m^2 I_1^2}$$

$$C_1 \lambda_n \left(\frac{\pi^2 N_0^2}{\sigma_m^2 I_1^2} \right)^n \cdot \frac{\pi N_0^2}{4\Gamma} = \dot{a}^n$$

so $$\frac{da}{dt} = \left(\frac{C_1 \lambda_n \pi^{2n+1}}{4\Gamma} \right)^{1/n} \frac{N_0^{2+2/n}}{\sigma_m^2 I_1^2} \tag{2.99}$$

For crack growth in one cycle, it is assumed that crack growth per cycle is small and it is furthermore assumed a wave shape of stress intensity factor, $\omega = \frac{N_0}{N_{0m}}$. N_{0m} is the maximum value of the stress intensity factor. Then,

$$\frac{da}{dN} = B N_{0m}^{2(1+\frac{1}{n})} \tag{2.100}$$

where $$B = \left(\frac{C_1 \pi^{2n+1} \lambda_n}{4} \right)^{1/n} \int_t^{t+t_p} \frac{\omega^{2(1+\frac{1}{n})}}{\Gamma^{1/n} \sigma_m^2 I_1^2} \, dt$$

Schapery argues that if bitumen completely surrounds the tip and for temperatures not close to the glass transition temperature, the slope may be taken as 1 and the Paris power law is retrieved. Usually though, $0 \leq n \leq .5$ for viscoelastic materials, implying the power is 6.

C. Generalized Fatigue Models: Dimensional Analysis

The above review of fracture and fatigue in viscoelastic media indicates that there is much similarity in the fatigue process for elastic and viscoelastic media. The next few pages will deal with fatigue laws obtained from dimensional analysis, applying in general to any material.

Kang and Liu (26), assuming a plane strain condition and small scale yielding, applied dimensional analysis to the problem of crack growth. For these assumptions, he argued, the crack tip region can be scaled by the size of the plastic zone. This means that the stresses and strains at the geometrically similar points are the same for various levels of stress intensity factors. Therefore, stresses and strains must be the same within crack increments ∂a if ∂a is proportional to the size of the plastic zone. If the material is homogeneous, then da/dN is proportional to r_p:

$$da/dN = f_1(R)\, r_p , \tag{2.101}$$

where r_p is the size of the plastic region and is proportional to $(\Delta K)^2$. Therefore,

$$da/dN = f_2(R)\, (\quad K)^2 \tag{2.102}$$

In analyzing actual data, Kang and Liu found that the power of the above model varied depending on the level of ΔK. The following figure illustrates this variation.

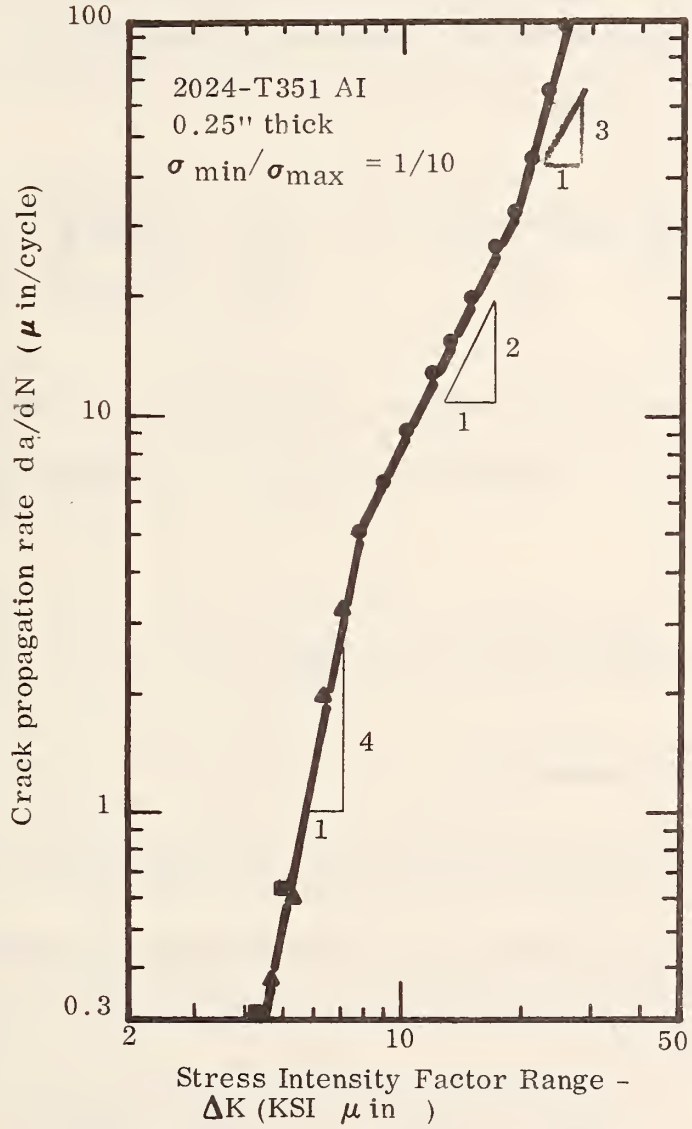

Figure 2.39 Typical fatigue crack propagation data for 2024-T351 aluminum alloy (from Kang and Liu)

The figure shows that for low ΔK, the power (the slope) is 4 or more. Also, for high ΔK, the slope is also 4 or more. For the intermediate region, the slope is close to 2. Kang and Liu also point out that these regions might be better fitted by curves rather than straight lines. This has been the recent experience at Ohio State University as well (41).

To illustrate this point further, the dimensional analysis of Cherepanov and Halmanov will be reviewed. Assuming continuous crack growth and a constant dissipation energy, they obtain:

$$\frac{da}{dN} = -\beta\left(\frac{K_{max}^2 - K_{min}^2}{K_C^2} + \ln\frac{K_C^2 - K_{max}^2}{K_C^2 - K_{min}^2}\right) \qquad (2.103)$$

where β is a material constant that depends on yield stress, σ_y, modulus of elasticity, E, Poisson's ratio ν, prehistory of loading σ_0, and the fracture toughness K_C. In general,

$$\beta = \alpha\left(\frac{\sigma_y}{E}, \frac{\sigma_0}{E}, \nu\right)\frac{EK_C^2}{2\sigma_y^2} \qquad (2.104)$$

being a non-dimensional constant.

To simplify the above rate of propagation model, the second term $\ln\left(\frac{K_C^2 - K_{max}^2}{K_C^2 - K_{min}^2}\right)$ can be expanded in a Taylor series around (0, 0). Substituting back in the above model yields:

$$\frac{da}{dN} = \beta\left(\frac{K_{max}^4 - K_{min}^4}{K_C^4} + \frac{K_{max}^6 - K_{min}^6}{K_C^6} + \ldots\right) \qquad (2.105)$$

This is not quite similar to Liu's result but it confirms the presence of high order powers. If $K_{min} = 0$, then one obtains:

$$\frac{da}{dN} = \beta\left(\frac{K_{max}}{K_C}^4 + \frac{K_{max}}{K_C}^6 + \ldots\right) \qquad (2.106)$$

It is obvious here that for different ranges of K_{max}, one obtains different powers if only one term is used to describe the process. This was the case in the work done by Majidzadeh et al. (41) where the generality of the power law was investigated.

If K_{max}/K_C is high (low cycle fatigue), then higher order terms should be retained and the last part of Figure 2.39is obtained. Here the points may not lie on a straight line as was observed. If K_{max}/K_C is low (high cycle fatigue), then higher order terms can be neglected as compared to the leading term and the Paris power law is obtained.

It is conceivable to think of a region between the above two extremes where a second power law might replace the above model. In this region, the above law will still describe the process better. But for the sake of simplicity, if one wants to choose only one power, then the power would be two. In a previous work by the authors, this was found to be precisely the case. Asphaltic concrete specimens were fatigued at different temperatures but approximately in the same range of crack growth rate (41). It was found that the best fit would be obtained if one uses three or more terms and the next best would be a two term fit. The one term fit led invariably to a power of 2. This one term fit was considered good because of the simple power law that results.

PART II

LIST OF REFERENCES

1. ASTM Special Committee on Fracture Testing of High-Strength Metallic Materials, "Progress in Measuring Fracture Toughness and Using Fracture Mechanics," Materials Research and Standards, Vol. 4, No. 3, pp. 107-119, March 1964.

2. ASTM Special Technical Publication 463, Review of Developments in Plane Strain Fracture Toughness Testing, National Aeronautics and Space Administration, September 1970.

3. ASTM Special Technical Publication 381, Fracture Toughness Testing and Its Applications, 1965.

4. Barenblatt, G. I., "The Mathematical Theory of Equilibrium Cracks in Brittle Fracture," Advances in Applied Mechanics, Vol. VII, Academic Press, 1962.

5. Brown, W. F., Jr. and Srawley, J. E., Plane Strain Crack Toughness Testing of High-Strength Matallic Materials, ASTM STP 410, American Society for Testing and Materials, 1967.

6. Cherepanov, G. P. and Halmanov, H., "On The Theory of Fatigue Crack Growth," Engineering Fracture Mechanics, Vol. 4, 1972.

7. Deverall, L. L. and Lindsey, G. H., "A Comparison of Numerical Methods for Determining Stress-Intensity Factors," ICRPG Paper, 1969.

8. Erdogan, F., "Crack Propagation Theories," Fracture, An Advanced Treatise, Vol. 2, (H. Liebowitz, Editor), Academic Press, New York, New York, 1971.

9. Fukakura, Juichi, "The Effect of Specimen Thickness and Temperature on Plastic Yielding and Fracture Properties of Mild Steel," Engineering Fracture Mechanics, Vol. 6, pp. 231-244, Pergamon Press, 1974.

10. George, K. P., "Theory of Brittle Fracture Applied to Soil Cement," Journal of the Soil Mechanics and Foundation Division, ASCE, Vol. 96, No. SM3, pp. 991-1010, May 1970.

11. Graham, G. A. C., "The Correspondence Principle of Linear Viscoelasticity Theory for Mixed Boundary Value Problems Involving Time Dependent Regions," Quarterly of Applied Mathematics, 26, 1968.

12. Griffith, A. A., "The Phenomena of Rupture and Flow in Solids," Philosophical Transactions of the Royal Society of London, 221, 163-168, 1921

13. _____, "The Theory of Rupture," Proceedings of the First International Congress in Applied Mechanics, 1924.

14. Gross, B. and Srawley, J. E., "Stress-Intensity Factors for Three Point Bend Specimens by Boundary Collocation," NASA TN D-3092, Lewis Research Center, Cleveland, Ohio.

15. Hahn, G. T. and Rosenfield, A. R., "Sources of Fracture Toughness: The Relation Between K_{IC} and Ordinary Tensile Properties of Metals," Applications Related Phenomena in Titanium Alloys, ASTM STP 432, American Society for Testing and Materials, pp. 3-31, March 1968.

16. Herrin, M. and Bahgat, A. G., "Brittle Fracture of Asphaltic Mixes," Presented at the Annual Meeting of the Association of Asphalt Paving Technologists, February, 1968.

17. Hoeppner, D. W. and Knopp, W. E., "Prediction of Component Life by Application of Fatigue Crack Growth Knowledge," Engineering Fracture Mechanics, Vol. 6, 1974.

18. Irwin, G. R., "Analysis of Stresses and Strains Near the End of a Crack Traversing a Plate," J. of Appl. Mechanics, Trans. ASME, 79:361-4, 1957.

19. Irwin, G. R. and Kies, J. A., "Critical Energy Rate Analysis of Fracture Strength," Welding Journal Research Supplement, Vol. 33, pp. 193s - 198s, 1954.

20. Irwin, G. R., "Fracture," Encyclopedia of Physics, Vol. 6, pp. 557-590, Springer Press, Berlin, 1958.

22. Irwin, G. R. and Wells, A. A., "A Continuum Mechanics View of Crack Propagation," Metallurgical Review, 10 (58), pp. 223-270, 1965.

21. Irwin, G. R. and Kies, J., "Fracturing and Fracture Dynamics," Welding Journal Research Supplement, February 1952.

23. Irwin, G. R., Structural Mechanics, Pergamon Press, Great Britain, p. 557, 1960.

24. Irwin, G. R., "Fracture Mechanics," Proceedings, First Symposium on Naval Structures Mechanics, MacMillan Press, 1958.

25. Irwin, G. R., "Plastic Zone Near a Crack Tip and Fracture Toughness," Seventh Sagamore Ordinance Materials Research Conference, August 1960.

26. Kang, T. S. and Liu, H. W., "Fatigue Crack Propagation and Cyclic Deformation at a Crack Tip," International Journal of Fracture Mechanics, Vol. 10, 1974.

27. Kaplan, M. F., "Crack Propagation and the Fracture of Concrete," Journal of the American Concrete Institute, Vol. 58, No. 5, pp. 591-610, 1961.

28. Kauffmann, E. M., "The Application of Fracture Mechanics Concepts to Predict Cracking of Flexible Pavements," Ph.D. Dissertation, The Ohio State University, 1973.

29. Knauss, W. G., "On the Steady Propagation of a Crack in a Viscoelastic Sheet: Experiments and Analysis," Deformation and Fracture of High Polymers, H. H. Kausch, J. A. Hassell, and R. I. Jaffee, Editors, Plenum Press, 1974.

30. Knauss, W. G., "Delayed Failure--The Griffith Problem for Linearly Viscoelastic Materials," International Journal of Fracture Mechanics, Vol. 6, 1970.

31. Knauss, W. G. and Dietmann, H., "Crack Propagation Under Variable Load Histories in Linearly Viscoelastic Solids," International Journal of Engineering Science, Vol. 8, 1970.

32. Kobayashi, Albert S., Editor, Experimental Techniques in Fracture Mechanics, The Iowa State University Press, Ames, Iowa, 1973.

33. Majidzadeh, K.; Ramsamooj, D. V. and Chan, A. T., "Fatigue and Fracture of a Bituminous Paving Mixtures," AAPT, 1969.

34. Majidzadeh, K.; Kauffmann, E. M. and Ramsamooj, D. V., "Application of Fracture Mechanics in the Analysis of Pavement Fatigue," AAPT, Vol. 40, 1971.

35. Majidzadeh, K. and Ramsamooj, D. V., "Development of Testing Procedures and a Method to Predict Fatigue Failures of Asphaltic Concrete Pavement Systems," Final Report, Project RF 2873, The Ohio State University Research Foundation, March 1971.

36. Majidzadeh, K.; Kauffmann, E. M. and Saraf, C. L., "Analysis of Fatigue of Paving Mixtures from the Fracture Mechanics Viewpoint," Fatigue of Compacted Bituminous Aggregate Mixtures, ASTM STP 508, 1972.

37. Majidzadeh, K.; Ramsamooj, D. V. and Chan. A., "Analysis of Fatigue and Fracture of Bituminous Paving Mixtures—Phase I, RF 2845, The Ohio State University Research Foundation, May 1970.

38. Majidzadeh, K. and Kauffmann, E., "Analysis of Fatigue and Fracture of Bituminous Paving Mixtures—Phase II," The Ohio State University Research Foundation, RF 2845, March 1971.

39. Majidzadeh, K. and Ramsamooj, D. V., "Development of Testing Procedures and Method to Predict Fatigue of Asphalt Concrete Pavement Systems," RF 2873, The Ohio State Research Foundation, March 1971.

40. Majidzadeh, K. and Kauffmann, E., "Verification of Fracture Mechanics Concepts to Predict Cracking of Flexible Pavements," RF3200, The Ohio State University Research Foundation, June 1973.

41. Majidzadeh, K.; Ilves, George; Makdisi-Ilyas, F. and Saraf, C. L., "A Laboratory and Field Durability Study of Asphaltic Mixtures," Engineering Experiment Station (EES 356), The Ohio State University, 1974.

42. Markstrom, Karl, "On Fracture Toughness and Its Size Dependence for Steels Showing Thickness Delamination," Engineering Fracture Mechanics, Vol. 4, pp. 593-603, Pergamon Press, Great Britain, 1972.

43. McElivy, A. J.; Boettner, R. C. and Johnson, T. L., "On Foundation and Growth of Fracture Cracks in Polymers," Fatigue, An Interdisciplinary Approach, Syracuse University Press, 1964.

44. Moavenzadeh, Fred, "Asphalt Fracture," Professional Paper P67-5, Massachusetts Institute of Technology, Cambridge, Massachusetts, February 1967.

45. Moavenzadeh, F. and Kuguel, R., "Fracture of Concrete," Journal of Materials, Vol. 41, No. 3, pp. 497-579, 1969.

46. Monismith, C. L.; Hicks, R. G. and Salam, Y.M., "Basic Properties of Pavement Components," Report FHWA-RD-72-19, Federal Highway Administration, University of California at Berkeley, September 1971.

47. Mueller, H. K., "Stress Intensity Factor and Crack Opening for a Linearly Viscoelastic Strip with a Slowly Propagating Central Crack," International Journal of Fracture Mechanics, Vol. 7, No. 2, 1971.

48. Mueller, H. K. and Knauss, W. G., "Crack Propagation in a Linearly Viscoelastic Strip," Journal of Applied Mechanics, Transactions, ASME, June 1971.

49. Mukherejee, B. and Burns, D. J., "Growth of Part Through Thickness Fatigue Cracks in Sheet Polymethylmethacrylate," Engineering Fracture Mechanics, Vol. 4, No. 4, December 1972.

50. Naus, D. J. and Lott, J. L., "Fracture Toughness of Portland Cement Concretes," Proceedings, ACI, Vol. 66, pp. 481-489, 1969.

51. Neuber, H., "Theory of North Stresses," Translation published by J.W. Edwards Co., Ann Arbor, Michigan, 1946.

52. Orowan, E., "Energy Criteria of Fracture," Welding Journal Research Supplement, pp. 157-160, March 1955.

53. Orowan, E. and Felbeck, D. K., "Experiments on Brittle Fracture of Steel Plates," Welding Journal Research Supplement, pp. 570-575, November 1955.

54. Orowan, E., Fatigue and Fracture of Metals, John Wiley & Sons, Inc. 1952.

55. Orowan, E., "Fundamentals of Brittle Behavior of Metals," Fatigue and Fracture of Metals, John Wiley & Sons, Inc., 139-167, 1952.

56. Paris, P. C., "The Fracture Mechanics Approach to Fatigue," Proceedings of the 10th Sagamore Conference, Syracuse University Press, 107-132, 1965.

57. Paris, P.C. and Sih, G. C., "Stress Analysis of Cracks," Fracture Toughness Testing and Its Applications, ASTM STP 381, 39-76, 1965.

58. Paris, P. C., Fatigue—An Interdisciplinary Approach, Syracuse University Press, 1964.

59. Paris, P. C.; Gomez, M. P. and Anderson, W. E., "A Rational Analytic Theory of Fatigue," Trend in Engineering (University of Washington), Seattle, Washington, Vol. 13, No. 1, 1961.

60. Paris, P.C., "The Growth of Cracks Due to Variation in Load," Ph.D. Dissertation, Lehigh University, September 1962.

61. Paris, P.C. and Erdogan, F. J., "A Critical Analysis of Crack Propagation Laws," Journal of Basic Engineering, Trans. ASME, Series D, Vol. 85, pp. 528-553, 1963.

62. Pearson, S., "The Effect of Mean Stress on Fatigue Crack Propagation in Half Inch Thick Specimens of Aluminum Alloys of High and Low Fracture Toughness," Engineering Fracture Mechanics, Vol. 4, p. 9, 1972.

63. Porter, T. R., "Method of Analysis and Prediction for Variable Amplitude Fatigue Crack Growth," Engineering Fracture Mechanics, Vol. 4, No. 4, 1972.

64. Ramsamooj, D. V., "The Design and Analysis of the Flexibility of Pavements," Ph.D. Dissertation, The Ohio State University, 1970.

65. Ramsamooj, D. V.; Majidzadeh, K. and Kauffmann, E. M., "The Analysis and Design of the Flexibility of Pavements," Proceedings, Third International Conference on the Structural Design of Asphalt Pavements, University of Michigan, 1972.

66. Rice, J. R. and Rosengren, G. F., Journal of the Mechanics and Physics of Solids, Vol. 16, pp. 1-12, 1968.

67. Rice, J. R., Journal of Applied Mechanics, "Tranactions of the American Society of Mechanical Engineers," June 1968, pp. 379-386.

68. Rice, J. R., "Mathematical Analysis in the Mechanics of Fracture," Fracture, H. Liebowitz, Editor, pp. 191-311, 1968.

69. Schapery, R. A., " A Theory of Crack Growth in Viscoelastic Media," Mechanics and Materials Research Center, Texas A&M University, College Station, Texas, 1973.

70. Sih, G. C., "A Review of the Three-Dimensional Stress Problem for a Cracked Plate," International Journal of Fracture Mechanics, Vol. 7, No. 1, pp. 39, 1971.

71. Sih, G. C. and Liebowitz, H., "Mathematical Theories of Brittle Fracture," Fracture, H. Liebowitz, Editor, pp. 67-190, 1968.

72. Sih, G. C., "Three-Dimensional Stress-State in a Cracked Plate," Proceedings of the Air Force Conference on Fatigue and Fracture of Aircraft Structures and Materials, September 1970.

73. Sih, G. C., " A Special Theory of Crack Propagation," Methods of Analysis and Solutions to Crack Problems, edited by G. C. Sih, Wolters-Noordhoff Publishing, 1972.

74. Srawley, J. E.; Jones, M. H. and Brown, W. F., "Determination of Plane Strain Fracture Toughness," Materials Research and Standards, Vol. 7, No. 6, pp. 262-266, June 1967.

75. Srawley, J. E., "Plane Strain Fracture Toughness," Fracture—An Advanced Treatise, edited by H. Liebowitz, Vol. IV, Chapter II, pp. 45-68, 1969.

76. Williams, M. L., "Initiation and Growth of Viscoelastic Fracture," International Journal of Fracture Mechanics, 1965.

77. Winne, D. H. and Wundt, B. M., "Application of the Griffith-Irwin Theory of Crack Propagation to the Bursting Behavior of Disce, Including Analytical and Experimental Studies," Trans. ASME, Vol. 80, pp. 1643-1655, 1968.

78. Wnuk, M. P., "Subcritical Growth of Fracture (Inelastic Fatigue), International Journal of Fracture Mechanics, 1971.

79. Wnuk, M. P., "Slow Growth of Cracks in a Rate Sensitive Tresca Solid," Engineering Fracture Mechanics, 5, 1973.

80. Wnuk, M. P., "Prior to Failure Extension of Flaws Under Monotonic and Pulsating Loadings," Engineering Fracture Mechanics, 5, 1973.

81. Wnuk, M. P. and Knauss, W. G., "Delayed Fracture in Viscoelastic Plastic Solids," International Journal of Solids and Structures, 6, 1970.

PART III. A MATHEMATICAL INVESTIGATION OF GEOMETRICAL MODELING AND FRACTURE AND FATIGUE ANALYSIS OF ASPHALTIC BEAMS ON ELASTIC FOUNDATION

I. INTRODUCTION

Previous research studies at The Ohio State University (12, 13, 14, 15), have led to the formulation of a fracture mechanics method of pavement fatigue design subsystem. This design principle, which provides a unique methodology for fatigue life prediction of pavement structures, also includes recommendations for material testing and evaluation procedures. The proposed laboratory testing method for fatigue and fracture analysis involves experimentation on beams on elastic foundations. In such a fatigue experiment, a two-dimensional elastic system of asphaltic beams on elastic foundation is subjected to repeated loading, and it is generally assumed that the fatigue crack propagation rate follows a power law relating the crack growth rate to the stress-intensity factor, K --- ($dc/dN = A K^n$). The material constants associated with the crack growth rate, A and n, are affected by such parameters as load frequency, external boundary conditions, temperature, and statistical distribution of flaws in the materials, as well as the dimensions of the models used.

In such an analysis, a pavement system is treated as a two-dimensional elasticity problem, and the laboratory investigation of beams on an

elastic foundation subjected to repeated loading is carried out to simulate the dynamic behavior of the pavement system under actual traffic loads. However, before this simulation can be accurately carried out, the effect of the model dimension on the material constants needs to be determined. This report, therefore, is concerned with the development of proper criteria for the design of such models and will include procedures to establish proper criteria for selection of suitable beam geometries, determination of allowable loads for fatigue testing experiments, and graphical determination of stress-intensity calculations for beams on elastic geometry as needed for fatigue and fracture analysis.

II. A REVIEW OF THEORETICAL CONCEPTS: BEAM ON ELASTIC FOUNDATION

A. An Infinitely Long Beam Resting on an Elastic Foundation of Finite Depth

To investigate the behavior of an asphaltic beam tested on an elastic foundation, first consider the effect of a sinusoidal load of value q per unit length acting directly on top of an infinitely long elastic foundation of unit width and a finite depth, d_f, resting on a rigid base as shown in Figure 1.

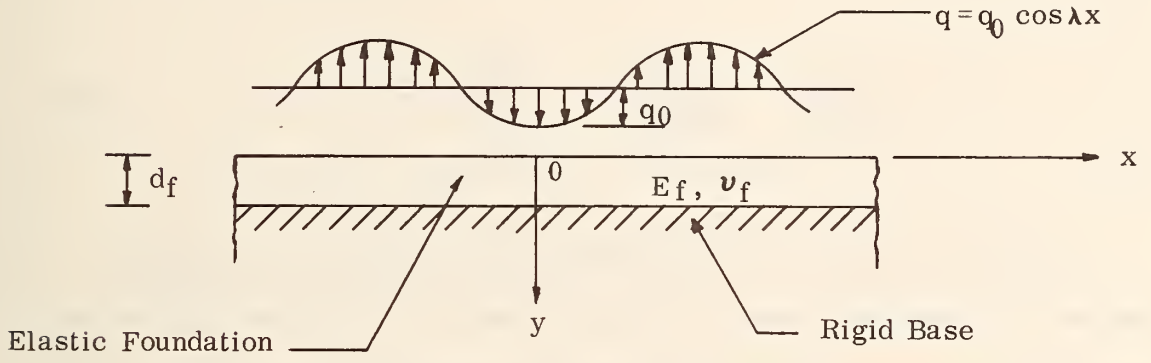

Figure 3.1

Under this condition, the value of the load is:

$$q(x) = q_0 \cos \lambda x \qquad (3.1)$$

This problem is a two-dimensional elasticity problem, the governing differential equation of which, in terms of the Airy's stress function and neglecting the body force, is given by:

$$\nabla^4 \phi = 0 \ , \qquad (3.2)$$

where ϕ is the Airy's stress function related to the stress components by:

$$\sigma_x = \frac{\partial^2 \phi}{\partial y^2}$$

$$\sigma_y = \frac{\partial^2 \phi}{\partial x^2} \tag{3.3}$$

$$\tau_{xy} = \frac{\partial^2 \phi}{\partial x \, \partial y}$$

and

$$\nabla^4 = \frac{\partial^4}{\partial x^4} + 2\frac{\partial^4}{\partial x^2 \partial y^2} + \frac{\partial^4}{\partial y^4} \tag{3.4}$$

Besides the well-known assumptions of linear elasticity, it will be assumed that there is no shearing stress acting at the interface of the foundation and the rigid base. With this additional assumption, the boundary conditions of the problem are:

$$\left.\begin{aligned} \tau_{xy} &= 0 \\ \sigma_y &= -q \cdot \cos \lambda x \end{aligned}\right\} \text{ at } y = 0 \tag{3.5}$$

$$\left.\begin{aligned} \tau_{xy} &= 0 \\ v &= 0 \end{aligned}\right\} \text{ at } y = d_f \tag{3.6}$$

where v is the vertical displacement along the y-axis. It can be shown that the stress function given by:

$$\phi(x,y) = \cos\lambda x \left[c_1 \cosh\lambda y + c_2 \lambda^2 \sinh\lambda y + c_3 \lambda(2\sinh\lambda y + \lambda y \cosh\lambda y) + c_4 \lambda(2\cosh\lambda y + \lambda y \sinh\lambda y)\right] \quad (3.7)$$

satisfies the biharmonic equation (3.2). Consequently, the corresponding stress components are:

$$\sigma_x = \cos\lambda x \left[c_1 \lambda^2 \cosh\lambda y + c_2 \lambda^2 \sinh\lambda y + c_3 \lambda(2\sinh\lambda y + \lambda y \cosh\lambda y) + c_4 \lambda(2\cosh\lambda y + \lambda y \sinh\lambda y)\right] \quad (3.8)$$

$$\sigma_y = -\lambda^2 \cos\lambda x \left[c_1 \cosh\lambda y + c_2 \sinh\lambda y + c_3 y \cosh\lambda y + c_4 y \sinh\lambda y\right] \quad (3.9)$$

$$\tau_{xy} = \lambda \sin\lambda x \left[c_1 \lambda \sinh\lambda y + c_2 \lambda \cosh\lambda y + c_3(\cosh\lambda y + \lambda y \sinh\lambda y) + c_4(\sinh\lambda y + \lambda y \cosh\lambda y)\right] . \quad (3.10)$$

Applying the boundary conditions (3.5) to (3.9) and (3.10) yields:

$$\left.\begin{aligned} c_3 &= -c_2 \lambda \\ c_1 &= q_0/\lambda^2 \end{aligned}\right\} \quad (3.11)$$

Also, from Equations (3.6.a) and (3.10), we get:

$$c_4 = \frac{(q_0/\lambda)\sinh\lambda d_f - c_2 \lambda^2 d_f \sinh\lambda d_f}{\sinh\lambda d_f + \lambda d_f \cosh\lambda d_f} \quad (3.12)$$

Now, for the plane stress problem, the vertical strain, ϵ_y, is related to the stress components by the relation:

$$\epsilon_y = \frac{\partial v}{\partial y} = \frac{1}{E_f}(\sigma_y - \nu_f \sigma_x) , \quad (3.13)$$

where

E_f = modulus of elasticity of the foundation

ν_f = Poisson's ratio of the foundation.

Upon substitution of Equations (3.8) and (3.9) in (3.13), and integrating with respect to y , one gets:

$$\begin{aligned} \nu(x,y) = -\frac{\cos\lambda x}{E_f} \Big[& c_1(1+\nu_f)\lambda \sinh\lambda y + c_2(1+\nu_f)\lambda\cosh\lambda y \\ & + c_3(1+\nu_f)\lambda y \sinh\lambda y - c_3(1-\nu_f)\cosh\lambda y \\ & + c_4(1+\nu_f)\lambda y\cosh\lambda y - c_4(1-\nu_f)\sinh\lambda y \Big] + h(x), \end{aligned} \tag{3.14}$$

where

$h(x)$ is the function of x alone.

Similarly,

$$\epsilon_x = \frac{\partial u}{\partial x} = \frac{1}{E_f}(\sigma_x - \nu_f \sigma_y), \tag{3.15}$$

where

u = the deformation in the x-direction

ϵ_x = axial strain in the x-direction.

Substituting Equations (3.8) and (3.9) in (3.15) and integrating with respect to x yields:

$$\begin{aligned} u(x,y) = \frac{\sin\lambda x}{E_f} \Big[& c_1\lambda\cosh\lambda y + c_2\lambda\sinh\lambda y \\ & + c_3(2\sinh\lambda y + \lambda y\cosh\lambda y) + c_4(2\cosh\lambda y \\ & + \lambda y\sinh\lambda y)\Big] + g(y) , \end{aligned} \tag{3.16}$$

where g(y) is the function of y alone.

From Equations (3.14) and (3.16), together with the stress-strain relation:

$$\gamma_{xy} = \frac{\partial u}{\partial y} + \frac{\partial v}{\partial x} = \frac{\tau_{xy}}{G} = \frac{2(1+\nu_f)}{E_f}\tau_{xy}, \qquad (3.17)$$

we get:

$$\frac{dh(x)}{dx} = -\frac{dg(y)}{dy} = C_5 \qquad (3.18)$$

Equation (3.18) leads to:

$$h(x) = C_5 x + C_6 , \qquad (3.19)$$

$$g(y) = C_5 y + C_7 . \qquad (3.20)$$

In this particular problem, there is no rigid body displacement. This implies that one must have:

$$C_5 = C_6 = C_7 = 0. \qquad (3.21)$$

Substituting Equations (3.11), (3.12), and (3.21) into (3.14), and using the boundary condition (3.6.b) yields:

$$c_2 = -\frac{q_0 \sinh^2 \lambda d_f}{\lambda^2(\lambda d_f + \sinh \lambda d_f \cosh \lambda d_f)} . \qquad (3.22)$$

With Equation (3.22), one obtains from Equations (3.11) and (3.12):

$$c_3 = \frac{q_0 \sinh^2 \lambda d_f}{\lambda(\lambda d_f + \sinh \lambda d_f \cosh \lambda d_f)} \qquad (3.23)$$

and

$$c_4 = -\frac{q_0 \sinh \lambda d_f}{\lambda(\sinh \lambda d_f + \lambda d_f \cosh \lambda d_f)} - \frac{q_0 d_f \sinh^3 \lambda d_f}{(\sinh \lambda d_f + \lambda d_f \cosh \lambda d_f)(\lambda d_f + \sinh \lambda d_f \cosh \lambda d_f)} \tag{3.24}$$

Substituting Equations (3.11.b), (3.22), (3.23) and (3.24) into Equation (3.14) leads to the following expression for the vertical deflection:

$$w(x) = v(x, 0)$$

or,

$$w(x) = 2q_0 \cos \lambda x \left[\frac{\sinh^2 \lambda d_f}{E_f \lambda (\lambda d_f + \sinh \lambda d_f \cosh \lambda d_f)}\right] \tag{3.25}$$

or, in view of Equation (3.1):

$$q(x) = \frac{E_f \lambda (\lambda d_f + \sinh \lambda d_f \cosh \lambda d_f)}{2 \sinh^2 \lambda d_f} \cdot w(x) \tag{3.26}$$

If one denotes,

$$Q(x) = 2bq(x) \tag{3.27}$$

to be the load acting across the width 2b of the foundation, then one has from Equation (3.26):

$$Q(x) = k'w(x), \tag{3.28}$$

where

$$k' = \frac{b\lambda E_f (\lambda d_f + \sinh \lambda d_f \cosh \lambda d_f)}{\sinh^2 \lambda d_f} \quad . \tag{3.29}$$

The load Q, acting on top of the foundation, can then be expressed in terms of the surface deflection.

Consider next an infinitely long beam of width 2b, resting on top of the elastic foundation subjected to the sinusoidal load, p(x), per unit length, acting on top of the beam over the width 2b, with the foundation reaction Q(x) defined in Equation (3. 28) as shown in Figure 2.

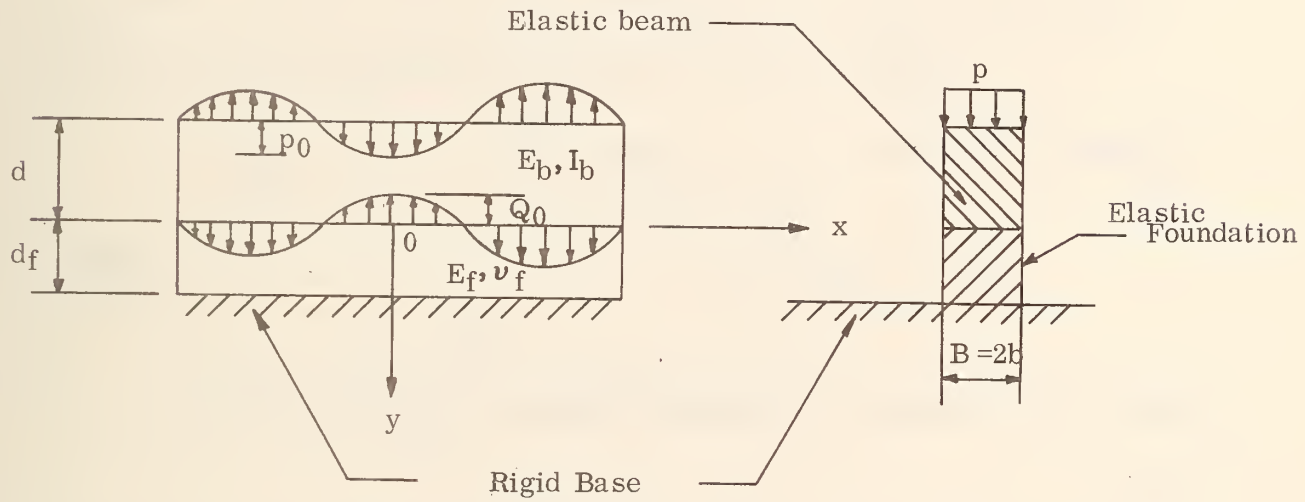

Figure 3.2

The load p(x) is expressed as:

$$p(x) = p_0 \cos \lambda x \tag{3.30}$$

Also note that:

$$Q(x) = Q_0 \cos \lambda x = 2b\, q_0 \cos \lambda x \quad . \tag{3.31}$$

According to the beam theory, the vertical deflection of the beam, w , is given by the differential equation:

$$E_b I_b \frac{d^4 w}{dx^4} = p - Q \ , \tag{3.32}$$

where

E_b = modulus of elasticity of the beam

I_b = moment of inertia of the beam section.

Substituting Equations (3.28) and (3.30) in (3.32) yields:

$$E_b I_b \frac{d^4 w}{dx^4} + k'w = p_0 \cos \lambda x \ . \tag{3.33}$$

To find the particular solution of (3.33), let:

$$w(x) = w_0 \cos \lambda x \ . \tag{3.34}$$

Substituting (3.34) into (3.33), one gets:

$$w_0 = \frac{p_0}{\lambda^4 E_b I_b + k'} \ . \tag{3.35}$$

Hence, upon substitution of Equations (3.35) and (3.29) into (3.34), we get:

$$w(x) = \frac{p(x) \sinh^2 \lambda d_f}{\lambda^4 E_b I_b \sinh^2 \lambda d_f + b \lambda E_f (\lambda d_f + \sinh \lambda d_f \cosh \lambda d_f)} \ , \tag{3.36}$$

where p(x) is given in Equation (3.30).

The bending moment due to the load p can be evaluated from the relation:

$$M(x) = -E_b I_b \frac{d^2 w}{dx^2} \ . \tag{3.37}$$

With Equations (3.36) and (3.37), it follows that:

$$M(x) = \frac{\lambda p(x)}{\lambda^3 + \frac{E_f b}{E_b I_b} \psi(\lambda d_f)} , \tag{3.38}$$

where

$$\psi(\lambda d_f) = \frac{\lambda d_f + \sin h\, \lambda d_f \cos h \lambda d_f}{\sin h^2 \lambda d_f} . \tag{3.39}$$

By means of Equation (3.38), it is possible to calculate the bending moment due to any loading condition using the superposition principle and the Fourier integral. Recall that any arbitrary load p(x) symmetrical about the y-axis can be represented in the form of a Fourier integral:

$$p(x) = \frac{1}{\pi} \int_0^\infty A(\lambda) \cos \lambda x \, d\lambda , \tag{3.40}$$

where

$$A(\lambda) = \int_{-\infty}^{\infty} p(v) \cos \lambda v \, dv . \tag{3.41}$$

Consequently, the bending moment due to any arbitrary load p(x), expressed in terms of the Fourier integral, is given by:

$$M(x) = \frac{1}{\pi} \int_0^\infty \frac{[A(\lambda) \cos \lambda x] \, \lambda d\lambda}{\lambda^3 + \frac{E_f b}{E_b I_b} \psi(\lambda d_f)} . \tag{3.42}$$

B. An Infinite Beam Subjected to a Uniform Strip Load

Suppose that the beam is subjected to a uniform strip load of intensity p and width 2ϵ as shown in Figure 3.

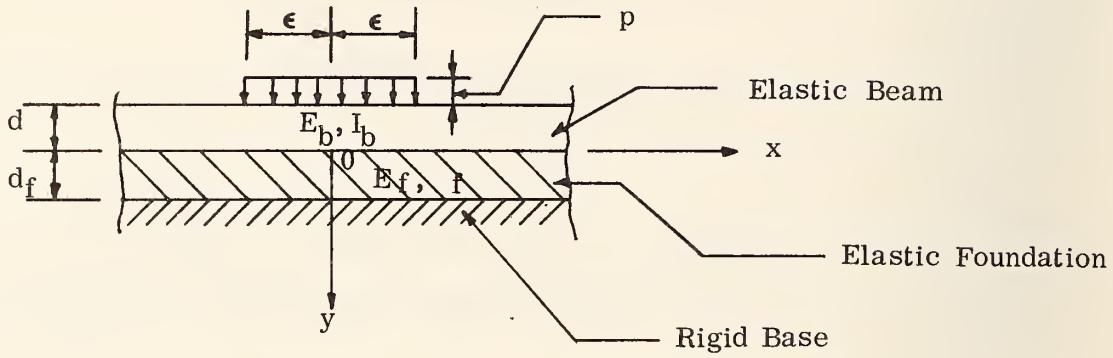

Figure 3.3

In this case, one has:

$$p(x) = \begin{cases} p & , -\epsilon \leq x \leq \epsilon \\ 0 & \text{elsewhere} \end{cases} \tag{3.43}$$

Hence:

$$A(\lambda) = \int_{-\epsilon}^{\epsilon} p \cos \lambda v \, dv$$

or,

$$A(\lambda) = 2p\epsilon \frac{\sin \lambda \epsilon}{\lambda \epsilon} \tag{3.44}$$

Substituting (3.44) in (3.42), and letting

$$a = \left[\frac{E_b I_b}{E_f b}\right]^{1/3} \tag{3.45}$$

and

$$\alpha = a\lambda \quad , \tag{3.46}$$

where a = a fundamental length

α = a dimensionless parameter,

leads to:

$$M(x) = \frac{2pa^2}{\pi} \int_0^\infty \frac{\sin(\alpha\epsilon/a)\cos(\alpha x/a)}{\alpha^3 + \psi(\alpha d_f/a)} \, d\alpha \quad . \tag{3.47}$$

Similarly, it can be shown that the corresponding expressions for the deflection w(x), the shearing force V(x) in the beam, and the contact pressure Q(x) (load per unit length) at the interface of the beam and the foundation are:

$$w(x) = \frac{2pa^4}{\pi E_b I_b} \int_0^\infty \frac{\sin(\alpha\epsilon/a)\cos(\alpha x/a)}{\alpha^2\left[\alpha^3 + \psi(\alpha d_f/a)\right]} \cdot d\alpha \tag{3.48}$$

$$V(x) = -\frac{2pa}{\pi} \int_0^\infty \frac{\sin(\alpha\epsilon/a)\sin(\alpha x/a)}{\alpha^3 + \psi(\alpha d_f/a)} \cdot d\alpha \tag{3.49}$$

$$Q(x) = \frac{2p}{\pi} \int_0^\infty \frac{\psi(\alpha d_f/a)\sin(\alpha\epsilon/a)\cos(\alpha x/a)}{\alpha\left[\alpha^3 + \psi(\alpha d_f/a)\right]} \cdot d\alpha \tag{3.50}$$

C. An Infinite Beam Subjected to a Concentrated Load

The elastic solution to the problem of an infinite beam subjected to a concentrated load, P, acting along the y-axis can be obtained as a limiting case of the uniform strip load problem. As the loaded region

$\epsilon \longrightarrow 0$, one has:

$$P = 2p\epsilon \quad ,$$

$$\lim_{\epsilon \longrightarrow 0} \frac{\sin(\alpha\epsilon/a)}{\alpha\epsilon/a} = 1.$$

Consequently, the expressions for w(x), M(x), V(x), and Q(x) due to the load P take the forms:

$$w(x) = \frac{Pa^3}{\pi E_b I_b} \int_0^\infty \frac{\cos(\alpha x/a)}{\alpha\left[\alpha^3 + \psi(\alpha d_f/a)\right]} \cdot d\alpha \qquad (3.51)$$

$$M(x) = \frac{Pa}{\pi} \int_0^\infty \frac{\alpha\cos(\alpha x/a)}{\alpha^3 + \psi(\alpha d_f/a)} \cdot d\alpha \qquad (3.52)$$

$$V(x) = -\frac{P}{\pi} \int_0^\infty \frac{\alpha^2 \sin(\alpha x/a)}{\alpha^3 + \psi(\alpha d_f/a)} \cdot d\alpha \qquad (3.53)$$

$$Q(x) = \frac{P}{\pi a} \int_0^\infty \frac{\psi(\alpha d_f/a)\cos(\alpha x/a)}{\alpha^3 + \psi(\alpha d_f/a)} \cdot d\alpha \qquad (3.54)$$

D. An Infinite Beam On A Semi-Infinite Foundation

This is a limiting case of an infinite beam resting on a finite depth foundation solutions. Rewrite Equation (3.39) in terms of the new parameter α:

$$\psi(\alpha d_f/a) = \frac{\alpha d_f/a + \sinh(\alpha d_f/a)\cosh(\alpha d_f/a)}{\sinh^2(\alpha d_f/a)} \cdot \qquad (3.39.a)$$

It is seen that as $d_f \longrightarrow \infty$, $\psi(\alpha d_f/a) \longrightarrow 1$ as a limit. Hence, for the case of a semi-infinite foundation, Equations (3.47) through (3.54) are still valid upon substitution of $\psi(\alpha d_f/a) = 1.0$.

It is noted that the expressions thus obtained for the deflections, bending moments, shearing forces, and the contact pressures are very similar in character to those obtained by Biot(1), Vesic (8), Drapkin (2), and Selvadurai (5). The solutions for the case of plane stress problem of an infinite beam on a semi-infinite foundation are exactly the same as those obtained by Biot.

For a plane strain problem, one simply replaces E_f with $E_f/(1 - \nu_f^2)$ in the expression for the fundamental length 'a' as defined in Equation (3.45). That is, for a plane strain problem, one has:

$$a = \left[\frac{(1 - \nu_f^2) E_b I_b}{E_f b} \right]^{1/3} \tag{3.55}$$

With 'a' defined in Equation (3.55), the expressions for the deflections, bending moments, etc. for the plane stress problem can then be used for the plane strain problem.

E. Numerical Evaluation of Related Integrals

A numerical technique that can be used to evaluate the finite integrals appearing in the preceding section is shown here in detail for the case of the beam subjected to a concentrated line load. The same technique also applies to the other cases.

Consider, for example, the expression for the bending moment of the

beam due to a concentrated line load given by Equation (3.52). Transform the equation to the form:

$$\frac{M(x)}{Pa} = \frac{1}{\pi} \int_0^{\infty} e^{-\alpha} \left[\frac{e^{\alpha} \alpha \cos(\alpha x/a)}{\alpha^3 + \psi (\alpha d_f/a)} \right] d\alpha \qquad (3.56.a)$$

or

$$\frac{M(x)}{Pa} = \frac{1}{\pi} \int_0^{\infty} e^{-\alpha} f(\alpha, x/a, d_f/a)\, d\alpha \qquad (3.56.b)$$

In this form, the integral can be evaluated by a Gauss-Laguerre quadrature formula.

A computer program was written to evaluate Equation (3. 56) for various values of x/a and d_f/a, using the 32-point Gauss-Laguerre quadrature formula. As a check for accuracy, one might use Equation (3. 52) to evaluate the maximum moment (at $x = 0$) when $d_f \longrightarrow \infty$, which results in:

$$M_{max} = \frac{Pa}{\pi} \int_0^{\infty} \frac{\alpha}{\alpha^3 + 1} \, d\alpha \qquad (3.57)$$

This integral can be integrated exactly to get:

$$M_{max} = 0.385\ Pa \qquad (3.58)$$

as compared to the computer output:

$$M_{max} = 0.382\ Pa \quad . \qquad (3.59)$$

Hence, the error is in the order of 1% or less.

Figure 4 shows a series of normalized bending moment curves obtained from numerical evaluations of Equation (3.56).

From Equation (3.56), the maximum moments for different values of d_f/a are given by:

$$\frac{M_{max}}{Pa} = \frac{1}{\pi} \int_0^{\infty} \frac{\alpha \, d\alpha}{\alpha^3 + \psi(\alpha d_f/a)} \quad . \qquad (3.60)$$

If the numerical results of Equation (3.60) are plotted on logarithmic paper, it is found that for $0.1 \leq d_f/a \leq 1.5$, Equation (3.60) can be represented, with an approximation on the order of 0.5%, as:

$$\frac{M_{max}}{Pa} = 0.2904 \left(\frac{d_f}{a}\right)^{0.2438} \quad , \quad 0.1 \leq d_f/a \leq 1.5$$

or

$$M_{max} = 0.2904 \left(\frac{d_f}{a}\right)^{0.2438} Pa \qquad (3.61)$$

Now, from the fundamental theory based on Winkler's assumption, it is given that:

$$M_{max} = 0.353554 \, P \left(\frac{E_b I_b}{k}\right)^{1/4} \qquad (3.62.a)$$

where k = modulus of subgrade reaction .

Hence, in order to obtain the same maximum bending moment by the approximate theory as by the exact one, one might have to use a modified

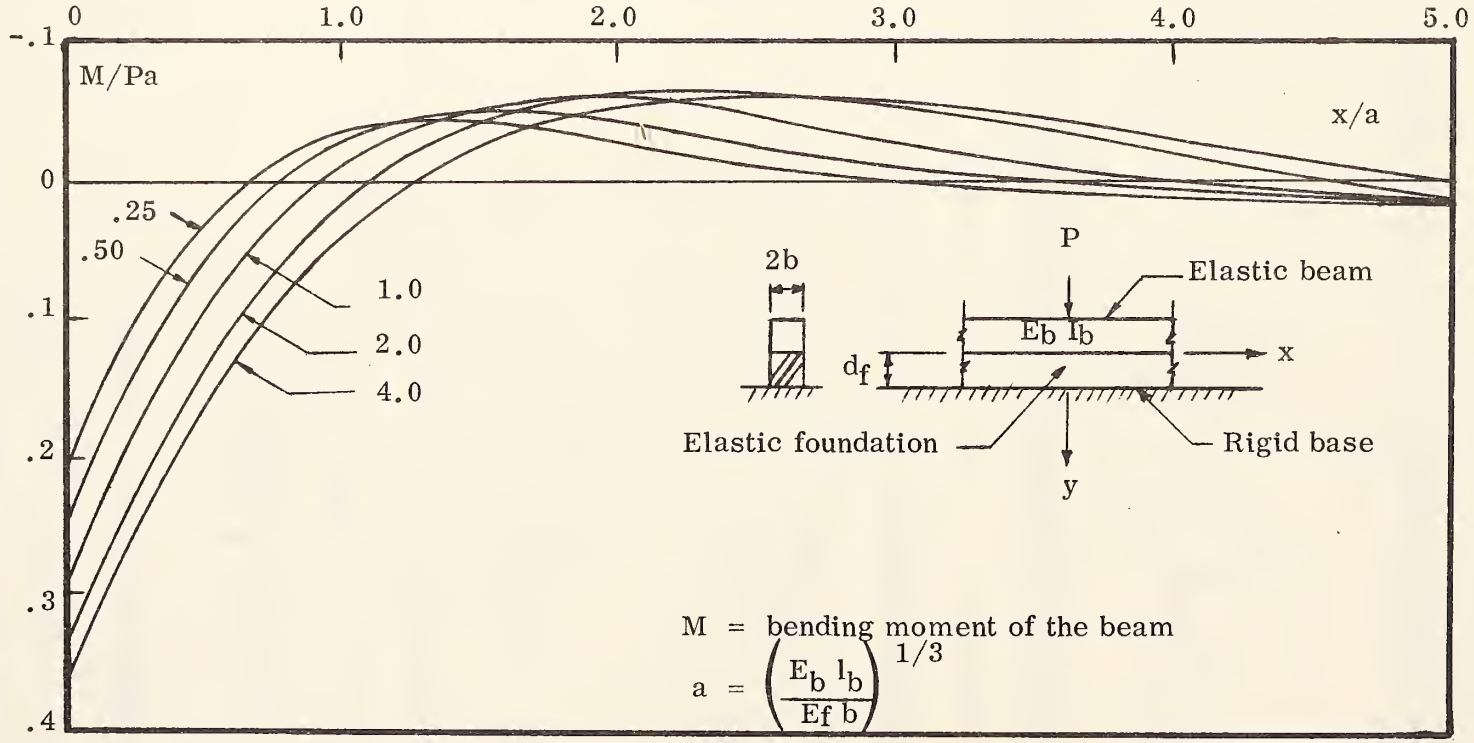

Figure 3.4. Normalized Bending Moment Curves for an Infinitely Long Beam

value of k found by equating Equations (3.61) and (3.62.a), i.e.:

$$0.353554\ P\left(\frac{E_b I_b}{k}\right)^{1/4} = 0.2904\left(\frac{d_f}{a}\right)^{0.2438} P\left(\frac{E_b I_b}{E_f b}\right)^{1/3}$$

or

$$\frac{k}{E_f} = 2.197\left[\frac{d_f}{a}\right]^{-0.9752}\left[\frac{b}{a}\right], \quad 0.1 \leq d_f/a \leq 1.5 \tag{3.63}$$

where a is given by Equation (3.45).

It should be noted that Equation (3.62.a) is derived from the general expression for the bending moment:

$$M(x) = \frac{P}{4\beta}\, e^{-\beta x}(\cos \beta x - \sin \beta x) \tag{3.64}$$

from which

$$M_{max} = \frac{P}{4\beta} \tag{3.62b}$$

where

$$\beta = \left[\frac{k}{4\ E_b I_b}\right]^{1/4} \tag{3.65}$$

So, in view of Equations (3.61) and (3.62.b), one gets:

$$\beta a = 0.8609\left[\frac{d_f}{a}\right]^{-0.2438}, \tag{3.66}$$

where $0.1 \leq d_f/a \leq 1.5$.

Hence, knowing β, one can also compute k from Equation (3.65), which gives:

$$k = 4\beta^4 E_b I_b \tag{3.67}$$

Equations (3.66) and (3.67) are suitable forms for evaluating β and k respectively. Equation (3.66) has been evaluated numerically and is plotted in Figure 5.

Knowing the stresses and the contact pressure in the uncracked beam, it is then possible to use these stresses as known boundary conditions to the approximation of the stresses in the beam having a centrally located vertical crack.

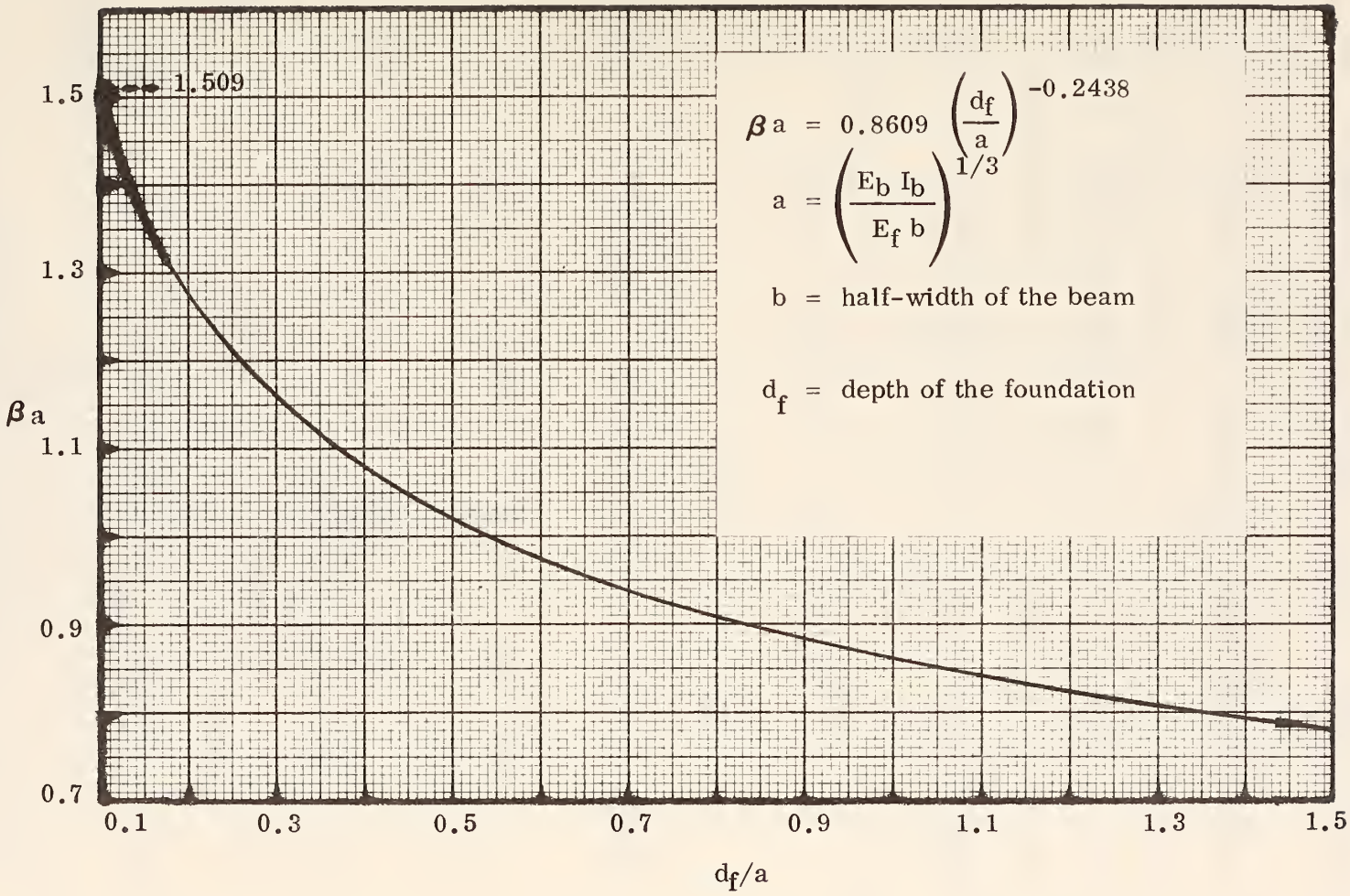

Figure 3.5 Relation between βa and d_f/a

III. AN ANALYSIS OF STRESSES AND THE OPENING-MODE STRESS INTENSITY FACTOR FOR A CRACKED BEAM

A method of analysis consists of finding a stress function, χ, that satisfies the biharmonic equation $\nabla^4 \chi = 0$, and also the boundary conditions along the boundary of the cracked beam. The biharmonic equation and the boundary condition along the crack are satisfied by the Williams stress function (9), which in the case of symmetry of loading, is given by:

$$\chi(r, \theta) = \sum_{n=1,2,\ldots}^{\infty} \left\{ (-1)^{n-1} d_{2n-1} r^{(n+1/2)} \left[-\cos(n-3/2)\theta + \frac{2n-3}{2n+1} \cos(n+1/2)\theta \right] + (-1)^n d_{2n} r^{(n+1)} \left[-\cos(n-1)\theta + \cos(n+1)\theta \right] \right\} \qquad (3.68)$$

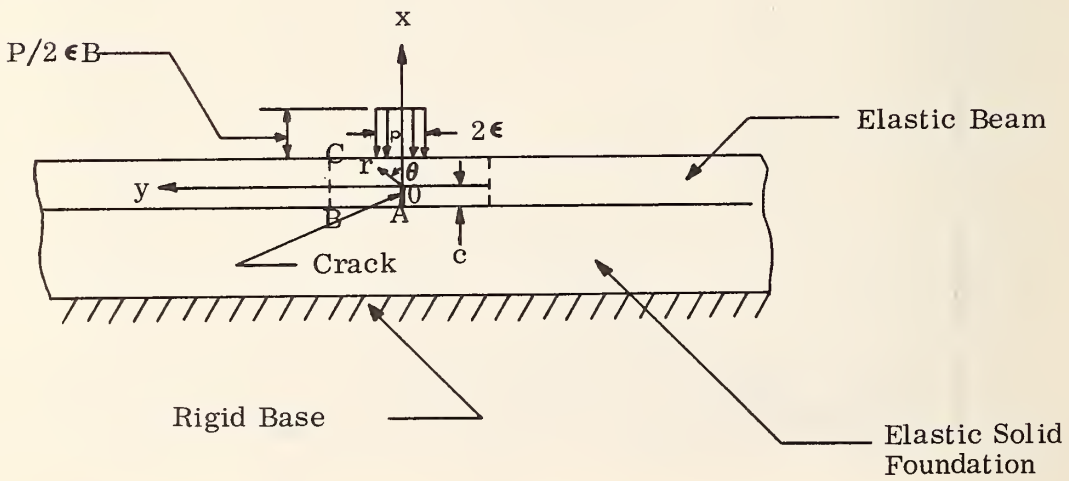

Figure 3.6 Cracked Beam on Elastic Foundation

According to the coordinate system shown, the stresses in terms of χ are:

$$\sigma_y = \frac{\partial^2 \chi}{\partial x^2} = \frac{\partial^2 \chi}{\partial r^2} \cos^2\theta - 2 \frac{\partial^2 \chi}{\partial \theta \partial r} \frac{\sin\theta \cos\theta}{r}$$

$$+ \frac{\partial \chi}{\partial r} \frac{\sin^2\theta}{r} + 2 \frac{\partial \chi}{\partial \theta} \frac{\sin\theta \cos\theta}{r^2}$$

$$+ \frac{\partial^2 \chi}{\partial \theta^2} \frac{\sin^2\theta}{r^2}$$

$$\sigma_x = \frac{\partial^2 \chi}{\partial y^2} = \frac{\partial^2 \chi}{\partial r^2} \sin^2\theta + 2 \frac{\partial^2 \chi}{\partial \theta \partial r} \frac{\sin\theta \cos\theta}{r} + \frac{\partial \chi}{\partial r} \frac{\cos^2\theta}{r}$$

$$- 2 \frac{\partial \chi}{\partial \theta} \frac{\sin\theta \cos\theta}{r^2} + \frac{\partial^2 \chi}{\partial \theta^2} \frac{\cos^2\theta}{r^2}$$

$$\tau_{xy} = - \frac{\partial^2 \chi}{\partial x \partial y} = - \sin\theta\cos\theta \frac{\partial^2 \chi}{\partial r^2} - \frac{\cos 2\theta}{r} \frac{\partial^2 \chi}{\partial \theta \partial r}$$

$$+ \frac{\partial^2 \chi}{\partial \theta^2} \frac{\sin\theta \cos\theta}{r^2} + \frac{\partial \chi}{\partial r} \frac{\sin\theta \cos\theta}{r}$$

$$+ \frac{\partial \chi}{\partial \theta} \frac{\cos 2\theta}{r^2} , \qquad (3.69)$$

where

$$\frac{\partial \chi}{\partial r} = \sum_{n=1,2,\ldots}^{\infty} \left\{ (-1)^{n-1} (n+1/2)\, d_{2n-1}\, r^{(n-1/2)} \left[-\cos(n-3/2)\theta \right.\right.$$

$$\left. + \frac{2n-3}{2n+1} \cos(n+1/2)\theta \right] + (-1)^n (n+1)\, d_{2n}\, r^n$$

$$\left. \left[- \cos(n-1)\theta + \cos(n+1)\theta \right] \right\} \qquad (3.70.a)$$

$$\frac{\partial^2 \chi}{\partial r^2} = \sum_{n=1,2,\ldots}^{\infty} \Big\{ (-1)^{n-1} (n^2-1/4)\, d_{2n-1}\, r^{(n-3/2)} \Big[-\cos(n-3/2)\,\theta + \frac{2n-3}{2n+1} \cos(n+1/2)\,\theta \Big] + (-1)^n (n+1)\, d_{2n}\, r^{n-1} \Big[-\cos(n-1)\,\theta + \cos(n+1)\,\theta \Big] \Big\} \tag{3.70.b}$$

$$\frac{\partial \chi}{\partial \theta} = \sum_{n=1,2,\ldots}^{\infty} \Big\{ (-1)^{n-1}\, d_{2n-1}\, r^{(n+1/2)} \Big[(n-3/2) \sin(n-3/2)\,\theta - (n-3/2) \sin (n+1/2)\,\theta \Big] + (-1)^n\, d_{2n}\, r^{n+1} \Big[(n-1) \sin (n-1)\,\theta - (n+1) \sin (n+1)\,\theta \Big] \Big\} \tag{3.70.c}$$

$$\frac{\partial^2 \chi}{\partial \theta^2} = \sum_{n=1,2,\ldots}^{\infty} \Big\{ (-1)^{n-1}\, d_{2n-1}\, r^{(n+1/2)} \Big[n-3/2)^2 \cos(n-3/2)\,\theta - (n-3/2)(n+1/2) \cos (n+1/2)\,\theta \Big] + (-1)^n\, d_{2n}\, r^{n+1} \Big[(n-1)^2 \cos(n-1)\,\theta - (n+1)^2 \cos(n+1)\,\theta \Big] \Big\} \tag{3.70.d}$$

$$\frac{\partial^2 \chi}{\partial \theta \partial r} = \sum_{n=1,2,\ldots}^{\infty} \Big\{ (-1)^{n-1}\, d_{2n-1}\, (n+1)\, r^{(n-1/2)} \Big[(n-3/2) \sin (n-3/2)\,\theta - (n-3/2) \sin (n+1/2)\,\theta \Big] + (-1)^n (n+1)\, d_{2n}\, r^{n} \Big[(n-1) \sin(n-1)\,\theta - (n+1) \sin (n+1)\,\theta \Big] \Big\} \tag{3.70.e}$$

If it is assumed that the presence of the crack does not have any signi-

ficant effect on the stresses beyond the boundary BC, as well as along the interface of the beam and the foundation, the stresses along those boundaries can then be closely approximated from the conditions of the uncracked beam. Taking symmetry into consideration and considering the portion of the beam cut along BC as a free body, one has the following additional boundary conditions:

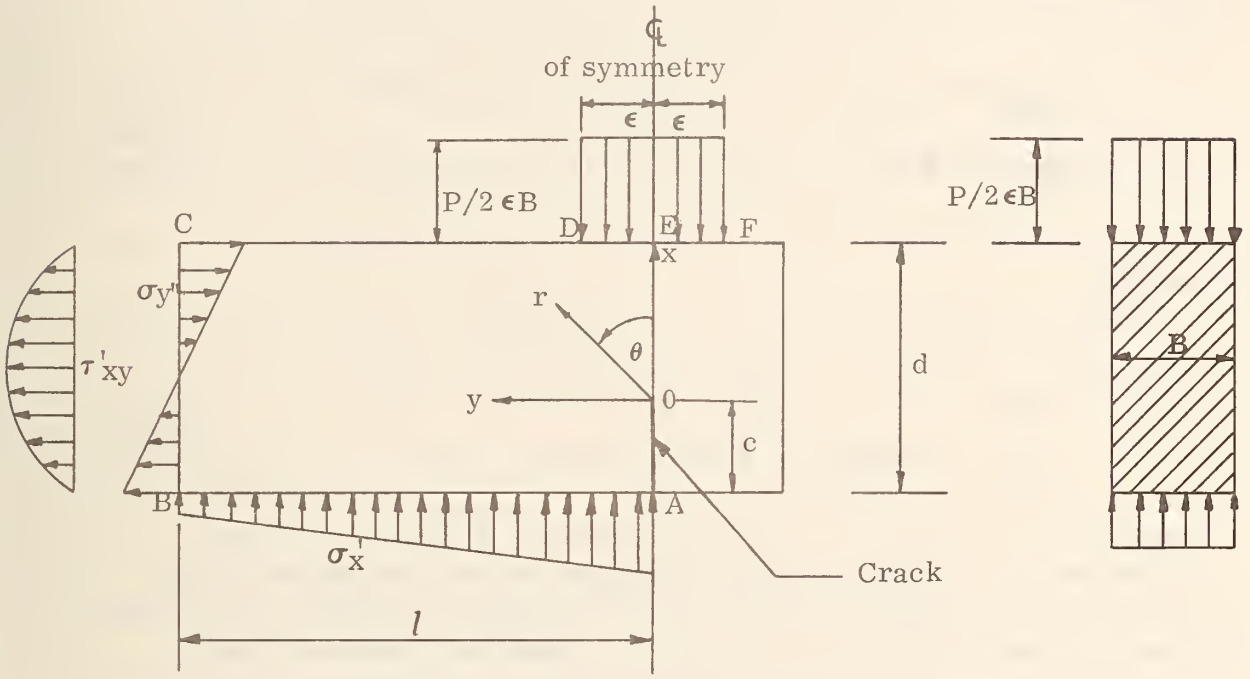

Figure 3.7

Along AB:

$$\left.\begin{aligned} \tau_{xy} &= 0 \\ \sigma_x &= \sigma'_x = -\frac{P}{\pi \epsilon B} \int_0^\infty \frac{\psi(\alpha d_f/a)\sin(\alpha \epsilon/a)\cos(\alpha y/a)}{\alpha\left[\alpha^3 + \psi(\alpha d_f/a)\right]}\, d\alpha \end{aligned}\right\} \quad (3.71)$$

Along BC:

$$\left.\begin{aligned} \tau_{xy} &= \tau'_{xy} = f(x) \cdot \frac{Pa}{\pi \epsilon B} \int_0^\infty \frac{\alpha \sin(\alpha \epsilon/a)\sin(\alpha l/a)}{\alpha^3 + \psi(\alpha d_f/a)}\, d\alpha \\ \sigma_y &= \sigma'_y = g(x)\,\frac{(Pa^2)}{\pi \epsilon B} \int_0^\infty \frac{\sin(\alpha \epsilon/a)\cos(\alpha l/a)}{\alpha^3 + \psi(\alpha d_f/a)}\, d\alpha \end{aligned}\right\} \quad (3.72)$$

where

$$f(x) = \frac{6}{d^3}\left[cd + xd - 2xc - c^2 - x^2 \right]$$

$$g(x) = \frac{1}{I_b}\left[x - \frac{d}{2} + c \right].$$

Along CD:

$$\left.\begin{aligned} \tau_{xy} &= 0 \\ \sigma_x &= 0 \end{aligned}\right\} \qquad (3.73)$$

Along DE:

$$\left.\begin{aligned} \tau_{xy} &= 0 \\ \sigma_x &= -P/2\epsilon B \end{aligned}\right\} \qquad (3.74)$$

The problem will be explicitly solved if we can find the coefficients of the Williams stress function, d_i , $i = 0, 1, 2, \ldots$, such that Equation (3.69) satisfies the boundary conditions given by Equations (3.71) through (3.74).

As for the opening-mode stress intensity factor, K_1, we have, according to Irwin (3), in the immediate vicinity of the crack tip (as r approaches zero):

$$\sigma_y = \frac{K_I}{\sqrt{2\pi r}} \cos\frac{\theta}{2}\left(1 + \sin\frac{\theta}{2}\sin\frac{3\theta}{2}\right) \qquad (3.75)$$

while in terms of the Williams stress function,

$$\sigma_y = -\frac{d_1}{\sqrt{r}} \cos\frac{\theta}{2}\left(1 + \sin\frac{\theta}{2}\sin\frac{3\theta}{2}\right) \qquad (3.76)$$

hence,

$$K_I = -\sqrt{2\pi}\, d_1 \qquad (3.77)$$

Therefore, only the value of the first coefficient, d_1, is needed to determine the value of the stress-intensity factor, K_I.

A. An Approximation of the Stress-Intensity Factor by the Boundary Collocation Procedure

Gross and Srawley (6,7) used a boundary collocation procedure in conjunction with the Williams stress function in the approximation of stress-intensity factors for single-edge-notch beams in bending and combined bending and tension. Later, Majidzadeh and Ramsamooj (4) adopted the same method to approximate the stress-intensity factor, K_I, for beams having a centrally located crack, supported on a three-dimensional semi-infinite elastic solid, and subjected to a centrally located, vertically concentrated load.

The same technique is employed here for solving the two-dimensional problem of an infinitely long beam having a centrally-located vertical crack at the bottom, supported on an elastic solid of any thickness, and subjected to a uniform strip load (a concentrated line load is merely a limiting case).

The boundary-collocation procedure consists of solving $2m$ simultaneous algebraic equations corresponding to the known values of stresses and displacements at a finite number of stations, m, along the boundary A B C D E (Figure 7) of the free body of a cracked beam. The solution yields the values of the first $2m$ coefficients of the Williams stress function. For the present purpose, only the first coefficient, d_1, is needed in the determination of the stress-intensity factor, K_I.

For given values of geometrical dimensions and loading conditions, the value of d_1 varies somewhat with the number of terms, 2n , of the stress function, the number of boundary stations, m, and the length l. It has been found that for a given 2n, the solution for d_1 converged rapidly with $l/d = 1.0$ and with the stations spacing within the range d/8 to d/16. To further optimize the solution, it has been recommended (4) to use the linear least-squares optimization scheme in solving the problem; using more equations than unknowns. Using this particular technique, it was noted that the optimal number of d_i terms, 2n, varies somewhat with each particular beam's dimensions as well as with the crack length over beam depth ratio; however, their effects on the values of K_I is practically small.

A value of K_I obtained by this method corresponds to a particular set of values of P, d, l, c, m, and n. For application, the results are better expressed more generally in terms of the dimensionless quantity,

$$K_I' = K_I / (\sigma_{max}\sqrt{d}) \tag{3.78}$$

where σ_{max} is the maximum tensile stress at the bottom of the uncracked beam on elastic solid. With $l/d \geq 1.0$, it was found that K_1' is practically dependent on the c/d ratio for a set of m and n.

For computation convenience, a beam section and loading conditions shown below was selected for the approximation of K_I' for various c/d ratios:

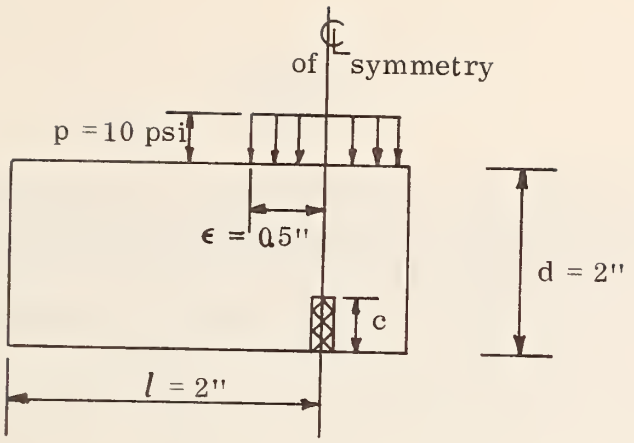

Figure 3.8

It was found that the optimum number of d_i terms, 2n , for various c/d ratios, lies between 60 and 80. Hence, for each particular c/d ratio, the value of K_I' was obtained by taking the average of three values computed for 2n equal to 60, 70, and 80.

The results of the computations are plotted in Figure 9. To verify the validity of this normalized relation, different beam sizes were selected to compute K_I' for a particular c/d ratio. The results agreed very well. The computer program used in the boundary collocation method is presented in Appendix A.

B. Applications to Analysis of Fracture Propagation

For a particular c/d ratio, the value of σ_{max} under a set of geometrical and loading conditions must be known in order to compute the absolute value of K_I from the normalized K_I'. For a rectangular cross section, one

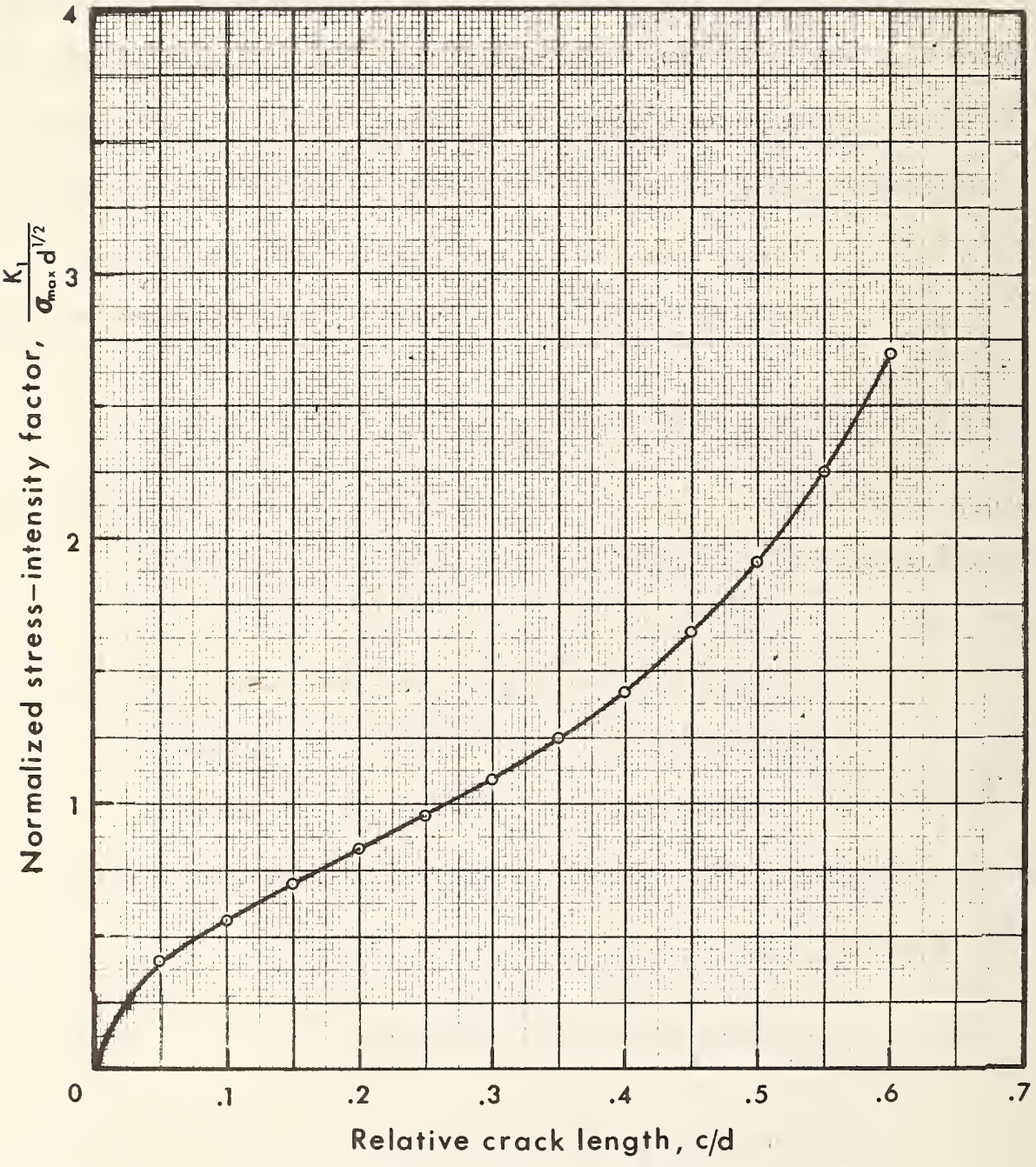

Figure 3.9 Relation Between the Normalized Stress-Intensity Factor and the Relative Crack Length.

has:

$$\sigma_{max} = \frac{6M_{max}}{Bd^2} \tag{3.79}$$

where M_{max} is the maximum bending moment in the beam. M_{max} can either be computed from Equation (3.47) for a uniform strip load, or from Equation (3.52) for a concentrated load. However, this direct method for evaluating M_{max} requires a numerical integration which is only feasible with the aid of a computer. A practical approach in the evaluation of σ_{max} is proposed in the following.

It has been shown that the bending moment in a beam resting on an elastic solid of a finite depth and subjected to a concentrated load may be computed from the conventional beam-on-elastic-foundation formula; i.e.:

$$M(y) = \frac{P}{4\beta} e^{-\beta y} (\cos \beta y - \sin \beta y) \tag{3.64}$$

if β is taken as:

$$\beta = \frac{0.8609}{a} \left[\frac{d_f}{a}\right]^{-0.2438}, \quad 0.1 \leq d_f/a \leq 1.5 \ . \tag{3.66}$$

Consequently, one gets:

$$M_{max} = \frac{P}{4\beta} \tag{3.62.b}$$

Substituting Equations (3.66) and (3.62.b) into Equation (3.79) yields:

$$\frac{\sigma_{p\,max}\, Bd^2}{Pa} = 1.7424 \left[\frac{d_f}{a}\right]^{0.2438}, \quad 0.1 \leq d_f/a \leq 1.5 \ . \tag{3.80}$$

It is noted that Equation (3.80) is applicable for $0.1 \leq d_f/a \leq 1.5$, which is considered to be within the practical range of d_f/a in an experimental set-up. For a special case of semi-infinite foundation, it can be shown that:

$$\frac{\sigma_{p\,max}\, Bd^2}{Pa} = 2.3094 \qquad (3.81)$$

The plot of Equation (3.80) is presented in Figure 10.

Thus far, one has been able to approximate the maximum tensile stress $\sigma_{p\,max}$ in the beam due to a concentrated load, P. To extend the application to a uniform loading conditions, a set of numerical integrations of M_{max} from Equation (3.37) were carried out for $0 < \epsilon/a \leq 2.0$. The results were expressed in terms of $\sigma_{s\,max} / \sigma_{p\,max}$, where $\sigma_{s\,max}$ is the maximum tensile stress due to a uniform load and $\sigma_{p\,max}$ is the maximum tensile stress due to a concentrated load. Figure 11 shows the plot of $\sigma_{s\,max}/\sigma_{p\,max}$ against ϵ/a ratios. For a particular ϵ/a ratio, the corresponding ratio of $\sigma_{s\,max}/\sigma_{p\,max}$ can then be read from Figure 9. Knowing this ratio and $\sigma_{p\,max}$ from Equation (3.80) or Equation (3.81), or from Figure 10, one can then compute $\sigma_{s\,max}$.

Having obtained the maximum tensile stress for the uncracked beam, the absolute value of the stress-intensity factor, K_I, may then be computed from Figure 9. However, instead of directly reading the value of K_I' for a c/d ratio off of Figure 9, the following empirical equation was found to be a compact expression of the present results for $0.1 \leq c/d \leq 0.6$,

$$K_I' = 6.898(c/d) - 17.425(c/d)^2 + 22.438(c/d)^3 \qquad (3.82)$$

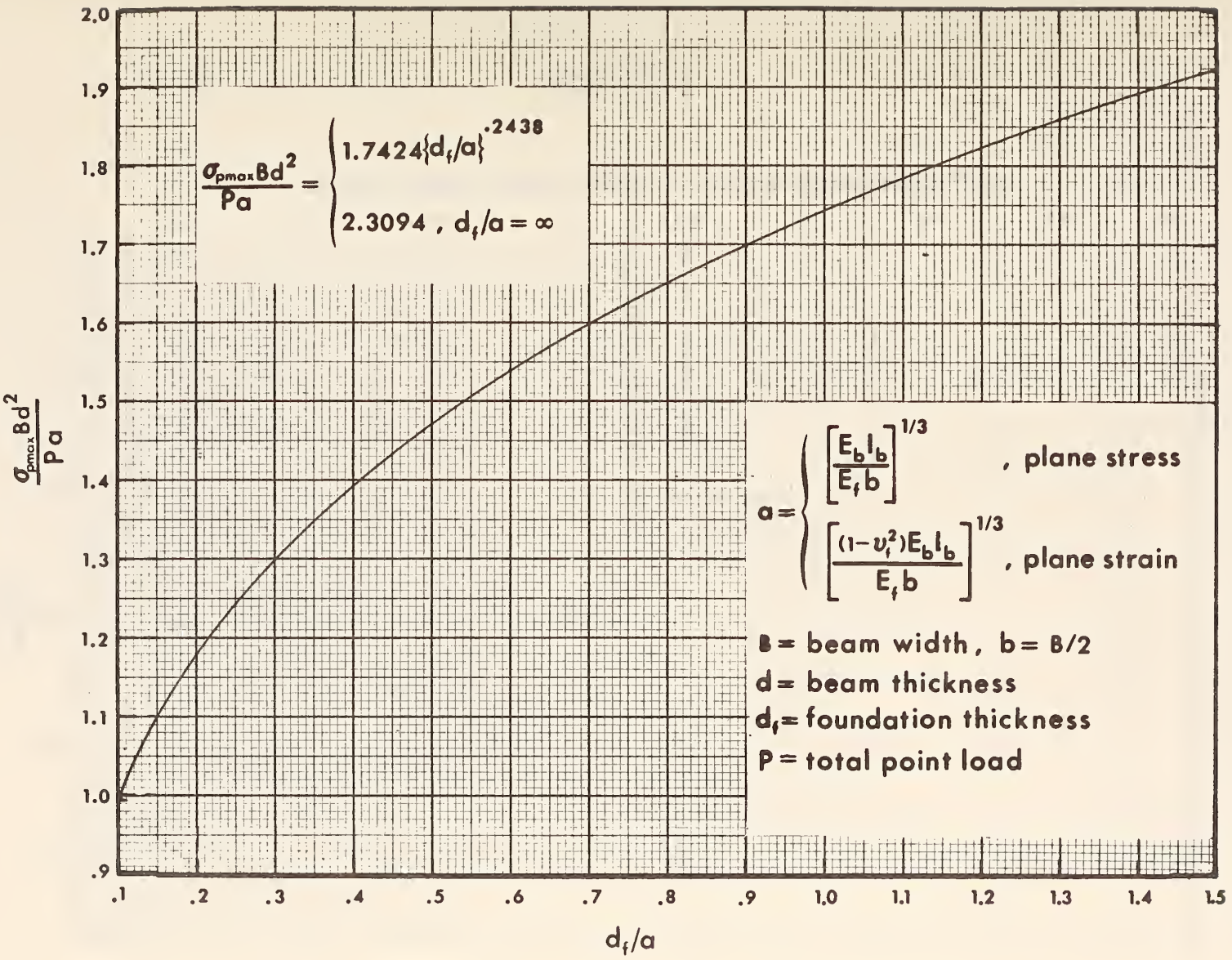

Figure 3.10 Relation Between $\frac{\sigma_{pmax}Bd^2}{Pa}$ And $\frac{d_f}{a}$ Ratio.

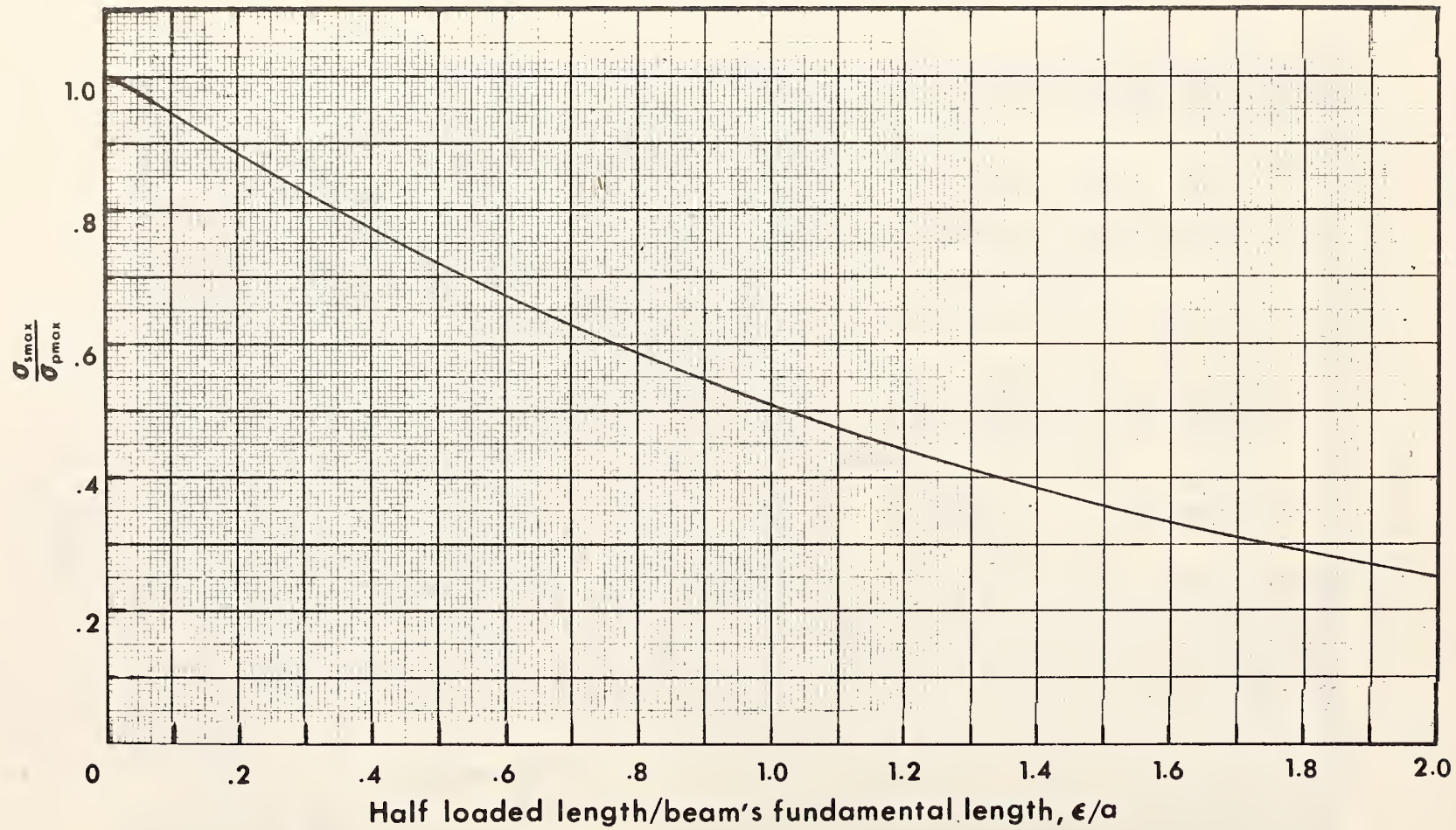
1.0
.8
.6
.4
.2
$\frac{\sigma_{smax}}{\sigma_{pmax}}$
0
.2
.4
.6
.8
1.0
1.2
1.4
1.6
1.8
2.0
Half loaded length/beam's fundamental length, ϵ/a

Figure 3.11

Equation (3.82) is plotted in Figure 3.12. K may then be approximated from Equation (3.82).

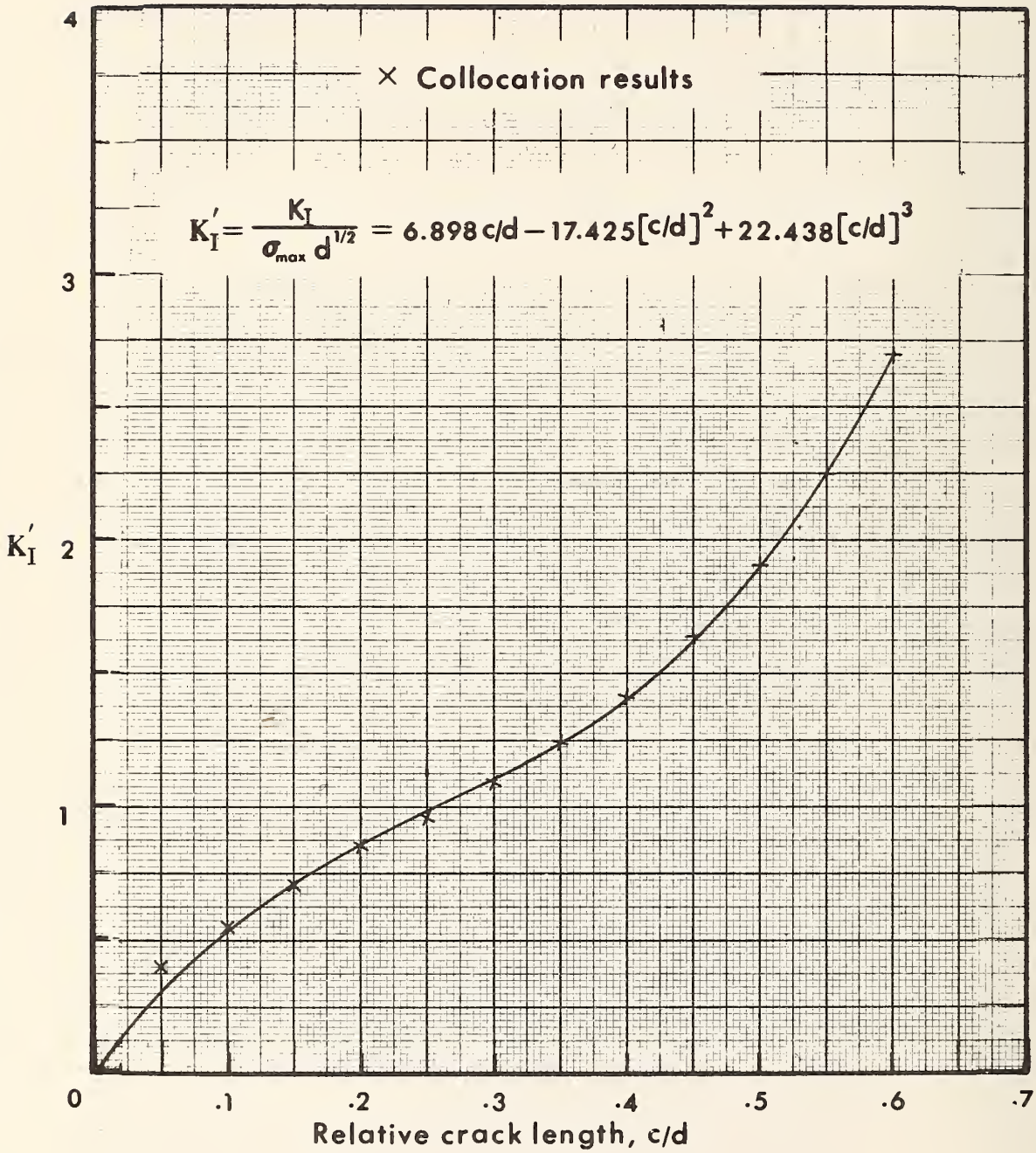

Figure 3.12 Approximation of the Normalized Stress-Intensity Factor as a Function of the Relative Crack Length

IV. GEOMETRICAL DESIGN OF BEAM SAMPLES AND EVALUATION OF K_I

A. A Criterion For the Length of a Beam Sample

It is known from the approximate theory based on Winkler's assumption that if

$$\beta l \geq 5 \quad , \tag{3.83.a}$$

where l = the length of the beam,

then the end conditioning forces at either end of the beam of finite length l will have an insignificant influence at the other end and, therefore, all the formulas derived from the infinitely long beam can be applied to this case. In this case, knowing the value of β from Equation (3.66), the minimum length of the beam sample then should not be less than:

$$l = 5/\beta \tag{3.83.b}$$

B. Criteria For the Cross Section of the Beam

According to the ASTM Specification C31-69, it is recommended that for flexure tests, a beam should have the minimum dimension of three times the maximum nominal size of the coarse aggregate in the mix. Furthermore, the depth of the beam should not exceed four times its width. Hence, the beam cross section should be such that:

$$B = 2b \geq 3 \text{ (max. size of aggregate)} \tag{3.84}$$

and

$$B \leq d \leq 4B \tag{3.85}$$

where B = the width of the beam

d = the depth of the beam.

C. A Criterion For the Determination of the Load Magnitude

In order to prevent excessive rutting of the beam top surface under the load, as well as to assure that the maximum tensile stress at the bottom of the beam surface is below the yield stress, it is recommended that the applied load should be of such a magnitude as to cause:

$$\sigma_{max} \leq 0.5 \ \sigma_y \tag{3.86}$$

where σ_y = yield stress in tension.

Knowing the beam and the foundation dimensions, together with the related material properties, one can then select the required magnitude of the applied load from Figures 11 and 10 respectively.

D. Procedure For the Design of a Beam Sample

a) Selection of the beam dimension:

1. Evaluate the values of

E_b = modulus of elasticity of the beam

E_f = modulus of elasticity of the foundation from the experiments

2. Select a minimum width of the beam from

   $B = 3$ (maximum nominal size of aggregate)

3. Select a series of beam depths, d, such that

   $B \leq d \leq 4B$

4. Find the section property $I_b = \frac{1}{12} Bd^3$ and from which calculate:

$$a = \left(\frac{E_b I_b}{E_f b} \right)^{1/3}, \text{ where } b = B/2$$

5. Select a foundation depth d_f and then compute d_f/a. Read off the curve in Figure 5 the corresponding value of βa. Then compute β.

6. The required length of the beam is computed from:

$$l = 5/\beta$$

7. For optimum solution for each particular E_b and E_f, try different beam depths as well as different foundation depths.

Example: Given the following properties:

Beam size: 3" x 3" $\quad I_b = \frac{1}{12} (3)^4 = 6.75 \text{ in.}^4$

$E_b = 65,000 \text{ lb./in.}^2$, $\quad E_f = 250 \text{ lb./in.}^2$

$$a = \left(\frac{E_b I_b}{E_f b} \right)^{1/3} = \left(\frac{65,000 \times 6.75}{250 \times 1.5} \right)^{1/3} = 10.54 \text{ in.}$$

For $d_f/a = 1.5''$

$$d_f/a = 1.5/10.54 = 0.142$$

From curve, one gets with $d_f/a = 0.142$,

$$\beta a = 1.375$$

$$\beta = 1.375/10.54 = 0.1305 \text{ in.}^{-1}$$

$$l = 5/\beta = 5/0.1305 = 38 \text{ in.}$$

Similarly, for $d_f = 2''$, one gets $l = 41''$

$d_f = 3''$, one gets $l = 45''$

$d_f = 4''$, one gets $l = 48.5''$

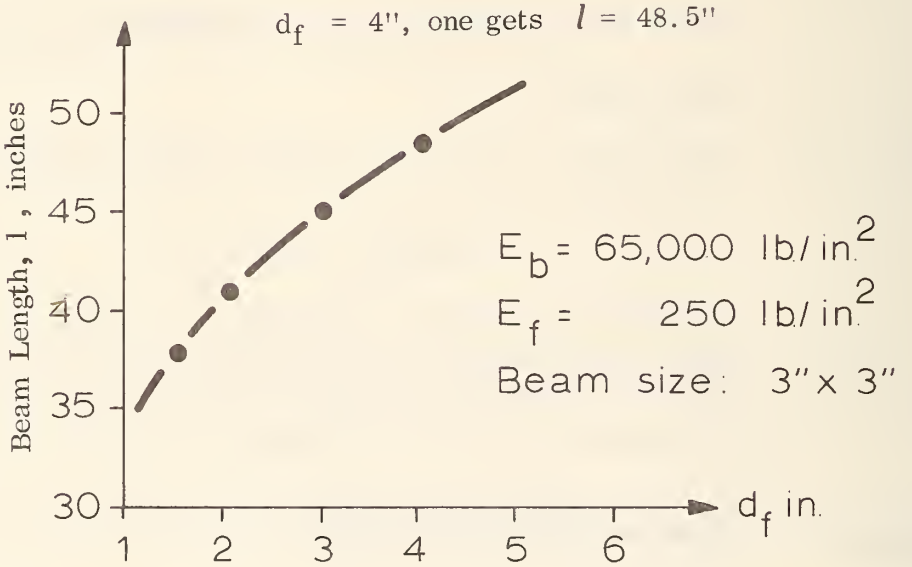

Figure 13. Relation between the required beam length and foundation depth

b) Selection of the magnitude of the applied load

1. Select the length, 2ϵ, of the cushion used to transfer the load from the loading piston onto the beam surface (the width of which should equal the width of the beam) as shown in Figure 14.

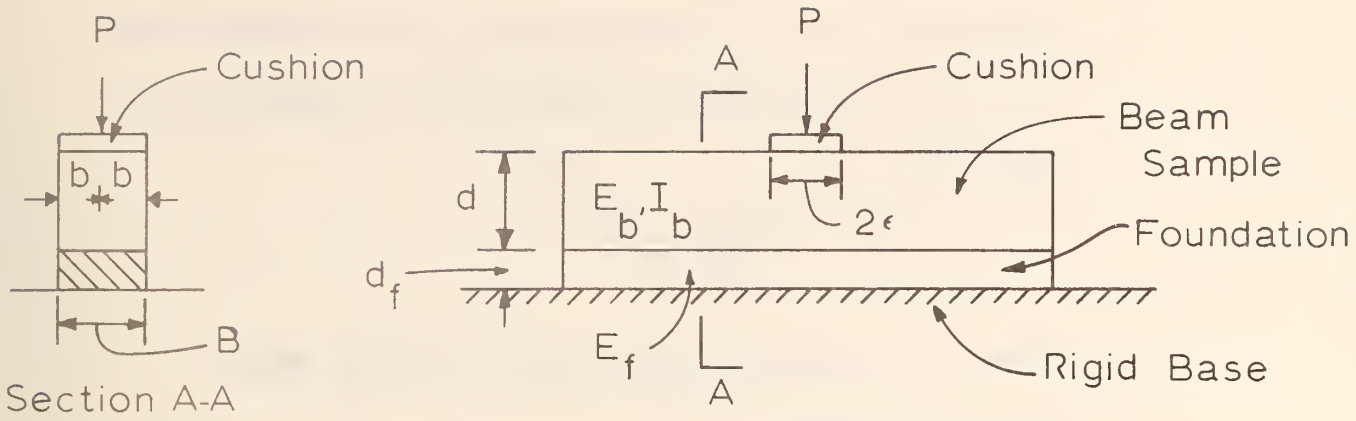

FIGURE 14

2. Compute ϵ/a and use this value to read off the curve in Figure 11 the magnitude of $\sigma_{s\ max}$ in terms of $\sigma_{p\ max}$, denote this by:

$$\sigma'_{p\ max} = \sigma_{s\ max} = \alpha_1 \sigma_{p\ max},$$

when α_1 is the value read off from the curve.

3. Select a desired value of $\sigma_{p\ max}$ such that,

$$\sigma_{p\ max} = \alpha_2\ \sigma_y\ , \quad \alpha_2 < 1$$

where σ_y = yield stress in tension
α_2 = a desired load factor

4. Compute the value of $\sigma'_{p\ max}$, i.e.

$$\sigma'_{p\ max} = \alpha_1 \alpha_2\ \sigma_y$$

5. Compute the value of d_f/a and read off from Figure 10 the corresponding value of $\sigma_{p\ max}\ Bd^2/Pa$, say

$$\frac{\sigma_{p\ max}\ Bd^2}{Pa} = \alpha_3$$

6. Substitute the value of $\sigma'_{p\ max}$ for $\sigma_{p\ max}$ in the above expression. The required magnitude of the applied load, P, can then be computed from:

$$P = \frac{\alpha_1 \alpha_2\ \sigma_y\ Bd^2}{\alpha_3\ a}$$

7. Check for the contact pressure between the cushion and the beam surface from:

$$p = P/2\epsilon B,$$

where B is the width of the cushion. The pressure p should be considerably less than σ_y in order to prevent excessive rutting; it is recommended that

$$p \leq 0.5\ \sigma_y.$$

8. If the contact pressure p is considerably large, one can either select a new dimension of the cushion and repeat the entire calculation, or simply select a new load factor, α_2, and repeat the computation from step 6.

Example:

Beam size: B = 3", d = 3"

$E_b = 65,000\ lb/in.^2$, $E_f = 250\ lb/in.^2$

$2\epsilon = 2$ in.

$d_f = 1.5$ in.

$\sigma_y = 150\ lb/in.^2$

One has from the preceding example:

$$a = 10.54 \text{ in.}$$

$$d_f/a = 0.142$$

$$\epsilon/a = 0.095$$

With $\epsilon/a = 0.095$, we get from Figure 11:

$$\sigma'_{p\,max} = \sigma_{s\,max} = 0.95\ \sigma_{p\,max}$$

Select $\sigma_{p\,max} = 0.5\ \sigma_y$, i.e. $\alpha_2 = 0.5$,

one gets:

$$\sigma'_{p\,max} = 0.95 \times 0.5 \times 150 = 71.5 \text{ lb/in.}^2$$

With $d_f/a = 0.142$ one obtains from Figure 10:

$$\frac{\sigma_{p\,max}\ B d^2}{P a} = \alpha_3 = 1.09$$

Hence, substitution of $\sigma'_{p\,max}$ for $\sigma_{p\,max}$ in the above equation leads to:

$$P = \frac{71.5 \times 3^3}{1.09 \times 10.54} = 168 \text{ lb.}$$

Next, check the contact pressure, assuming that the cushion has the same width, $B = 3''$,

$$p = \frac{P}{2 \epsilon B} = \frac{168}{2 \times 3} = 28 \text{ lb./in.}^2$$

$$<< \sigma_y \quad \text{o.k.}$$

c) Determination of K_I value for a particular crack length:

1. Compute for each particular crack length c the ratio c/d.

2. For each c/d ratio, read off from Figure 12 the corresponding K_I' value.

3. Let $\sigma_{max} = \sigma'_{p\,max} = \alpha_1 \alpha_2 \sigma_y$ as obtained from the preceeding example.

4. Compute for each crack length the corresponding value of K_I from the following equation:

$$K_I = \sigma_{max} \cdot \sqrt{d} \quad K_I'$$

Example: Using the same data as given in the preceeding example, supposing that the value of K_I for a crack length $c_o = 1.05$ inches is required.

1. $c/d = 1.05/3.0 = 0.35$.

2. With $c/d = 0.35$, from Figure 12 the corresponding $K_I' = 1.25$

3. From the preceeding example,

$$\sigma_{max} = \sigma'_{p\,max} = 71.5 \text{ lb/in}^2$$

4. With $d = 3.0$ in.,

$$K_I = \sigma_{max} \sqrt{d} \quad K_I'$$

$$= 71.5 \sqrt{3} \quad (1.25)$$

$$= 154.8 \text{ lb-in.}^{-3/2}$$

PART III

LIST OF REFERENCES

1. Biot, M. A., "Bending of an Infinite Beam on an Elastic Foundation," Journal of Applied Mechanics, Transactions, A.S.M.E., Vol. 59, A1-A7, 1937.

2. Drapkin, B., "Grillage Beams on Elastic Foundation," Proceedings, A.S.C.E., Vol. 81, No. 771, pp. 1-19.

3. Irwin, G. R., "Analysis of Stresses and Strains Near the End of a Crack Transversing a Plate," Journal of Applied Mechanics, Vol. 24, No. 3, pp. 361-364, September 1957.

4. Majidzadeh, K. and Ramsamooj, D. V., "Development of Testing Procedures and a Method to Predict Fatiuge Failures of Asphalt Concrete Pavement Systems," Research Foundation, The Ohio State University, Columbus, Ohio, March 1971.

5. Selvadurai, A.P.S., "Bending of an Infinite Beam Resting on a Porous Elastic Medium," Geotechnique, Vol. 23, No. 3, pp. 407-421, 1973.

6. Srawley, J. E. and Gross, B., "Stress-Intensity Factors for Single-Edge-Notch Specimens in Bending or Combined Bending and Tension by Boundary Collocation of a Stress Function," NASA TN D-3092, January 1965.

7. Srawley, J. E. and Gross, B., "Stress-Intensity Factors for Three-Point Bend Specimens by Boundary Collocation," NASA TN D-2603, February 1966.

8. Vesic, A., "Bending of Beams Resting on an Isotropic Elastic Solid," Journal of Engineering Mech. Div., A.S.C.E., Vol. 87, EM2, No. 1, pp. 35-53, 1961.

9. Williams, M. L., "On The Stress Distribution at the Base of a Stationary Crack," Journal of Applied Mechanics, Vol. 24, No. 1, pp. 109-114, March 1957.

10. Srawley, J. E., "Plane Strain Fracture Toughness," Fracture, An Advanced Treatise, Edited by H. Liebowitz, Vol. IV, Chapter 2, pp. 45-68, 1969.

11. Saraf, C.L., "Effect of Mix Variables on the Fatigue Response of Asphaltic Mixes," Ph.D. Dissertation, The Ohio State University, Columbus, Ohio, 1973.

12. Majidzadeh, K.; Ramsamooj, D. and Chan, A., "Analysis of Fatigue and Fracture of Bituminous Paving Mixtures—Phase I, RF 2845, The Ohio State University Research Foundation, May 1970.

13. Majidzadeh, K. and Kauffmann, E., "Analysis of Fatigue and Fracture of Bituminous Paving Mixtures—Phase II," The Ohio State University Research Foundation, RF 2845, March 1971.

14. Majidzadeh, K. and Ramsamooj, D.V., "Development of Testing Procedures and Method to Predict Fatigue of Asphalt Concrete Pavement Systems," RF 2873, The Ohio State University Research Foundation, March 1971.

15. Majidzadeh, K. and Kauffmann, E., "Verification of Fracture Mechanics Concepts to Predict Cracking of Flexible Pavements," RF 3200, The Ohio State University Research Foundation, June 1973.

APPENDIX A

Description and Use of the Collocation Computer Program for the Calculation of the Stress-Intensity Factor, K_1, for Two Dimensional Problems of a Beam With a Centrally-Located Finite Crack, Resting on an Elastic Solid.

IA. GENERAL DESCRIPTION

This program uses the Williams stress function, χ, in conjunction with the boundary stresses from the elastic theory of beams on elastic foundation to compute an opening-mode stress-intensity factor, K_1, and then normalizes it to K_1'. The method chosen to solve the problem is the "boundary collocation of stresses", which consists of solving a set of 2m simultaneous algebraic equations corresponding to the known values of stresses at a finite number of boundary stations m of the cracked beam.

Since it is impossible to deal with the exact form of the Williams stress function given by Equation (46) in the text (involving an infinite sum of series), only the first 2n terms of it were included in the analysis, i.e., the Williams stress function was approximated by:

$$\bar{\chi} = \sum_{n=1}^{NOOFM} \left\{ (-1)^{n-1} d_{2n-1} r^{(n+1/2)} \left[-\cos(n-3/2)\theta + \frac{2n-3}{2n+1} \cos(n+1/2)\theta \right] + (-1)^{n} d_{2n} r^{(n+1)} \left[-\cos(n-1)\theta + \cos(n+1)\theta \right] \right\} \qquad (A-1)$$

The corresponding stress components are given by:

$$\sigma_x = \frac{\partial^2 \bar{\chi}}{\partial r^2} \sin^2\theta - 2 \frac{\partial^2 \bar{\chi}}{\partial \theta \partial r} \frac{\sin\theta\cos\theta}{r} + \frac{\partial \bar{\chi}}{\partial r} \frac{\cos^2\theta}{r} - \frac{2\partial \bar{\chi}}{\partial \theta} \frac{\sin\theta\cos\theta}{r^2} + \frac{\partial^2 \bar{\chi}}{\partial \theta^2} \frac{\cos^2\theta}{r^2}$$

$$\sigma_y = \frac{\partial^2 \bar{\chi}}{\partial r^2} \cos^2\theta - 2 \frac{\partial^2 \bar{\chi}}{\partial \theta \partial r} \frac{\sin\theta\cos\theta}{r} + \frac{\partial \bar{\chi}}{\partial r} \frac{\sin^2\theta}{r} + \frac{2\partial \bar{\chi}}{\partial \theta} \frac{\sin\theta\cos\theta}{r^2} + \frac{\partial^2 \bar{\chi}}{\partial \theta^2} \frac{\sin^2\theta}{r^2} \qquad (A-2)$$

$$\tau_{xy} = -\frac{\partial^2 \bar{\chi}}{\partial r^2} \sin\theta\cos\theta - \frac{\partial^2 \bar{\chi}}{\partial\theta\partial r} \frac{\cos 2\theta}{r} + \frac{\partial^2 \bar{\chi}}{\partial\theta^2} \frac{\sin\theta\cos\theta}{r^2}$$

$$+ \frac{\partial \bar{\chi}}{\partial r} \frac{\sin\theta\cos\theta}{r} + \frac{\partial \bar{\chi}}{\partial\theta} \frac{\cos 2\theta}{r^2} ,$$

where

$$\frac{\partial \bar{\chi}}{\partial r} = \sum_{n=1,2,\ldots}^{NOOFM} \left\{ (-1)^{(n-1)} (n+1/2)\ d_{2n-1}\ r^{(n-1/2)} \right.$$

$$\left[-\cos(n-3/2)\theta + \frac{2n-3}{2n+1} \cos(n+1/2)\theta \right]$$

$$\left. + (-1)^n\ d_{2n}\ r^n \left[-\cos(n-1)\theta + \cos(n+1)\theta \right] \right\} \qquad (A-3.a)$$

$$\frac{\partial^2 \bar{\chi}}{\partial r^2} = \sum_{n=1,2,\ldots}^{NOOFM} \left\{ (-1)^{(n-1)} (n^2 - 1/4)\ d_{2n-1}\ r^{(n-3/2)} \left[-\cos(n-3/2)\theta \right.\right.$$

$$\left. + \frac{2n-3}{2n+1} \cos(n+1/2)\theta \right] + (-1)^n\ (n+1)\ n d_{2n}\ r^{(n-1)} \qquad (A-3.b)$$

$$\left. \left[-\cos(n-1)\theta + \cos(n+1)\theta \right] \right\}$$

$$\frac{\partial \bar{\chi}}{\partial\theta} = \sum_{n=1,2,\ldots}^{NOOFM} \left\{ (-1)^{(n-1)}\ d_{2n-1}\ r^{(n+1/2)} \left[(n-3/2)\sin(n-3/2)\theta \right.\right.$$

$$\left. - (n-3/2)\sin(n+1/2)\theta \right] + (-1)^n\ d_{2n}\ r^{(n+1)} \qquad (A-3.c)$$

$$\left. \left[(n-1)\sin(n-1)\theta - (n+1)\sin(n+1)\theta \right] \right\}$$

$$\frac{\partial^2 \bar{\chi}}{\partial\theta^2} = \sum_{n=1,2,\ldots}^{NOOFM} \left\{ (-1)^{(n-1)}\ d_{2n-1}\ r^{(n+1/2)} \left[(n-3/2)^2 \cos(n-3/2)\theta \right.\right.$$

$$\left. - (n-3/2)(n+1/2)\cos(n+1/2)\theta \right] + (-1)^n\ d_{2n}\ r^{(n+1)} \qquad (A-3.d)$$

$$\left. \left[(n-1)^2 \cos(n-1)\theta - (n+1)^2 \cos(n+1)\theta \right] \right\}$$

$$\frac{\partial^2 \bar{X}}{\partial \theta \partial r} = \sum_{n=1,2,\ldots}^{NOOFM} \left\{ (-1)^{(n-1)} d_{2n-1} (n+1/2) r^{(n-1/2)} \left[(n-3/2)\sin(n-3/2)\theta \right. \right.$$

$$\left. - (n-3/2) \sin (n+1/2)\theta \right] + (-1)^n (n+1) d_{2n} r^n \qquad \text{(A - 3.e)}$$

$$\left. \left[(n-1) \sin (n-1)\theta - (n+1) \sin (n+1)\theta \right] \right\}$$

To solve the problem, it was assumed that the stresses along the boundary of the free body of the beam can be closely approximated from the conditions of the uncracked beam. According to this assumption, we have the following boundary conditions:

Along AB:

$$\tau_{xy} = 0$$

$$\sigma_x = \sigma'_x = -\frac{P}{\pi \epsilon B} \int_0^\infty \frac{\psi(\alpha d_f/a) \sin(\alpha\epsilon/a) \cos(\alpha y/a)}{\alpha \left[\alpha^3 + \psi(\alpha d_f/a) \right]} \cdot d\alpha$$

Along BC:

$$\tau_{xy} = \tau'_{xy} = f(x) \cdot \frac{Pa}{\pi \epsilon B} \int_0^\infty \frac{\alpha \sin(\alpha\epsilon/a)\sin(\alpha l/a)}{\left[\alpha^3 + \psi(\alpha d_f/a) \right]} \cdot d\alpha$$

$$\sigma_y = \sigma_y' = g(x) \frac{(-Pa^2)}{\pi \epsilon B} \int_0^\infty \frac{\sin(\alpha\epsilon/a) \cos(\alpha l/a)}{\alpha^3 + \psi(\alpha d_f/a)} \cdot d\alpha$$

where

$$f(x) = \frac{6}{d^3} \left[cd + xd - 2xc - c^2 - x^2 \right]$$

$$g(x) = \frac{12}{d^3} \left[x - \frac{d}{2} + c \right]$$

Along CD:

$$\tau_{xy} = 0$$

$$\sigma_x = 0$$

Along DE:

$$\tau_{xy} = 0$$

$$\sigma_x = - P/2 \epsilon B$$

In the above expressions, one has:

$$a = \begin{cases} \left[\frac{E_b I_b}{E_f b}\right]^{1/3} & \text{for plane stress} \\ \left[\frac{(1 - \nu_f^2)\ E_b I_b}{E_f b}\right]^{1/3} & \text{for plane strain} \end{cases}$$

$$\psi(\alpha d_f/a) = \frac{\alpha d_f/a + \sinh(\alpha d_f/a) \cosh(\alpha d_f/a)}{\sinh^2(\alpha d_f/a)}$$

B = width of the beam

b = B/2

c = crack length

d = depth of the beam

d_f = depth of the foundation

E_b = modulus of elasticity of the beam

E_f = modulus of elasticity of the foundation

I_b = moment of inertia of the beam

l = effective length of the beam

P = total applied load

2ϵ = length of the loaded area

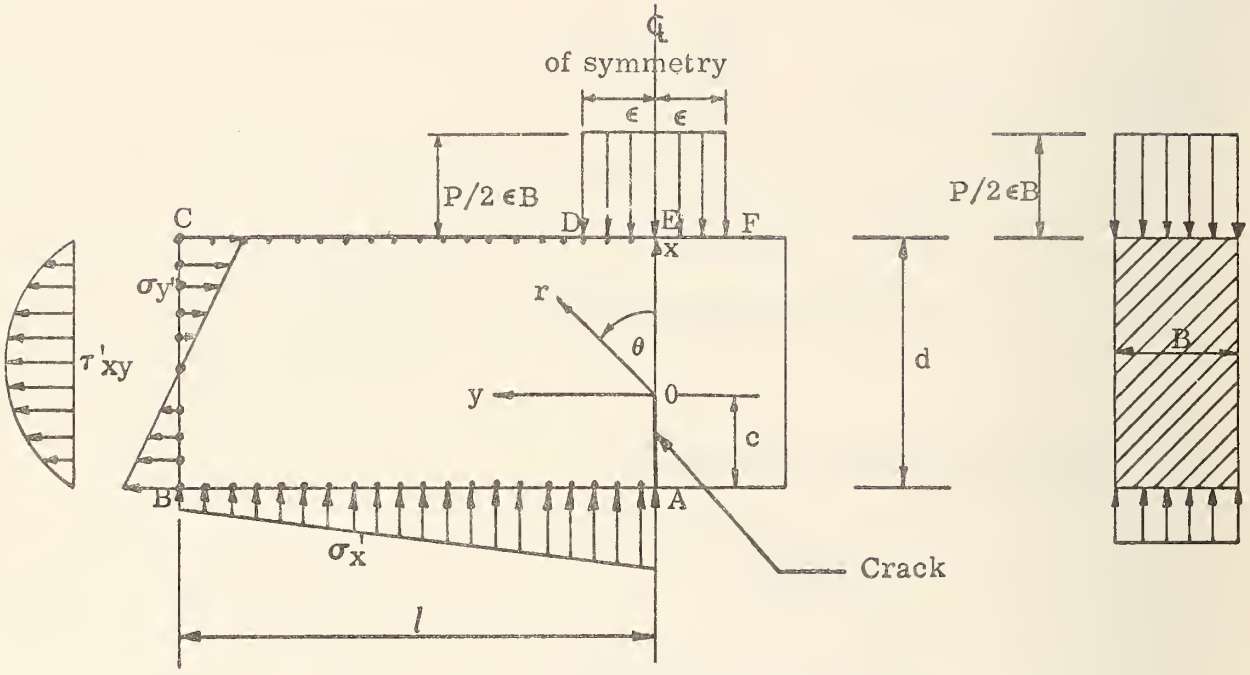

Figure A-1. Collocation Grid and the System of Loading

Having mathematically described the boundary conditions, the system of simultaneous algebraic equations for the collocation procedure is set up in the matrix form as follows:

		Boundary
σ_x	$-P/2\epsilon B$	D - E
σ_x	0	C - D
σ_x	σ'_x	A - B
σ_y	σ'_y	B - C
τ_{xy}	0	D - E
τ_{xy}	0	C - D
τ_{xy}	τ'_{xy}	B - C
τ_{xy}	0	A - B

Expressing the above system of equations in terms of the Williams stress function coefficient, d_i, yields:

$$\begin{bmatrix} C_{1,1} & C_{1,2} \cdots\cdots C_{1,2\,(NOOFM)} \\ C_{2,1} & C_{2,2} \cdots\cdots C_{2,2\,(NOOFM)} \\ \vdots & \vdots \\ C_{NOOFXY,1} & \cdots\cdots C_{NOOFXY,2(NOOFM)} \end{bmatrix} \begin{bmatrix} d_1 \\ d_2 \\ \vdots \\ d_{2(NOOFM)} \end{bmatrix} = \begin{bmatrix} a_1 \\ a_2 \\ \vdots \\ a_{(NOOFXY)} \end{bmatrix} \qquad (A - 4)$$

where $C_{i,j}$ represent the coefficients of d_j, a_i represent the numerical values of the boundary conditions to a particular i^{th} boundary station, 2(NOOFM) is

the number of d_i terms, and NOOFXY is the total number of equations used in the program.

The program will solve for the d_i , $i = 1, 2, \ldots . 2(NOOFM)$. Because solution convergence could be a problem, the least-squares optimization technique was employed in solving the system of equations. This technique and its computer listing is described in the IBM computer manual "The Scientific Subroutine Package" -- Subroutines LLSQ and DLLSQ, pp. 160 - 164. This method of solution has an advantage in that the number of equations can exceed the number of unknowns: i.e.,

$$2(NOOFM) \leq NOOFSY \qquad (A - 5)$$

In the program, NOOFXY is calculated from:

$$NOOFXY = 2\left[NOOFXL + NOOFXU + NOOFXS + NOOFXB\right] - 4 \qquad (A - 6)$$

where NOOFXL, NOOFXU, NOOFXS, and NOOFXB are the number of collocation stations under the load on the top boundary, outside the load on the top boundary, on the side boundary, and on the bottom boundary respectively In view of Equation (A - 6), Equation (A - 5) becomes:

$$NOOFM + 2 \leq NOOFXL + NOOFXU + NOOFXS + NOOFXB \qquad (A - 7)$$

This equation gives the criterion for the allowable size of the system of equations (A - 4).

Once the values of d_i have been solved, the stress-intensity factor is then calculated from:

$$K_1 = -\sqrt{2\pi}\ d_1 \qquad (A - 8)$$

and the corresponding normalized value K'_1 ,

$$K'_1 = \frac{K_1}{\sigma_{max}\sqrt{d}} \qquad (A-9)$$

where

$$\sigma_{max} = \frac{6Pa^2}{\pi\epsilon Bd^2} \int_0^{\infty} \frac{\sin(\alpha\epsilon/a)}{\alpha^3 + \psi(\alpha d_f/a)}\, d\alpha \qquad (A-10)$$

Note should be taken of the fact that the optimum number of the Williams stress function coefficients, d_i, depends somewhat on the geometrical and loading conditions of the beam. Therefore, a sensitivity analysis similar to the one shown in Figure A-2 should be done to determine, at the least, the range of d_i terms (= 2(NOOFM)) within which lies the maximum value of the stress-intensity factor. Although it was noted that the optimum value of d_i terms varies slightly with the crack length, only one set of sensitivity analysis is practically sufficient with regard to the economical viewpoint; the average values of the stress-intensity factors for other crack lengths of the system computed from three or more values of d_i terms within the optimum range should give sufficiently accurate results for practical purposes.

Example of Sensitivity Analysis

Input data:

Beam: Effective length = 3 inches
Width B = 1 inch
Depth d = 3 inches
Young's modulus E_b = 10^6 psi

Foundation:
Depth d_f = semi-infinite
Young's modulus E_f = 10^4 psi

Others: Total applied load P = 10 lbs.
Loaded area's length = 1 inch
Station spacing = 1/8 inch
Crack length = 0.6 inch

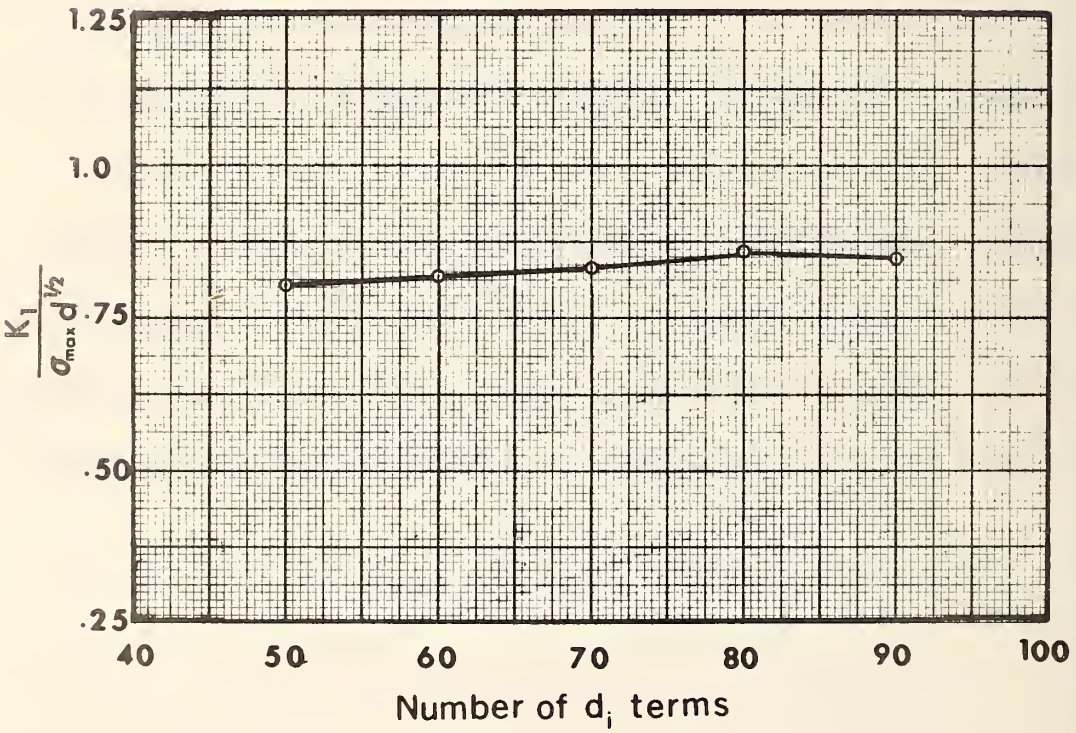

Figure A-2. Value of Normalized Stress-Intensity Factor Against Number of Williams Stress Function Coefficients, d_i.

IIA. USE OF THE PROGRAM

A. Input Data

The first step in the analysis is to select a suitable effective length, l, of the beam and a proper station spacing, s. It is recommended that the effective length be greater than or equal to the beam depth, d, and the station spacing be not greater than 1/8 of the beam depth. An equal spacing between each boundary station is assumed in the program. The next step is to choose an initial value of NOOFM (one-half of the number of the Williams stress function coefficients). After all the computations corresponding to this value of NOOFM and a specified crack length are completed, the value of NOOFM will automatically be increased by an increment of 5 and the computations are repeated for that particular crack length and the new NOOFM. This process will continue through the last NOOFM specified. The value of NOOFM will then be automatically set to the initial value again, and the execution continues with a new crack length. The program will stop executing when all the computations for the last specified crack length have been carried out.

The following is a sequence of punched cards which numerically define all the parameters needed by the program.

1. Method of Analysis for Boundary Conditions (I 1)

This is the first card in the data deck to give the program a control, whether the plane stress or plane

strain analysis is to be used in the establishment of the boundary conditions. If the number in column 1 is

0 the plane stress analysis is to be used

1 the plane strain analysis is to be used.

2. Job Title (18A4)

This card will give the descriptive identification for the job. It is the second card in the data deck.

3. Geometrical Properties, Material Properties, and Control Information Cards

The third card through the seventh card will give the following information:

Card Number	Format	Information	Columns
3	3D24.16	Effective length, l, of the beam	1 - 24
		Depth, d, of the beam	25 - 48
		Width, B, of the beam	49 - 72
4	3D24.16	Young's modulus, E_b, of the beam	1 - 24
		Young's modulus, E_f, of the foundation	25 - 48
		Depth of the foundation, d_f, (0 for semi-infinite)	49 - 72
5	3D24.16	Poisson's ratio, υ_f, of the foundation	1 - 24
		One-half of the loaded area's length, ϵ	25 - 48
		Total applied load, P	49 - 72
6	3D24.16	Initial crack length	1 - 24
		Crack increment required	25 - 48
		Final crack length required	49 - 72

7	(2I 10, L10, D24.16)	Initial NOOFM	1 - 10
		Final NOOFM required	11 - 20
		Logical constant, PRISCK (.TRUE., or .FALSE.)	21 - 30
		Station spacing, s.	31 - 54

B. Output Information

The following information is developed and printed by the program:

1. Reprint of geometrical and material properties.
2. Stress-intensity factor, K_1.
3. Normalized stress-intensity factor, K'_1.
4. Maximum tensile stress in the uncracked beam, based on the infinite beam on elastic solid, σ_{max}.
5. Fundamental length of the beam, a.
6. Relative crack length, c/d.

IIIA. ACKNOWLEDGMENT

The program is based, in part, upon the one used in Reference (4) by Majidzadeh and Ramsamooj. The modifications include some corrections to the original program, and the introduction of an improved method of analyzing the boundary conditions.

```
C****
C****     THIS PROGRAM CALCULATES THE 'K1' STRESS-INTENSITY FACTOR
C****          DEFINED BY :
C****                        K1 = -2.5066282746310D0*SOL(1)
C****          WHERE SOL(I) IS THE FIRST COEFFICIENT OF WILLIAMS
C****          STRESS FUNCTION
C****     NCODE IS 0 FOR PLANE STRESS, 1 FOR PLANE STRAIN
C****     COND IS THE BEAM'S EFFECTIVE LENGTH
C****     CONH IS THE BEAM'S DEPTH
C****     CONW IS THE BEAM'S WIDTH
C****     CONE IS THE BEAM'S YOUNG'S MODULUS
C****     CONEF IS THE FOUNDATION'S YOUNG'S MODULUS
C****     CONFD IS THE FOUNDATION'S DEPTH
C****     CONVF IS THE FOUNDATION'S POISSON'S RATIO
C****     CONA IS ONE-HALF OF THE LOADED AREA'S LENGTH
C****     CONP IS THE TOTAL APPLIED LOAD
C****     C1 IS THE CRACK LENGTH REQUIRED IN THE COMPUTATION
C****     CINC IS THE INCREMENT OF THE CRACK LENGTH .
C****     C1END IS THE FINAL CRACK LENGTH  REQUIRED
C****     NOOFM IS ONE-HALF OF THE NUMBER OF WILLIAMS STRESS FUNCTION
C****          COEFFICIENTS REQUIRED IN THE COMPUTATION
C****     LNOOFM IS THE MAXIMUM VALUE OF  NOOFM REQUIRED
C****     PRISCK IS THE LOGICAL CONSTANSTANT, '.TRUE.' INDICATES THAT
C****          AN ACCURACY CHECK OF THE SOLUTION WILL BE MADE
C****     SPACE IS THE REQUIRED SPACING BETWEEN EACH BOUNDARY STATION
C****
      IMPLICIT REAL*8 (A-H,O-Z)
      REAL*8 LAGUER
      REAL*4 NAME(18)
      REAL*4 FXL, FXS, FXB
      LOGICAL  PRISCK,ZEROCK,SOLUCK,BASEK
C****
      COMMON /DOUB/ PRIS, B,  D , CONE, COR, CORR, CONA, CONP, CONH,
     *COND,C1,CONEF,CONW,CONFD,C1END,CINC,CONVF,SPACE,AMAX,SIGMAX,
     *CONI,CONSTA,DELXL,DELXU,DELXS,DELXB
      COMMON /SING/ NOOFM, NOOFXU, NOOFXS, NOOFXB, NOOFXL, LNOOFM, IARG,
     * JARG,KARG,LARG,NAME,NOOFI,NCODE,NOOFTO,NOOFXT,NOOFT1,
     * NOOFTS,NOOFT2,NOOFTX,NOOFXX,NOOFY1,NOOFYY,NOOFB1,NOOFC1,NOOFD1,
     * NOOFF1,NOOFG1,NOOFXY,NOOFS
      COMMON /LOG/ PRISCK , BASEK
      DIMENSION  X(00100),Y(00100),R(00100),PHI(00100),V9(00200),SOL(010
     *0),COEF(0200,100),COEFCK(200,100),CALC(200),CADD(200),CON(200),
     *CONCHK(0200),IPIV(0100)
      EXTERNAL  FUNCTN
      READ(5,116)NCODE
  116 FORMAT(I1)
    3 CONTINUE
      BASEK =.FALSE.
      READ(5,801,END=1001) (NAME(I),I=1,18)
  801 FORMAT(18A4)
C
C     READ IN CONSTANTS
C
      PRIS = 1.0D-14
      READ(5,800)COND,CONH,CONW,CONE,CONEF,CONFD,CONVF,CONA,CONP,C1,
     *CINC,C1END
      IF(CONFD.GT.0.1) BASEK = .TRUE.
  800 FORMAT(3D24.16)
      READ(5,802) NOOFM, LNOOFM, PRISCK, SPACE
      NOOFI  =  NOOFM
  802 FORMAT( 2I10,L10,D24.16)
      FXL = CONA/SPACE + 1.05
```

```
      NOOFXL = IFIX(FXL)
      FXB = COND/SPACE + 1.05
      NOOFXB = IFIX(FXB)
      NOOFXU = NOOFXB - NOOFXL
      FXS = CONH/SPACE + 1.05
      NOOFXS = IFIX(FXS)
      DELXL = CONA/(NOOFXL-1)
      DELXU = (COND - CONA)/NOOFXU
      DELXS = CONH/(NOOFXS - 1)
      DELXB = COND/(NOOFXB - 1)
      NOOFT0 = NOOFXL + 1
      NOOFXT = NOOFXL + NOOFXU
      NOOFT1 = NOOFXT + 1
      NOOFTS = NOOFXT + NOOFXS - 1
      NOOFT2 = NOOFTS + 1
      NOOFTX = NOOFTS + NOOFXB - 1
      NOOFXX = NOOFXT + NOOFXB
      NOOFY1 = NOOFXX + 1
      NOOFYY = NOOFXX + NOOFXS
      NOOFB1 = NOOFYY + 1
      NOOFC1 = NOOFYY + NOOFXT - 1
      NOOFD1 = NOOFC1 + 1
      NOOFF1 = NOOFC1 + NOOFXS - 2
      NOOFG1 = NOOFF1 + 1
      NOOFXY = NOOFYY + NOOFTX - 2
      NITWIT = NOOFXL + NOOFXU + NOOFXS + NOOFXB
      IARG = NOOFTX
      LARG = NOOFXY
      CONB = CONW/2.0D0
      CONI = CONW*CONH**3/12.0D0
      CONSTA = (CONE*CONI/CONEF/CONB)**(1.0D0/3.0D0)
      IF(NCODE.EQ.1)CONSTA=(1.0D0-CONVF**2)**(1.0D0/3.0D0)*CONSTA
C
C****     CHECK FOR SEMI-INFINITE DEPTH FOUNDATION.
C
      IF(BASEK) D = CONFD/CONSTA
      D = 10000.0D0
      B = CONA/CONSTA
      AMAX = LAGUER(1,B,0.0D0,D,FUNCTN)
      SIGMAX =  6.0D0*AMAX/(CONH**2*CONW)
 9000 CONTINUE
      IF(NOOFM.GT. LNOOFM) GO TO 9999
      IF (NOOFM.EQ.NOOFI) GO TO 9997
      GO TO 9998
 9999 C1 = C1 + CINC
      NOOFM = NOOFI
      C1END = C1END+0.1D-3
      IF(C1.GT. C1END) GO TO 3
 9997 CALL COORD (X,Y,R,PHI)
 9998 CONTINUE
      KARG = NOOFM*2
      JARG = 2*KARG
      NOOFS = KARG
      CALL STRESK        (X,Y,R,PHI,V9,SOL,COEF,COEFCK,CALC,CADD,CON,
     * CONCHK,IPIV)
      NOOFM = NOOFM + 5
      GO TO 9000
 1001 STOP
      END
      SUBROUTINE COORD  (X,Y,R,PHI)
      IMPLICIT REAL*8 (A-H,O-Z)
      REAL*4 NAME(18)
```

```
      COMMON /DOUB/ PRIS, B,  D , CONE, COR, CORR, CONA, CONP, CONH,
     *COND,C1,CONEF,CONW,CONFD,C1END,CINC,CONVF,SPACE,AMAX,SIGMAX,
     *CONI,CONSTA,DELXL,DELXU,DELXS,DELXB
      COMMON /SING/ NOOFM, NOOFXU, NOOFXS, NOOFXB, NOOFXL, LNOOFM, IARG,
     * JARG,KARG,LARG,NAME,NOOFI,NCODE,NOOFTO,NOOFXT,NOOFT1,
     * NOOFTS,NOOFT2,NOOFTX,NOOFXX,NOOFY1,NOOFYY,NOOFR1,NOOFC1,NOOFD1,
     * NOOFF1,NOOFG1,NOOFXY,NOOFS
      DIMENSION X(IARG), Y(IARG), R(IARG), PHI(IARG)
C
C        GENERATION OF X & Y
C
      Y(1) = 0.
      X(1) = CONH - C1
      DO 803 I=2,NOOFXL
      Y(I) = Y(I- 1) + DELXL
  803 X(I) = X(I-1)
      Y(NOOFXL) = CONA
      DO 863 I=NOOFTO,NOOFXT
      Y(I) = Y(I- 1) + DELXU
  863 X(I) = X(I-1)
      X(NOOFXT) = CONH - C1
      Y(NOOFXT) = COND
      DO 804 I=NOOFT1,NOOFTS
      Y(I) = Y(I-1)
  804 X(I) = X(I- 1) - DELXS
      Y(NOOFTS) = COND
      X(NOOFTS) = - C1
      DO 805 I=NOOFT2,NOOFTX
      Y(I) = Y(I- 1) - DELXB
  805 X(I) = X(I-1)
      Y(NOOFTX) = 0.
C
C        CALCULATION OF POLOR  COORDINATES
C
      DO 5 I=1, NOOFTX
      R(I)=DSQRT(X(I)**2+Y(I)**2)
    5 PHI(I)=DATAN2(Y(I),X(I))
C
      RETURN
C
      END
C
      SUBROUTINE STRESK (X,Y,R,PHI,V9,SOL,COEF,COEFCK,CALC,CADD,CON,
     * CONCHK,IPIV)
      IMPLICIT REAL*8 (A-H,O-Z)
      REAL*8 LAGUER
      REAL*4   STAR(30),NAME(18)
      LOGICAL  PRISCK,ZEROCK,SOLUCK,BASEK
      COMMON /DOUB/ PRIS, B,  D , CONE, COR, CORR, CONA, CONP, CONH,
     *COND,C1,CONEF,CONW,CONFD,C1END,CINC,CONVF,SPACE,AMAX,SIGMAX,
     *CONI,CONSTA,DELXL,DELXU,DELXS,DELXB
      COMMON /SING/ NOOFM, NOOFXU, NOOFXS, NOOFXB, NOOFXL, LNOOFM, IARG,
     * JARG,KARG,LARG,NAME,NOOFI,NCODE,NOOFTO,NOOFXT,NOOFT1,
     * NOOFTS,NOOFT2,NOOFTX,NOOFXX,NOOFY1,NOOFYY,NOOFR1,NOOFC1,NOOFD1,
     * NOOFF1,NOOFG1,NOOFXY,NOOFS
      COMMON /LOG/ PRISCK , BASEK
      DIMENSION X(IARG), Y(IARG), R(IARG), PHI(IARG), V9(JARG), SOL(KARG
     2),COEF(LARG,KARG),COEFCK(LARG,KARG),CALC(LARG),CADD(LARG),
     3 CON(LARG),CONCHK(LARG),IPIV(KARG),FOUND(4)
      DATA STAR/30*'****'/,FOUND(1)/'SEMI'/,FOUND(2)/'-INF'/,FOUND(3)/
     * 'INIT'/,FOUND(4)/'E'/
      EXTERNAL   FUNCTN
```

```
      ZEROCK = .TRUE.
      SOLUCK = .TRUE.
      IF(C1.EQ.0.0)  ZEROCK = .FALSE.
      IF(C1.EQ.0.0)  PRISCK = .FALSE.
      IF((NOOFM+2).GE.(NOOFXL+NOOFXU+NOOFXS+NOOFXB)) PRISCK=.FALSE.
      IF((NOOFM+2).GE.(NOOFXL+NOOFXU+NOOFXS+NOOFXB)) SOLUCK=.FALSE.
      IF((NOOFM+2).GE.(NOOFXL+NOOFXU+NOOFXS+NOOFXB)) GO TO 8000
      IF(C1.EQ.0.0)  GO TO 8000
C
C
C        ZEROING BLANK COEFFICIENTS
C
      DO 22 I = 1,NOOFXY
      CONCHK(I) = 0.
      CON(I) =0.
      DO 22 J=1,NOOFS
      COEFCK(I,J) = 0.
   22 COEF(I,J) = 0.
C
C     CALCULATION OF SIGMA XX COEFFICIENTS
C
      DO 15 I=1,NOOFXX
      N = I
      IF(I.GT.NOOFXT) N = I + NOOFXS - 2
      IF(I.LE.NOOFXL) CON(I) = -CONP/(2.0D0*CONA*CONW)
      IF(I.GT.NOOFXT) CON(I) =-LAGUER(3,B,Y(N)/CONSTA,D,FUNCTN)/CONW
      Q=1.D0
      DO 15 J=1,NOOFM
      IF(J-(J/2*2)) 80,80,81
   80 COR=1.D0
      GO TO 201
   81 COR=-1.D0
  201 CORR=-COR
      ESIN=  DSIN(PHI(N))
      ECOS=  DCOS(PHI(N))
      IF(DABS(ESIN).LT.PRIS)  ESIN=0.
      IF(DABS(ECOS).LT.PRIS)  ECOS=0.
      CALL STRES1 (Q,PHI(N),D1,D2,D3,D4,D5,R(N))
      COEF(I,2*J-1) =   D1*ESIN*ESIN  +D2*ECOS*ECOS/R(N)  + D3*2.D0*ESIN
     **ECOS/R(N)  +D5*ECOS*ECOS/R(N)**2  -  D4*2.D0*ECOS*ESIN/R(N)**2
      CALL STRES2 (Q,PHI(N),D1,D2,D3,D4,D5,R(N))
      COEF(I,2*J) =     D1*ESIN*ESIN  +D2*ECOS*ECOS/R(N)  + D3*2.D0*ESIN
     **ECOS/R(N)  +D5*ECOS*ECOS/R(N)**2  -  D4*2.D0*ECOS*ESIN/R(N)**2
   15 Q=Q+1.D0
C
C     CALCULATION OF SIGMA YY COEFFICIENTS
C
      C = Y(NOOFXT)/CONSTA
      CONM = LAGUER(1,B,C,D,FUNCTN)
      DO 17 I=NOOFY1,NOOFYY
      N = I - NOOFXB - 1
      CON(I)=-CONM*(X(N)-CONH/2.D0+C1)/CONI
      Q=1.D0
      DO 17 J=1,NOOFM
      IF(J-(J/2*2)) 84,84,85
   84 COR=1.D0
      GO TO 203
   85 COR=-1.D0
  203 CORR=-COR
      ESIN=  DSIN(PHI(N))
      ECOS=  DCOS(PHI(N))
      IF(DABS(ESIN).LT.PRIS)  ESIN=0.
```

```
      IF(DABS(ECOS).LT.PRIS)  ECOS=0.
      CALL STRES1 (Q,PHI(N),D1,D2,D3,D4,D5,R(N))
      COEF(I,2*J-1) =   D1*ECOS*ECOS  +D2*ESIN*ESIN/R(N)  -2.D0*D3*ESIN*
     *ECOS/R(N)  + 2.D0*D4*ECOS*ESIN/R(N)**2  +  D5*ESIN*ESIN/R(N)**2
      CALL STRES2 (Q,PHI(N),D1,D2,D3,D4,D5,R(N))
      COEF(I,2*J) =     D1*ECOS*ECOS  +D2*ESIN*ESIN/R(N)  -2.D0*D3*ESIN*
     *ECOS/R(N)  + 2.D0*D4*ECOS*ESIN/R(N)**2  +  D5*ESIN*ESIN/R(N)**2
   17 Q=Q+1.D0
C
C     CALCULATION OF SIGMA XY COEFFICIENTS
C
      CONQ = -LAGUER(2,B,C,D,FUNCTN)/CONW
      DO 16 I=NOOFB1,NOOFXY
      N = I - NOOFYY +1
      IF(N.LE.NOOFXT .OR. N.GE.NOOFTS) GO TO 550
      CON(I) = 6.0D0*CONQ/CONH**3*(C1*CONH+X(N)*CONH-2.0D0*X(N)*C1-C1**2
     * -X(N)**2)
  550 Q = 1.D0
      DO 16 J=1,NOOFM
      IF(J-(J/2*2)) 82,82,83
   82 COR=1.D0
      GO TO 202
   83 COR=-1.D0
  202 CORR=-COR
      FCOS=  DCOS(2.D0*PHI(N))
      ESIN=  DSIN(PHI(N))
      ECOS=  DCOS(PHI(N))
      IF(DABS(ESIN).LT.PRIS)  ESIN=0.
      IF(DABS(FCOS).LT.PRIS)  FCOS=0.
      IF(DABS(ECOS).LT.PRIS)  ECOS=0.
      CALL STRES1 (Q,PHI(N),D1,D2,D3,D4,D5,R(N))
      COEF(I,2*J-1) =  -D1*ECOS*ESIN   -D3*FCOS/R(N)  +D5*ECOS*ESIN/R(N)
     ***2   +D2*ECOS*ESIN/R(N)  +D4*FCOS/R(N)**2
      CALL STRES2 (Q,PHI(N),D1,D2,D3,D4,D5,R(N))
      COEF(I,2*J) =    -D1*ECOS*ESIN   -D3*FCOS/R(N)  +D5*ECOS*ESIN/R(N)
     ***2   +D2*ECOS*ESIN/R(N)  +D4*FCOS/R(N)**2
   16 Q=Q+1.D0
C
C****    SOLVING FOR SOLUTIONS
C
      DO 130 I = 1,NOOFXY
      CONCHK(I) = CON(I)
      DO 130 J = 1,NOOFS
  130 COEFCK(I,J) = COEF(I,J)
      CALL DLLSQ(COEFCK,CONCHK,NOOFXY,NOOFS,1,SOL,IPIV,1.E-72,IER,V9)
      SEFK1 = -2.5066282746310D0*SOL(1)
      YY = SEFK1/(SIGMAX*DSQRT(CONH))
      CH = C1/CONH
C
C        OUTPUT
C
 8000 WRITE(6,810)   (STAR(I),I=1,30)
  810 FORMAT(1H1/1H1 //  30A4)
      WRITE(6,873)    (NAME(I),I=1,18)
  873 FORMAT(   //30X,' S T R E S S  I N T E N S I T Y  F A C T O R  A N
     * A L Y S I S'///25X,'CASE :  ',18A4)
      IF(NCODE .LE. 0)WRITE(6,114)
      IF (NCODE .EQ. 1) WRITE(6,115)CONVF
  114 FORMAT(//30X,'PLANE STRESS SOLUTION.')
  115 FORMAT(//30X,'PLANE STRAIN SOLUTION.',21X,'FOUNDATION''S POISSON''
     *S RATIO =',F7.4)
      CON2A = 2.0D0*CONA
```

```
      IF(BASEK) GO TO 312
      WRITE(6,871)CONE,CONH,COND,C1,CONW,CONEF,  (FOUND(I),I=1,4),
     *CONP,CON2A,NOOFS,SPACE
      GO TO 313
  312 WRITE(6,872)CONE,CONH,COND,C1,CONW,CONEF,CONFD,
     *CONP,CON2A,NOOFS,SPACE
  313 CONTINUE
  871 FORMAT(//56X,'PARAMETERS'//25X,'BEAM  :'//30X,'YOUNG''S MODULUS',
     *F10.1,18X,'BEAM DEPTH',5X,F10.2,/73X,'BEAM LENGTH',4X,F10.2,/30X,
     *'CRACK LENGTH',1X,F10.4,20X,'BEAM WIDTH',5X,F10.2//25X,'FOUNDATION
     * :'//30X,'YOUNG''S MODULUS',F10.1,18X,'DEPTH',10X, 4A4 ,//25X,
     *'OTHERS  :'//30X,'LOAD',9X,F10.1,20X,'LOADED AREA''S LENGTH',F8.4,
     */30X,'NUMBER OF SOLUTIONS',I4,20X,'STATION SPACING',4X,F8.3)
  872 FORMAT(//56X,'PARAMETERS'//25X,'BEAM  :'//30X,'YOUNG''S MODULUS',
     *F10.1,18X,'BEAM DEPTH',5X,F10.2,/73X,'BEAM LENGTH',4X,F10.2,/30X,
     *'CRACK LENGTH',1X,F10.4,20X,'BEAM WIDTH',5X,F10.2//25X,'FOUNDATION
     * :'//30X,'YOUNG''S MODULUS',F10.1,18X,'DEPTH',10X,F12.5,//25X,
     *'OTHERS  :'//30X,'LOAD',9X,F10.1,20X,'LOADED AREA''S LENGTH',F8.4,
     */30X,'NUMBER OF SOLUTIONS',I4,20X,'STATION SPACING',4X,F8.3)
      IF(SOLUCK)  GO TO 6718
      WRITE(6,6719)
 6719 FORMAT(//15X, '* * * * * NOOFM > NUMBER OF BOUNDARY STATIONS -----
     *EXECUTION WAS TERMINATED * * * * *')
 6718 IF(ZEROCK)  GO TO 879
      WRITE(6,876)
  876 FORMAT(//  15X,'* * * * * THEORY IS NOT VALID FOR SPECIFIED CRACK
     *LENGTH  --  EXECUTION WAS TERMINATED * * * * *')
      GO TO 877
  879 IF(IER.EQ.0)GO TO 878
      WRITE(6,90)
   90 FORMAT(///01X'* * * * * SOLUTION PROCEDURE INDICATES MATRIX SEVERE
     *LY ILL-CONDITIONED OR RANK LESS THAN NUMBER OF COLUMNS * * * * *')
  878 WRITE(6,299)  SEEK1
  299 FORMAT(  ///  30X,'STRESS INTENSITY FACTER K1 =',D24.10)
      WRITE(6,813) SIGMAX, YY, CH,CONSTA
  813 FORMAT(  /,30X,'MAXIMUM STRESS IN UNCRACKED BEAM = ',F12.6,
     2//30X, 'NORMALIZED K = ',F12.6,//,30X,'CRACK/DEPTH RATIO =',
     3 F12.6,//30X,'FUNDAMENTAL LENGTH OF BEAM = ',F12.6)
  877 WRITE(6,811)   (STAR(I),I=1,30)
      IF(PRISCK) GO TO 293
      GO TO 1001
  293 WRITE(6,8107)  (STAR(I),I=1,30)
 8107 FORMAT(1H1//  30A4)
      DO 32  I=1, NOOFXY
      CALC(I)=0.
      DO 32  J=1, NOOFS
   32 CALC(I)= CALC(I) + SOL(J)*COEF(I,J)
      DO 5268 I=1, NOOFXY
 5268 CADD(I) = CON(I)-CALC(I)
      WRITE(6,296) NOOFXL,NOOFT0,NOOFXT,NOOFT1,NOOFXX,NOOFY1,NOOFYY,
     *NOOFB1,NOOFC1,NOOFD1,NOOFF1,NOOFG1,NOOFXY
  296 FORMAT(///35X,'* * * * * OUTPUT CHECK ON SOLUTION FIT * * * * * '
     *///43X,'SUMMARY OF BOUNDARY REQUIREMENTS'//30X,'EQUATIONS    1 TO'
     *,I4,' SIGMA XX ON TOP BOUNDARY -- LOCATIONS UNDER LOAD'/30X,
     *'EQUATIONS ',I4,' TO',I4,' SIGMA XX ON TOP BOUNDARY -- REMAINING
     *LOCATIONS',/30X,'EQUATIONS ',I4,' TO',I4,' SIGMA XX ON BOTTOM BOUN
     *DARY',/30X,'EQUATIONS ',I4,' TO',I4,' SIGMA YY ON SIDE BOUNDARY',
     */30X,'EQUATIONS ',I4,' TO',I4,' SIGMA XY ON TOP BOUNDARY',/30X,
     *'EQUATIONS ',I4,' TO',I4,'SIGMA XY ON SIDE BOUNDARY',/30X,
     *'EQUATIONS ',I4,' TO',I4,'SIGMA XY ON BOTTOM BOUNDARY')
      WRITE(6,297)
  297 FORMAT( // 14X,'EQUATION NO.',13X,'THEORETICAL VALUE',12X,'CALCUAT
```

```
     *ED VALUE',15X,'DIFFERENCE'   )
      WRITE(6,291)  (I,CON(I),CALC(I),CADD(I),I=1,NOOFXY)
  291 FORMAT(17X,I3,10X,3D28.16)
      WRITE(6,811)    (STAR(I),I=1,30)
  811 FORMAT(///    30A4)
 1001 CONTINUE
C
      RETURN
      END
C
      SUBROUTINE STRES1 (S,PHEE,D2PDR2,DPDR,D2PDRP,DPDP,D2PDP2,RR)
      IMPLICIT REAL*8 (A-H,O-Z)
      COMMON /DOUB/ PRIS, B,  D , CONE, COR, CORR, CONA, CONP, CONH,
     *COND,C1,CONEF,CONW,CONFD,C1END,CINC,CONVF,SPACE,AMAX,SIGMAX,
     *CONI,CONSTA,DELXL,DELXU,DELXS,DELXB
      ECOS=  DCOS((S-1.5D0)*PHEE)
      FCOS=  DCOS((S+0.5D0)*PHEE)
      ESIN=  DSIN((S-1.5D0)*PHEE)
      FSIN=  DSIN((S+0.5D0)*PHEE)
      IF(DABS(ESIN).LT.PRIS)  ESIN=0.
      IF(DABS(ECOS).LT.PRIS)  ECOS=0.
      IF(DABS(FCOS).LT.PRIS)  FCOS=0.
      IF(DABS(FSIN).LT.PRIS)  FSIN=0.
      D2PDR2=(  -ECOS +((2.D0*S-3.D0)/(2.D0*S+1.D0))*FCOS)* (S**2-.25D0)
     **RR**(S-1.5D0)*(+1.D0)**(S-1.D0)*CORR
      DPDR=D2PDR2*RR/(S-.5D0)
      D2PDRP=((S-1.5D0)*ESIN -(S-1.5D0)*FSIN)*(S+.5D0)*RR**(S-.5D0)*
     *(+1.D0)**(S-1.D0)*CORR
      DPDP=D2PDRP*RR/(S+.5D0)
      D2PDP2=  ((S-1.5D0)**2*ECOS   -(S-1.5D0)*(S+.5D0)*FCOS)*RR**(S+.5
     *D0)*(+1.D0)**(S-1.D0)*CORR
C
      RETURN
      END
C
      SUBROUTINE STRES2 (S,PHEE,D2PDR2,DPDR,D2PDRP,DPDP,D2PDP2,RR)
      IMPLICIT REAL*8 (A-H,O-Z)
      COMMON /DOUB/ PRIS, B,  D , CONE, COR, CORR, CONA, CONP, CONH,
     *COND,C1,CONEF,CONW,CONFD,C1END,CINC,CONVF,SPACE,AMAX,SIGMAX,
     *CONI,CONSTA,DELXL,DELXU,DELXS,DELXB
      FSIN=  DSIN((S+1.D0)*PHEE)
      ECOS=  DCOS((S-1.D0)*PHEE)
      ESIN=  DSIN((S-1.D0)*PHEE)
      FCOS=  DCOS((S+1.D0)*PHEE)
      IF(DABS(ESIN).LT.PRIS)  ESIN=0.
      IF(DABS(ECOS).LT.PRIS)  ECOS=0.
      IF(DABS(FSIN).LT.PRIS)  FSIN=0.
      IF(DABS(FCOS).LT.PRIS)  FCOS=0.
      D2PDR2=   (-ECOS +FCOS)*(S*S+S)*RR**(S-1.D0)*(+1.D0)**S*COR
      DPDR=D2PDR2*RR/S
      D2PDRP=   ((S-1.D0)*ESIN -(S+1.D0)*FSIN)*(S+1.D0)*RR**S*(+1.D0)**S
     **COR
      DPDP=D2PDRP*RR/(S+1.D0)
      D2PDP2=  ((S-1.D0)**2*ECOS  -(S+1.D0)**2*FCOS)*RR**(S+1.D0)*(+1.D0
     *)**S*COR
C
      RETURN
      END
C
      REAL FUNCTION FUNCTN*8(NFUNCT,B,C,D,X)
      IMPLICIT REAL*8 (A-H,O-Z)
C
```

```
      S = D*X
      IF (S.GT.80.) GO TO 2
      PSI = (S+DSINH(S)*DCOSH(S))/(DSINH(S)*DSINH(S))
      GO TO 3
    2 PSI = 1.0D0
    3 IF(NFUNCT.EQ.1) FUNCTN= (DEXP(X)*DSIN(B*X)*DCOS(C*X))/(X**3+PSI)
      IF(NFUNCT.EQ.2) FUNCTN= (X*DEXP(X)*DSIN(B*X)*DSIN(C*X))/(X**3+PSI)
      IF(NFUNCT.EQ.3) FUNCTN= (DEXP(X)*PSI*DSIN(B*X)*DCOS(C*X))/
     *(X*(X**3+PSI))
C
      RETURN
      END
C
      REAL FUNCTION LAGUER*8(NFUNCT,BB,C,DD,FUNCTN)
      IMPLICIT REAL*8 (A-H,O-Z)
      COMMON /DOUB/ PRIS, B,  D , CONE, COR, CORR, CONA, CONP, CONH,
     *COND,C1,CONEF,CONW,CONFD,C1END,CINC,CONVF,SPACE,AMAX,SIGMAX,
     *CONI,CONSTA,DELXL,DELXU,DELXS,DELXB
C
      DIMENSION Z(32),W(32)
C
C.....PRESET Z AND W ARRAYS.....
C
      DATA PI/3.14159265358979D0/
      DATA Z/.44893658332670180-1,.2345261095196 1854,.57688462930188643
     1 ,.10724487538178176D1,.17224087764446454D1,.25283367064257949D1,
     2 .34922132730219945D1,.46164567697497674D1,.59039585041742439D1,
     3 .73581267331862410 1,.89829409242125960 1,.10783018632539972D2,
     4 .12763697986742725D2,.14931139755522557D2,.17292454336715315D2,
     5 .19855860940336055D2,.22630889013196774D2,.25628636022459248D2,
     6 .28862101816323475D2,.32346629153964737D2,.36100494805751974D2,
     7 .40145719771539442D2,.44509207995754938D2,.49224394987308639D2,
     8 .54333721333969070 2,.59892509162134018D2,.65975377287935053D2,
     9 .72687628096627102 2,.80187446977913520 2,.88735340417892400 2,
     I .98829542868283970 2,.11175139809793770D3/
C
      DATA W/.10921834195238497,.21044310793881323,.23521322966984801,
     1 .19590333597288104,.12998378628607176,.70578623865717442D-1,
     2 .31760912509175070D-1,.11918214834838557D-1,.37388162946115248D-2
     3 ,.98080330661495510-3,.21486491880136419D-3,.39203419679879472D-4
     4 ,.59345416128686329D-5,.74164045786675520-6,.76045678791207810-7,
     5 .63506022662580670-8,.42813829710409289D-9,
     6 .23058994918913361D-10,.97993792887270940-12,
     7 .32378016577292665D-13,.81718234434207190-15,
     8 .15421338333938234D-16,.21197922901636186D-18,
     9 .20544296737880454D-20,.13469825866373952D-22,
     I .56612941303973594D-25,.14185605454630369D-27,
     J .19133754944542243D-30,.11922487600982224D-33,
     K .26715112192401370D-37,.13386169421062563D-41,
     L .45105361938989742D-47/
C
      SUM = 0.0
      DO 5 J = 1,32
    5 SUM = SUM+W(J)*FUNCTN(NFUNCT,BB,C,DD,Z(J))
C
      AREA = 2.0D0*CONA
      IF(NFUNCT.EQ.1) LAGUER = 2.0D0*CONP*CONSTA**2*SUM/PI/AREA
      IF(NFUNCT.EQ.2) LAGUER = -2.0D0*CONP*CONSTA*SUM/PI/AREA
      IF(NFUNCT.EQ.3) LAGUER = 2.0D0*CONP*SUM/PI/AREA
C
      RETURN
      END
```

```
C
      SUBROUTINE DLLSQ(A,B,M,N,L,X,IPIV,EPS,IER,AUX)                    DLLS 630
      IMPLICIT REAL*8 (A-H,O-Z)
      REAL*4 EPS
      DIMENSION A(1),B(1),X(1),IPIV(1),AUX(1)
    1 PIV=0.D0                                                          DLLS 730
      IEND=0                                                            DLLS 740
      DO 4 K=1,N                                                        DLLS 750
      IPIV(K)=K                                                         DLLS 760
      H=0.D0                                                            DLLS 770
      IST=IEND+1                                                        DLLS 780
      IEND=IEND+M                                                       DLLS 790
      DO 2 I=IST,IEND                                                   DLLS 800
    2 H=H+A(I)*A(I)                                                     DLLS 810
      AUX(K)=H                                                          DLLS 820
      IF(H-PIV)4,4,3                                                    DLLS 830
    3 PIV=H                                                             DLLS 840
      KPIV=K                                                            DLLS 850
    4 CONTINUE                                                          DLLS 860
    5 SIG=DSQRT(PIV)                                                    DLLS 920
      TOL=SIG*ABS(EPS)                                                  DLLS 930
      LM=L*M                                                            DLLS 970
      IST=-M                                                            DLLS 980
      DO 21 K=1,N                                                       DLLS 990
      IST=IST+M+1                                                       DLLS1000
      IEND=IST+M-K                                                      DLLS1010
      I=KPIV-K                                                          DLLS1020
      IF(I)8,8,6                                                        DLLS1030
    6 H=AUX(K)                                                          DLLS1060
      AUX(K)=AUX(KPIV)                                                  DLLS1070
      AUX(KPIV)=H                                                       DLLS1080
      ID=I*M                                                            DLLS1090
      DO 7 I=IST,IEND                                                   DLLS1100
      J=I+ID                                                            DLLS1110
      H=A(I)                                                            DLLS1120
      A(I)=A(J)                                                         DLLS1130
    7 A(J)=H                                                            DLLS1140
    8 IF(K-1)11,11,9                                                    DLLS1170
    9 SIG=0.D0                                                          DLLS1180
      DO 10 I=IST,IEND                                                  DLLS1190
   10 SIG=SIG+A(I)*A(I)                                                 DLLS1200
      SIG=DSQRT(SIG)                                                    DLLS1210
      IF(SIG-TOL)32,32,11                                               DLLS1240
   11 H=A(IST)                                                          DLLS1270
      IF(H)12,13,13                                                     DLLS1280
   12 SIG=-SIG                                                          DLLS1290
   13 IPIV(KPIV)=IPIV(K)                                                DLLS1320
      IPIV(K)=KPIV                                                      DLLS1330
      BETA=H+SIG                                                        DLLS1370
      A(IST)=BETA                                                       DLLS1380
      BETA=1.D0/(SIG*BETA)                                              DLLS1390
      J=N+K                                                             DLLS1400
      AUX(J)=-SIG                                                       DLLS1410
      IF(K-N)14,19,19                                                   DLLS1420
   14 PIV=0.D0                                                          DLLS1450
      ID=0                                                              DLLS1460
      JST=K+1                                                           DLLS1470
      KPIV=JST                                                          DLLS1480
      DO 18 J=JST,N                                                     DLLS1490
      ID=ID+M                                                           DLLS1500
      H=0.D0                                                            DLLS1510
      DO 15 I=IST,IEND                                                  DLLS1520
```

```
      II=I+ID                                                          DLLS1530
   15 H=H+A(I)*A(II)                                                   DLLS1540
      H=BETA*H                                                         DLLS1550
      DO 16 I=IST,IEND                                                 DLLS1560
      II=I+ID                                                          DLLS1570
   16 A(II)=A(II)-A(I)*H                                               DLLS1580
      II=IST+ID                                                        DLLS1610
      H=AUX(J)-A(II)*A(II)                                             DLLS1620
      AUX(J)=H                                                         DLLS1630
      IF(H-PIV)18,18,17                                                DLLS1640
   17 PIV=H                                                            DLLS1650
      KPIV=J                                                           DLLS1660
   18 CONTINUE                                                         DLLS1670
   19 DO 21 J=K,LM,M                                                   DLLS1700
      H=0.D0                                                           DLLS1710
      IEND=J+M-K                                                       DLLS1720
      II=IST                                                           DLLS1730
      DO 20 I=J,IEND                                                   DLLS1740
      H=H+A(II)*B(I)                                                   DLLS1750
   20 II=II+1                                                          DLLS1760
      H=BETA*H                                                         DLLS1770
      II=IST                                                           DLLS1780
      DO 21 I=J,IEND                                                   DLLS1790
      B(I)=B(I)-A(II)*H                                                DLLS1800
   21 II=II+1                                                          DLLS1810
      IER=0                                                            DLLS1860
      I=N                                                              DLLS1870
      LN=L*N                                                           DLLS1880
      PIV=1.D0/AUX(2*N)                                                DLLS1890
      DO 22 K=N,LN,N                                                   DLLS1900
      X(K)=PIV*B(I)                                                    DLLS1910
   22 I=I+M                                                            DLLS1920
      IF(N-1)26,26,23                                                  DLLS1930
   23 JST=(N-1)*M+N                                                    DLLS1940
      DO 25 J=2,N                                                      DLLS1950
      JST=JST-M-1                                                      DLLS1960
      K=N+N+1-J                                                        DLLS1970
      PIV=1.D0/AUX(K)                                                  DLLS1980
      KST=K-N                                                          DLLS1990
      ID=IPIV(KST)-KST                                                 DLLS2000
      IST=2-J                                                          DLLS2010
      DO 25 K=1,L                                                      DLLS2020
      H=B(KST)                                                         DLLS2030
      IST=IST+N                                                        DLLS2040
      IEND=IST+J-2                                                     DLLS2050
      II=JST                                                           DLLS2060
      DO 24 I=IST,IEND                                                 DLLS2070
      II=II+M                                                          DLLS2080
   24 H=H-A(II)*X(I)                                                   DLLS2090
      I=IST-1                                                          DLLS2100
      II=I+ID                                                          DLLS2110
      X(I)=X(II)                                                       DLLS2120
      X(II)=PIV*H                                                      DLLS2130
   25 KST=KST+M                                                        DLLS2140
   26 IST=M+1                                                          DLLS2180
      IEND=0                                                           DLLS2190
      DO 29 J=1,L                                                      DLLS2200
      IEND = IEND + M
      H=0.D0                                                           DLLS2220
      IF(M-N)29,29,27                                                  DLLS2230
   27 DO 28 I=IST,IEND                                                 DLLS2240
   28 H=H+B(I)*B(I)                                                    DLLS2250
```

```
      IST=IST+M                                                    DLLS2260
   29 AUX(J)=H                                                     DLLS2270
      RETURN                                                       DLLS2280
   32 IER=K-1                                                      DLLS2390
C
      RETURN                                                       DLLS2400
      END                                                          DLLS2410
```

☆U.S. GOVERNMENT PRINTING OFFICE: 1977-240-897/268